2010

Autotaxin: A Regulator of Oligodendrocyte Differentiation

Larra Yuelling
Virginia Commonwealth University

Autotaxin: A Regulator of Oligodendrocyte Differentiation

A dissertation submitted in partial fulfillment of the requirements for the degree of Doctor of Philosophy at Virginia Commonwealth University

By

Larra Walling Yuelling
B.A. Drew University, 2003

Director: Babette Fuss, Ph.D.
Professor
Department of Anatomy and Neurobiology

Virginia Commonwealth University
Richmond, Virginia
December 2010

ACKNOWLEDGEMENTS

I would like to first extend my sincere gratitude to my advisor, Dr. Babette Fuss. Because of her knowledge, guidance and support, I have learned how to work and think independently as a scientist as well as be successful in my graduate career. Dr. Fuss is extremely hard working, creative and enthusiastic about her work, all great qualities for a mentor.

Dr. James Lister was instrumental for my studies with zebrafish. Not only did he give me the tools and knowledge necessary to perform experiments, he also mentored me through the years and I thank him for all of his help.

I would also like to thank the many faculty members who aided in my success as a graduate student. I would first like to thank the members of my graduate committee: Dr. Raymond Colello, Dr. Jeffrey Dupree, Dr. James Lister, Dr. Carmen Sato-Bigbee and Dr. Robert Tombes. I would also like to thank the director of the neuroscience program, Dr. John Bigbee as well as its past director Dr. Leslie Satin. Due to the dedication of Dr. Bigbee, the Neuroscience program has become more recognized and recently has been awarded its own Ph.D. degree. I would also like to thank the microscopy facility, including Dr. Scott Henderson, Judy Williamson and Natasha Purdie.

Through the years as a graduate student, members of the lab, both past and present, were there to celebrate in my successes and were also there for support during the failures. They have aided in my success as a graduate student with helpful suggestions, technical assistance and most importantly by provided comic relief and friendship. These people include Sati Afshari, Dr. Jameel Dennis, Dr. Audrey Lafrenaye, Chris Waggener, Dr. Luciana Nogaroli, Karen Gorse, Dr. Magdalena Svelag, Angali Hari and Jessicka Hall.

I finally would like to thank my family, especially my mother for teaching me the importance of an education for as long as I can remember and for her unconditional and continued support throughout my life. I am also grateful for my incredible husband John who has always been there for me and I want to thank him for his support, understanding and encouragement through the years.

Without the help and support of the above-mentioned people as well as many unmentioned friends and family, I would not be where I am today and I thank everyone for that.

TABLE OF CONTENTS

LIST OF FIGURES

Page

LIST OF ABBREVATIONS

ATX	autotaxin
bp	base pair
BSA	bovine serum albumin
CNS	central nervous system
cAMP	cyclic AMP
cldnk	claudink
CREB	cAMP response element binding protein
dpf	days post fertilization
DMEM	Dubecco's modified essential medium
ECM	extracellular matrix
ENPP	ecto-nucleotide pyrophosphatase / phosphodiesterase
ERK	extracellular signal-regulated kinase
FCS	fetal calf serum
FGF	fibroblast growth factor
FN	fibronectin
GalC	galactocerebroside
GPCR	G protein-coupled receptor
hpf	hours post fertilization
HRP	horseradish peroxidase
kDa	kilodalton
LPA	lysophosphatidic acid
LPC	lysophosphatidylcholine

lysoPLD	lysophospholipase D
MAPK	mitogen-activated protein kinase
MBP	myelin basic protein
MO	morpholino
MOG	myelin oligodendrocyte glycoprotein
MORFO	modulator of oligodendrocyte remodeling and focal adhesion organization
mRNA	messenger RNA
MS	Multiple Sclerosis
OLG	oligodendrocyte
OPC	oligodendrocyte progenitor cell
P	postnatal
P1	primer 1
P2	primer 2
P0	myelin protein zero
PBS	phosphate-buffered saline
PD-Iα/ATX	phosphodiesterase-1α/autotaxin
PDGF	platelet-derived growth factor
PDGFαR	platelet-derived growth factor alpha receptor
PLP	proteolipid protein
pMN	motor neuron progenitor domain
PNS	peripheral nervous system
qRT-PCR	quantitative RT-PCR

RT-PCR	reverse transcriptase – polymerase chain reaction
S1P	sphingosine-1-phosphate
Shh	sonic hedgehog
SEM	standard error of mean
siRNA	short interfering RNA
SPC	sphingosylphosphorylcholine
Twhh	tiggy winkle hedgehog

ABSTRACT

AUTOTAXIN: A REGULATOR OF OLIGODENDROCYTE DIFFERENTIATION

By Larra W. Yuelling

A dissertation submitted in partial fulfillment of the requirements for the degree of Doctor of Philosophy at Virginia Commonwealth University

Virginia Commonwealth University, 2010

Advisor: Babette Fuss, Ph.D., Professor, Department of Anatomy and Neurobiology

In order for oligodendrocyte progenitor cells (OPCs) to differentiate into fully mature, myelinating oligodendrocytes, they must be specified at the correct times and undergo coordinated changes in both gene expression and morphology. As oligodendrocytes differentiate, they transition from a bipolar morphology into a morphology characterized by a complex network of multiple processes, which will eventually generate membranous structures necessary for myelination of axonal segments. As changes are observed in cellular morphology, oligodendrocytes also undergo changes in their gene expression profile and express genes necessary for both early and later stages of development such as *olig1* and *myelin basic protein* (*mbp*), respectively.

Data from our laboratory demonstrate that autotaxin (ATX), also referred to as phosphodiesterase Iα/autotaxin (PD-Iα/ATX), is involved in all of these processes as a multifunctional protein by regulating lysophospholipid signaling

and cell-extracellular matrix interactions. Previously, our laboratory has identified ATX as an oligodendrocyte-secreted factor present in the extracellular environment that via a newly-identified functional domain, named the MORFO domain (modulator of oligodendrocyte remodeling and focal adhesion organization), can regulate adhesion of oligodendrocytes to naturally occurring extracellular matrix (ECM) proteins and ultimately the establishment of the oligodendrocyte's complex process network. *In vitro* data presented in this dissertation suggest that lysophosphatidic acid (LPA), via production from ATX's well characterized lysophospholipase D (lysoPLD) domain, can induce the expression of myelin basic protein (*mbp*) and the establishment of membranous structures by differentiating oligodendrocytes, both necessary for the initial stages of myelination. Interested in relating these functions to an *in vivo* model and due to the early embryonic lethality of atx-null mice, we utilized the zebrafish as an *in vivo* model. The *in vivo* data presented in this dissertation demonstrate that *atx* expression in the zebrafish is evolutionarily conserved within vertebrates. Interestingly, in both mouse and the zebrafish, *atx* was found expressed by cells of the cephalic floor plate in addition to differentiating oligodendrocytes. Functionally the *in vivo* data presented in this dissertation confirmed ATX's role in stimulating *mbp* expression during later stages of oligodendrocyte development. In addition, a novel function for ATX was revealed by the studies undertaken as part of this dissertation that has never been described before. More specifically, based on the timing of *atx* expression and the phenotype seen upon *atx* knock-down, the data presented here suggest that ATX, released by the cephalic floor

plate, regulates early oligodendrocyte development and/or specification. Taken together, these data identify ATX as a major regulator for early as well as late developmental stages of the oligodendrocyte lineage.

CHAPTER 1

Introduction to Oligodendrocyte Biology and Autotaxin

(The section of this chapter describing autotaxin includes parts of a review that was accepted in Biochimica et Biophysica Acta (BBA) - Molecular and Cell Biology of Lipids in April of 2008. The review was written by myself with guidance from Babette Fuss.)

Myelination and its biological significance

In mammals, myelination takes place in late embryonic and early postnatal life by oligodendrocytes, the myelinating cells of the central nervous system. Once mature, these cells produce the myelin sheath, a lipid rich multilamellar membrane that surrounds and insulates axons allowing for fast conduction of electrical impulses, called action potentials, over long distances. Action potentials are required for the nervous system to function efficiently.

The generation of the myelin sheath is an evolutionary adaptation common to the majority of vertebrates (Schweigreiter et al., 2006; Hartline and Colman, 2007). Without it, faster conduction speeds are attained through increased axon diameter (i.e. the squid giant axon). The myelin sheath conserves space by allowing axons of small caliber to communicate quickly over long distances (Hartline and Colman, 2007). The unmyelinated squid giant axon occupies 15,000 times more space than a myelinated mammalian axon with a comparable conduction speed (Salzer, 1997).

The myelin sheath is distributed along the axon in long segments called internodes, with intermittent gaps in between called the nodes of Ranvier. Sodium channels cluster at the nodes and increase conduction speed by

allowing action potentials to “jump” from node to node, a process referred to as saltatory conduction (Salzer, 1997). Myelin is crucial for saltatory conduction because it provides long-term maintenance of the nodal domain which contains sodium channels (Salzer, 1997; Dupree et al., 2004). Myelin also increases conduction speed by preventing the electrical current from dissipating through the insulation of the axon. This increases the electrical resistance across the cell membrane and decreases capacitance. Each oligodendrocyte can myelinate up to 40 internodal segments on multiple axons (Pfeiffer et al., 1993).

Along with promoting fast signal propagation, myelin has been shown to be important in maintenance of axonal integrity (Griffiths et al., 1998b; Nave and Trapp, 2008). The myelin sheath produced by oligodendrocytes is therefore crucial for proper signal conduction in the central nervous system. If oligodendrocytes are damaged or not present, the resulting signal disruption can lead to a wide range of disability as seen in disease.

Diseases affecting myelin

Diseases affecting myelin include dys-myelinating diseases such as leukodystrophies, hereditary neurodegenerative disorders when myelin is not produced, or acquired demyelinating diseases such as multiple sclerosis (MS), where myelin was present but has been damaged.

MS is the most common demyelinating disease and is usually seen in patients ranging from 20 to 50 years old. Current estimates are that approximately 2.1 million people worldwide have MS, with 400,000 cases in the

United States (Multiple Sclerosis Society, 2010). MS is the leading cause of nontraumatic disability and symptoms, although unpredictable and can vary from person to person, encompass sensory and motor abnormalities, visual difficulties and cognitive dysfunction (Fox et al., 2006).

MS is classified according to different courses of the disease: relapsing-remitting, primary progressive, secondary progressive and progressive-relapsing. Patients start the disease course as either having relapsing-remitting MS (85% of patients) or primary progressive MS (10-15% of patients). In relapsing-remitting MS, episodes of inflammation, called relapses, are accompanied by the introduction of new symptoms or resurfacing of old symptoms. Relapses can last several days to weeks followed by remission which leads to partial or full recovery and can take up to weeks or months to occur. In between relapses the disease does not get worse, but either shortly after being diagnosed with, or up to 10-20 years of having relapsing-remitting MS, conditions gradually get worse and the disease transitions into secondary progressive MS. There may be some relapses in the begininning of this stage but conditions continue to get worse in between leading to a steady decline with no recovery (Lublin and Reingold, 1996; Fox et al., 2006).

As stated above, some patients alternately start the disease course with primary progressive MS characterized by gradual worsening of symptoms with no relapses or remissions, similar to secondary progressive MS. It is thought that some patients in this group initially started with relapsing-remitting MS but either the areas of inflammation did not target white matter to cause symptoms or the

relapses were not recognized or remembered by the patients (Lublin and Reingold, 1996; Fox et al., 2006).

The least common form of MS is progressive-relapsing MS and usually, but not always, occurs in patients that initially had primary progressive MS. This course of the disease is characterized by acute attacks that may or may not have recovery associated with them (Multiple Sclerosis Society, 2010).

Because there are different disease courses that present themselves in MS, different patients may experience different courses of the disease. Also, each patient will likely experience more than one disease course through their life.

In MS lesions, remyelination occurs with great efficiency, especially early in the disease but frequently fails in chronic lesions leading to persistent demyelination. The pathogenesis of MS is still not completely understood and in order to gain an understanding about the process of myelination it is important to understand the cellular biology and development of the oligodendrocyte.

Oligodendrocyte specification

Oligodendrocytes are found distributed throughout the adult brain and spinal cord, accumulating mainly after birth in rodents but their progenitors are present much earlier in restricted locations in the central nervous system (Warf et al., 1991; Noll and Miller, 1993; Pringle and Richardson, 1993; Pringle et al., 1998).

The majority of research looking at oligodendrocyte specification and development has been conducted on ventrally derived oligodendrocytes in the rodent spinal cord. In the spinal cord, oligodendrocyte progenitor cells (OPCs) are specified from neuroepithelial precursors in a restricted domain of the ventral ventricular zone termed the motor neuron progenitor domain that also generates motor neurons (Warf et al., 1991; Noll and Miller, 1993; Fu et al., 2002). This domain is located immediately dorsal to the ventral midline structure termed the floor plate. OPCs are first identified in the cervical spinal cord of the rat on embryonic day 14, while motor neurons have been identified a few days earlier, between embryonic days 11-13 (Yu et al., 1994; Pringle et al., 1996). Please refer to more detailed descriptions of oligodendrocyte specification and early development in chapter three.

Oligodendrogenesis in the brain has not been studied as extensively as in the spinal cord. Oligodendrocyte development and myelination occurs in a caudal to rostral pattern, occurring earlier in the spinal cord than in the brain and subsequently earlier in caudal versus rostral regions of the brain. OPCs appear postnatally in both the ventricular and subventricular zones lining the ventricles of the brain and more specifically, they are generated from the subventricular zone of the lateral and fourth ventricles in the rat cerebrum and cerebellum, respectively (Reynolds and Wilkin, 1988, 1991; Levison and Goldman, 1993). As in the spinal cord, oligodendrocytes in the hindbrain and midbrain are generated from ventral ventricular zone precursors (Ono et al., 1997; Alberta et al., 2001;

Davies and Miller, 2001; Nery et al., 2001; Tekki-Kessaris et al., 2001; Lu et al., 2002; Zhou and Anderson, 2002).

There has been some debate through the years on whether oligodendrocytes are solely generated in ventral locations as initial chick-quail chimera experiments conducted in the spinal cord indicated dorsally derived oligodendrocytes at later stages (Cameron-Curry and Le Douarin, 1995). These studies were not confirmed until recently with further evidence pointing towards a later, dorsal origin in the hindbrain and spinal cord (Cai et al., 2005; Fogarty et al., 2005; Vallstedt et al., 2005; Richardson et al., 2006). One critical study in the forebrain of mice not only discovered different populations of oligodendrocytes generated from multiple locations induced at various times, but that these populations are able to spread and populate areas where one population was destroyed (Kessaris et al., 2006).

Oligodendrocyte development and differentiation

After OPCs are specified in the ventricular and subventricular zones, they migrate away from these zones and proliferate extensively to populate the brain and spinal cord where they ultimately differentiate into myelinating oligodendrocytes. Throughout their development, oligodendrocytes are characterized by the sequential expression of developmental markers (lipids, proteins and surface antigens). Presence of these markers as well as changes in cellular morphology have made it possible to identify different stages of the oligodendrocyte lineage (Pfeiffer et al., 1993).

OPCs are migratory and proliferative cells with a bipolar morphology. Once they are specified, they proliferate in the rat brain from a population of ~5 x 10^5 at birth to ~60x 10^6 cells in the adult and as they proliferate, they migrate throughout the central nervous system to their proper locations (Pfeiffer et al., 1993). The majority of proliferation occurs after they leave the ventricular and subventricular zones (Miller et al., 1997). In the rodent system, many OPCs can be identified via the expression of gangliosides recognized by the A2B5 antibody (Eisenbarth et al., 1979; Raff et al., 1984) and by expression of the α-receptor for platelet-derived growth factor (PDGFαR) (Fig. 1.1) (Hart et al., 1989b; Pringle et al., 1992; Ellison and de Vellis, 1994). The ability of OPCs to proliferate is dependent on extrinsic cues whereby activation of the PDGFαR by PDGF enhances the proliferation and survival of OPCs (Noble et al., 1988; Hart et al., 1989a). Fibroblast growth factor (FGF2) is also mitogenic and upregulates PDGFαR expression in OPCs and blocks their differentiation into oligodendrocytes (Bogler et al., 1990; McKinnon et al., 1990).

The transition from an OPC to a mature differentiated oligodendrocyte is a critical step during development. As oligodendrocytes begin to differentiate, they develop more processes and become multipolar. They can be identified by expressing an unidentified antigen, POA (pro-oligo antigen), on their surface recognized by the O4 monoclonal antibody (Fig. 1.1) (Sommer and Schachner, 1981; Bansal et al., 1992). This is the last stage where the cells have significant proliferative capabilities and the first stage where they become post-migratory (Warrington and Pfeiffer, 1992). Soon after onset of recognition of the O4

antibody with POA, reactivity to the A2B5 antibody disappears as well as proliferative responses to PDGF (Hardy and Reynolds, 1991; Pfeiffer et al., 1993).

Lineage progression then continues to the immature oligodendrocyte stage where the cells are post-migratory, only migrating short distances if needed, and still retain some proliferative capacity. These more mature cells express markers of differentiation such as 2,3 cyclic nucleotide-3-phosphodiesterase (CNP), sulfatide and galactocerebroside (GalC) (Fig. 1.1) (Pfeiffer et al., 1993). CNP is a myelin protein that catalyzes the hydrolysis of 2',3'-cyclic nucleotides to produce 2'-nucleotides (Wells and Sprinkle, 1981; Sprinkle et al., 1983; Kim et al., 1984; Sprinkle, 1989). It is confined to oligodendrocytes in noncompact regions of the myelin sheath (Braun et al., 1988) and has high binding affinity for cytoskeleton proteins and was recently shown to regulate branching and process formation of oligodendrocytes (Lee et al., 2005). Sulfatide and GalC are sphingolipids highly enriched in myelin and are recognized by the O4 and O1 monoclonal antibodies, respectively, on their cell surfaces (Fig. 1.1) (Bansal et al., 1989; Warrington and Pfeiffer, 1992).

Mature oligodendrocytes are postmitotic, terminally differentiating cells that express late myelin proteins such as myelin basic protein (MBP), proteopilid protein (PLP), myelin-associated glycoprotein (MAG) and myelin-oligodendrocyte glycoprotein (MOG) as well as maintain continued expression of sulfatide, GalC and CNP (Fig. 1.1). Expression of genes encoding the more mature proteins is followed by synthesis of myelin-specific lipids and elaboration of the myelin

sheath by oligodendrocytes (Pfeiffer et al., 1993). Myelination is a process that is developmentally regulated as it requires coordination of the above-described lipids and myelin proteins (Campagnoni and Macklin, 1988).

MBPs are a class of myelin proteins expressed by oligodendrocytes in the central nervous system. They are abundant in myelin, representing 30% of total myelin protein, are membrane associated and important for fusion (compaction) of the opposing cytoplasmic membranes of myelin (Omlin et al., 1982; Readhead et al., 1990). In the *shiverer* mutant mouse where a large portion of the *mbp* gene has been deleted, oligodendrocytes begin to myelinate but cannot form compacted myelin in the central nervous system (Readhead et al., 1990).

The *mbp* gene, first identified in the mouse, contains seven exons which, through alternative splicing of exons 2 and 6, account for the four major “classic” MBP variants which have different molecular weights (14kDa, 17kDa, 18.5kDa, and 21.5kDa) (Barbarese et al., 1977; Yu and Campagnoni, 1982; de Ferra et al., 1985; Takahashi et al., 1985). A few years later, a third exon (exon 5), was found to also be differentially spliced out in the processing of the mouse MBP gene transcript creating a second 17kDa isoform (Newman et al., 1987). During this time there was evidence that more molecular forms exist (Greenfield et al., 1982; Sorg et al., 1986) and due to the newer discovery of an unidentified “exon 5a” it is now known that there are at least seven transcripts expressed (Aruga et al., 1991).

The splicing of the classic *mbp* transcripts is developmentally regulated in oligodendrocytes (Campagnoni et al., 1978; Carson et al., 1983; Campagnoni,

1988). Transcripts containing exon 2 (21.5 and 17kDa isoforms) are expressed at high levels early during myelination then decline with development (Barbarese et al., 1978; Campagnoni, 1988) while the more mature isoforms (14 and 18.5kDa) are expressed later and are incorporated into the myelin sheath (Newman et al., 1987; Jordan et al., 1990).

As well as being expressed during developmental myelination, exon 2-containing *mbp* transcripts are also expressed in oligodendrocytes during remyelination as they react to demyelination with widespread *mbp* mRNA synthesis (Kristensson et al., 1986) as seen in lesions of a demyelinating animal model and during remyelination in adult mice after viral depletion of oligodendrocytes (Jordan et al., 1990; Nagasato et al., 1997).

Differing from other myelin protein mRNAs such as *plp* (Trapp et al., 1987), mRNAs for *mbp* have to be transported through oligodendrocyte processes to intracellular regions and translated locally where myelin compaction occurs because their proteins are highly charged and have a strong affinity for membranes (Campagnoni et al., 1980; Colman et al., 1982; Kristensson et al., 1986; Verity and Campagnoni, 1988). The transport of *mbp* mRNA requires a RNA transport signal in the 3' untranslated region and localization of mRNA to the myelin compartment requires an additional element, the RNA localization region (Ainger et al., 1997).

Proteolipid protein (PLP) is a membrane spanning protein that constitutes about 50% of the protein in the myelin sheath. PLP consists of four hydrophobic transmembrane domains on the outer membranes of myelin (Popot et al., 1991;

Nave, 2001) and although it is an abundant protein in myelin, its function has been mainly attributed to axonal survival. Initially, the function of PLP was thought to be directly associated with myelin sheath deficits because of observations in PLP mutant mice. The *jimpy* mutation was the first mutation identified in the *plp* gene and mice harboring this mutation lack the majority of central nervous system-specific myelin due to the absence of mature oligodendrocytes because of cell death. The little myelin that remains has ultrastructural abnormalities as would be expected for an integral myelin protein (Meier and Bischoff, 1974, 1975; Duncan et al., 1989; Skoff, 1995). It was later unexpectedly discovered that *plp*-null mice, in which the *plp* gene is inactivated, display no myelin abnormalities or oligodendrocyte loss, but develop axonal degeneration and so it then was suggested that the observations in the PLP mutant mice were a result from misfolded protein responses (Griffiths et al., 1998a; Griffiths et al., 1998b).

PLP has a splice variant that it is co-expressed with named DM20 which differs by a 35-amino acid deletion in exon 3B of the gene (Agrawal et al., 1972; Trifilieff et al., 1986; Macklin et al., 1987; Nave et al., 1987). The splicing of the PLP/DM20 gene is developmentally regulated and the appearance of DM20 precedes PLP in many species (Yu et al., 1994; Dickinson et al., 1996; Spassky et al., 1998). As development proceeds, expression of DM20 declines as PLP increases (Griffiths et al., 1998a) and during these later stages of development DM20 protein has been identified in compacted myelin (Nave, 2001).

The myelin membrane is also composed of other proteins beside MBP and PLP, such as myelin oligodendrocyte glycoprotein (MOG). MOG is a minor membrane protein composing 0.1% of total protein and is found on the surface of oligodendrocytes. It is the last myelin protein expressed and is a marker for mature oligodendrocytes (Kettenmann and Ransom, 2005). The function of MOG is not yet known but it has been suggested to function in the myelin sheath and not during development (Roth et al., 1995).

.

The oligodendrocyte cytoskeleton

Along with the expression of various lipids and proteins during oligodendrocyte differentiation, cell shape changes also occur and are mediated by the cytoskeleton. The cytoskeleton of oligodendrocytes is composed of microtubules and microfilaments and devoid on intermediate filaments (Wilson and Brophy, 1989).

In less mature, younger oligodendrocytes, microfilaments are much more abundant than microtubules, and are found in many processes emerging from the cell where they mediate process outgrowth resulting in the formation of filapodia and lamellopodia (Wilson and Brophy, 1989). Alternately, microtubules serve as mechanical stability for processes in more mature oligodendrocytes and are present in the cell body and primary processes, not at the distal tips (Lunn et al., 1997; Song et al., 2001; Bauer et al., 2009).

Microtubules are made of subunits of α-tubulin and β-tubulin which assemble as heterodimers and form a hollow cylindrical shape. In order to

promote stability of oligodendrocyte processes as seen in more mature oligodendrocytes, tubulin subunits must undergo posttranslational modifications including acetylation of α-tubulin (Song et al., 2001). Acetylation of α-tubulin is important for maintaining the complex process arborization necessary for proper morphological differentiation. As oligodendrocytes mature, they generate larger processes and membranous structures. These membranous structures are mainly devoid of tubulin but have a few, large acetylated α-tubulin-containing processes that extend throughout the structure (Richter-Landsberg, 2000).

In order for oligodendrocytes to develop in a proper, timely manner they must not only express the correct genetic profile, but it is also crucial that process morphology is regulated correctly. It is still debated whether gene expression is directly linked to cyoskeletal development or if the two processes can be uncoupled, but regardless of the mechanism, it is necessary that both processes function together at the correct time to develop functional myelinating oligodendrocytes.

Oligodendrocytes and remyelination

It is of interest to note that not all OPCs differentiate during development as they are present in the adult CNS. These cells still have proliferative capabilities (Wolswijk and Noble, 1989; Wolswijk et al., 1991) and have been shown to respond to demyelination by increasing in numbers and repopulating the lesion site (Reynolds et al., 2001).

Either due to the presence of these OPCs or from OPCs recruited from the subventricular zone, MS patients have extensive spontaneous remyelination in early phases of the disease, occurring more than previously thought, but eventually remyelination will fail as the disease progresses (Patani et al., 2007).

OPC recruitment and differentiation are both very important for remyelination to occur. Studies in older animals have suggested that even though both processes are not as efficient, failure of differentiation of OPCs and not recruitment may be the reason for limited remyelination (Sim et al., 2002; Woodruff et al., 2004; Shen et al., 2008). In agreement with these studies, it has been reported that MS lesions contain substantial numbers of OPCs with no evidence of remyelination (Wolswijk, 1998; Chang et al., 2000; Chang et al., 2002; Wolswijk, 2002; Kuhlmann et al., 2008). Even though OPCs are present and recruited in MS lesions initially, over time they do become depleted (Kuhlmann et al., 2008) which could be the reason behind progressive stages of MS. In the case where there are large areas of demyelination, OPC recruitment may not be efficient enough to repopulate the whole area and so experimental studies have found that transplanted OPCs could repopulate those areas with much greater efficiency than endogenous OPCs (Chari and Blakemore, 2002).

Limited remyelination in MS lesions suggests that myelination is possible but needs to be stimulated (Armstrong, 2007). One such molecule that can stimulate oligodendrocyte differentiation is the oligodendrocyte-secreted protein autotaxin (ATX) (Fuss et al., 1997; Fox et al., 2003; Dennis et al., 2005; Dennis et al., 2008; Yuelling and Fuss, 2008; Nogaroli et al., 2009). *Atx* expression is

reduced in MS lesions (Comabella and Martin, 2007) and could be a potential target for treatment.

Autotaxin

Autotaxin (ATX), also designated phosphodiesterase Iα/autotaxin (PD-Iα/ATX) or (ecto)nucleotide pyrophosphatase/phosphodiesterase 2 [(E)NPP2], was originally discovered as an autocrine motility stimulating factor released by human melanoma cells (Stracke et al., 1992). This functional property was the foundation for its name autotaxin, which remains the most commonly used designation. cDNA cloning identified a brain-specific alternatively spliced isoform that based on the protein's enzymatic phosphodiesterase activity was designated phosphodiesterase Iα (PD-Iα) (Narita et al., 1994; Kawagoe et al., 1995). Possessing enzymatic activity, ATX was subsequently included in the family of nucleotide pyrophosphatase/phosphodiesterase (NPP)-type ectophosphodiesterases and additionally termed (E)NPP2 (Bollen et al., 2000; Goding et al., 2003; Stefan et al., 2005). To date, at least three splice variants/isoforms of ATX have been identified in both human and mouse, and they have been recently referred to as autotaxin α, β and γ, with autotaxin γ being identical to PD-Iα (Murata et al., 1994; Lee et al., 1996b; Kawagoe et al., 1997; Giganti et al., 2008). The known isoforms of ATX display characteristic expression patterns but do not appear to exert major differences in the substrate specificity of the enzymatically active site, and to our knowledge, no major

functional isoform differences have been identified so far (Lee et al., 1996b; Fuss et al., 1997; Giganti et al., 2008).

ATX has been found to be released by a large variety of tumor cells and to be expressed within a number of different tissues during normal development and in the adult (Narita et al., 1994; Kawagoe et al., 1995; Lee et al., 1996b; Fuss et al., 1997; Bachner et al., 1999; Ohuchi et al., 2007; Savaskan et al., 2007; Giganti et al., 2008). Furthermore, high protein levels of ATX have been observed in biological fluids, i.e. plasma and cerebrospinal fluid (CSF) (Tokumura et al., 2002; Umezu-Goto et al., 2002; Sato et al., 2005). Despite this rather broad expression pattern, a major focus in the research related to ATX has long remained in tumor cell biology.

More recently, ATX has gained new attention since it was discovered to act as the major extracellular enzyme generating the bioactive lipid signaling molecule lysophosphatidic acid (LPA) , i.e. as an extracellular lysophospholipase D (lysoPLD) (Tanaka et al., 2006; van Meeteren et al., 2006). In addition, current studies investigating ATX's role during CNS development uncovered a novel functionally active site and thus highlighted a multi-functional and multi-modular nature of ATX (Fox et al., 2003; Fox et al., 2004; Dennis et al., 2005; Dennis et al., 2008).

The first mentioning of ATX in the literature dates to the early 1990s, when it was discovered as part of a search for active cellular motility stimulating factors involved in tumor cell invasion (Stracke et al., 1992; Stracke et al., 1993). Isolation of a cDNA encoding this 125 kDa glycoprotein and subsequent

sequencing revealed that ATX did not exhibit any significant homologies to previously characterized motility and growth factors. However, ATX was found to contain a domain that displayed high homology with the enzymatically active domain of proteins known to possess nucleotide phosphodiesterase and pyrophosphatase activity, in particular bovine intestinal 5′ nucleotide phosphodiesterase and plasma cell glycoprotein-1 (PC-1) (Culp et al., 1985; van Driel and Goding, 1987; Buckley et al., 1990; Murata et al., 1994). Furthermore, it was found that the homology between ATX and PC-1 was not restricted to the enzymatically active site but extended through the entire length of their extracellular portions. Thus, both proteins shared additional properties and domains, namely two adjacent somatomedin B-like domains, a nuclease-like domain and a single EF hand-like motif (Fig. 1.2). Due to the homology to PC-1, ATX's N-terminus was originally thought to represent a transmembrane region thus rendering ATX a type II transmembrane protein. However, it is now clear that ATX is synthesized as a pre-pro-enzyme and secreted upon removal of the N-terminal signal peptide and further trimming by a furin-type protease (Jansen et al., 2005; van Meeteren et al., 2005; Koike et al., 2006; Pradere et al., 2007). In the years following ATX's first cDNA isolation and sequencing, proteins with similar structure–function domains were identified, leading to the creation of a novel protein family, namely the (E)NPP family, which currently consists of seven known members (Goding et al., 1998; Zimmermann, 1999; Bollen et al., 2000; Goding et al., 2003; Stefan et al., 2005).

Shortly after ATX's sequence had been identified, Lee et al.(Lee et al., 1996) by using mutant recombinant forms of ATX, discovered that the catalytic domain is crucial for motility stimulation. This finding prompted a more detailed characterization of the catalytic activity of ATX and its relationship to the catalytic activities of the other (E)NPP family members. Early studies showed that all (E)NPPs hydrolyze both pyrophosphate and phosphodiester bonds present in nucleotides and their derivatives (Bollen et al., 2000). However, their actual physiological substrates still remained unidentified. It was later found out that even though (E)NPPs have a structurally related catalytic domain, they differ in their enzymatic substrate specificities (Gijsbers et al., 2001; Cimpean et al., 2004; Stefan et al., 2005).

With regard to ATX, an important clue for its most likely physiological substrate came from research related to the lipid signaling molecule LPA. The discovery of an extracellular enzyme catalyzing the conversion from LPC to LPA, i.e. an extracellular lysoPLD, revealed that ATX is molecularly identical to this extracellular lysoPLD (Tokumura et al., 2002; Umezu-Goto et al., 2002; Ferry et al., 2003; Xie and Meier, 2004). Moreover, ATX's affinity for LPC was found to be significantly higher than its affinity for nucleotides (Tokumura et al., 2002; Umezu-Goto et al., 2002). This finding that ATX may exert various biological effects through its lysoPLD activity clearly marked a turning point in research related to ATX (Moolenaar, 2002).

ATX: enzymatic activity via the catalytic lysoPLD active site

Once the molecular identity of ATX as a lysoPLD had been identified, the characterization of ATX's enzymatic activities was revisited. ATX's NPP activity had long been known to be dependent on a single threonine residue located within the catalytic domain (Clair et al., 1997). Mutational analyses showed that the same residue is critical for ATX's lysoPLD activity and that lysoPLD activity shares a common reaction mechanism with the originally described 5′-nucleotide phosphodiesterase activity (Gijsbers et al., 2003; Koh et al., 2003). However, the lysoPLD activity appears unique to ATX within the (E)NPP protein family, and it seems to require in addition to the critical threonine residue, sequences within the N- and C-terminal domains of ATX (Gijsbers et al., 2003; Cimpean et al., 2004; Stefan et al., 2005). It was then proposed that the substrate specificity of ATX's lysoPLD activity extends to the phosphosphingolipid sphingosine phosphorylcholine (SPC), thus suggesting that ATX not only generates LPA but also sphingosine 1-phosphate (S1P) (Clair et al., 2003). While this ability of ATX has been well demonstrated *in vitro*, its physiological relevance still needs to be demonstrated (van Meeteren and Moolenaar, 2007). ATX's lysoPLD products, LPA and S1P, inhibit enzymatic activity at biologically relevant concentrations (van Meeteren et al., 2005). This was discovered after the observations that plasma ATX is constitutively active, LPC is abundant in plasma and serum, yet LPA levels are low (Croset et al., 2000); (Eichholtz et al., 1993; Baker et al., 2002; Sano et al., 2002). On the other hand, positive regulatory mechanisms

likely also exist since serum LPA levels gradually increase following platelet activation(van Meeteren and Moolenaar, 2007).

Physiological actions of LPA are mediated through the binding and activation of specific plasma membrane receptors belonging to the superfamily of G protein-coupled receptors (GPCRs) (Moolenaar, 1995, 1999; Chun et al., 2002; Takuwa et al., 2002; Anliker and Chun, 2004; Fukushima, 2004; Valentine et al., 2008). To date, there are six known LPA receptors. The three originally identified receptors belong to the endothelial differentiation gene (Edg) family: LPA1/Edg-2/vzg-1, LPA2/Edg-4 and LPA3/Edg-7 (Hecht et al., 1996; An et al., 1998; Bandoh et al., 1999). More recently identified receptors are only distantly related to the Edg family of receptors (20–24% sequence homology) and are more closely related to the purinergic family of receptors: GPR23/P2Y9 (LPA4), GPR92 (LPA5), P2Y5 (LPA6) GPR87(Noguchi et al., 2003; Kotarsky et al., 2006; Lee et al., 2006a; Tabata et al., 2007; Yanagida et al., 2009). Further complexity to the mechanism of LPA signaling is contributed by the discovery that PPARγ can function as an intracellular LPA receptor (McIntyre et al., 2003).

Biochemical pathways other than the conversion of LPC via lysoPLD activity have been identified to lead to the generation of LPA (Pages et al., 2001; Aoki et al., 2002; Xie and Meier, 2004). Thus, biological actions of LPA are not restricted to those described here involving ATX.

ATX and disease

ATX's enzymatic lysoPLD activity has been implicated in a large variety of biological processes during normal development and under pathological conditions (Goding et al., 2003). Developmental roles include adipogenesis, intestinal cell motility and neurite morphology (Sato et al., 2005; Simon et al., 2005; Khurana et al., 2008), while a contribution to disease has been described for Alzheimer's disease, chronic Hepatitis C, Multiple Sclerosis, neuropathic pain, obesity and rheumatoid arthritis (Santos et al., 1996; Ferry et al., 2003; Hammack et al., 2004; Boucher et al., 2005; Watanabe et al., 2007b; Watanabe et al., 2007a; Inoue et al., 2008a; Inoue et al., 2008b; Zhao et al., 2008). The functional importance of ATX's lysoPLD active site has, however, been investigated most intensively during tumor progression and vascular development.

Since its first description as a tumor cell motility stimulating factor for human melanoma cells, ATX has been found expressed by a large variety of tumor cells (Kawagoe et al., 1997; Yang et al., 1999; Zhang et al., 1999; Stassar et al., 2001; Yang et al., 2002; Kehlen et al., 2004; Hoelzinger et al., 2005; Kishi et al., 2006; Zhao et al., 2007). ATX promotes tumor cell penetration, metastatic capability, tumor aggressiveness as well as tumor cell motility (Stracke et al., 1992; Stracke et al., 1993; Kawagoe et al., 1997; Yang et al., 2002; Kishi et al., 2006; Hoelzinger et al., 2008). In the search for the molecular mechanism responsible for the tumor cell motility stimulating effect of ATX, a link with its enzymatic activity and the involvement of G-protein-coupled receptors was found

(Stracke et al., 1992; Lee et al., 1996a; Lee et al., 2002). However, it took the identification of ATX as a lysoPLD to unravel that the above effects are mediated, at least in part, via the conversion of LPC to LPA and via binding of LPA to one of its high affinity receptors (Tokumura et al., 2002; Umezu-Goto et al., 2002; Koh et al., 2003; Hama et al., 2004; Kishi et al., 2006; van Meeteren and Moolenaar, 2007; Hoelzinger et al., 2008).

The role of ATX in vascular development was revealed through the generation of ATX null mice (Tanaka et al., 2006; van Meeteren et al., 2006). ATX-deficient mice were found to die at midgestation (E9.5–E11.5) and to harbor severe vascular defects that were in particular noticeable in the yolk sac. Endothelial, smooth muscle and blood cell differentiation was not significantly impaired however, newly formed blood vessels failed to develop into mature vessels and this may be solely due to ATX's lysoPLD active site. Notably, in a mouse line expressing only a lysoPLD inactivated ATX gene product, embryonic lethality was observed to be similar to the one seen in the complete absence of ATX (Ferry et al., 2007).

ATX: matricellular properties via the MORFO domain

Studies in our laboratory characterized ATX, which we referred to as PD-Iα/ATX, as an extracellular factor involved in the differentiation of oligodendrocytes (Fox et al., 2003; Fox et al., 2004; Dennis et al., 2005; Dennis et al., 2008). Most interestingly, these studies revealed a novel functionally active domain, the MORFO domain, that 1) is located at the C-terminal end of the

protein, 2) entails a nuclease-like domain not thought to be catalytically active and 3) functions independently of ATX's enzymatic activity (see Fig. and (Gijsbers et al., 2001; Fox et al., 2003; Fox et al., 2004; Dennis et al., 2005; Stefan et al., 2005; Dennis et al., 2008). Early studies uncovered that the MORFO domain antagonizes adhesion of oligodendrocytes to naturally occurring extracellular matrix (ECM) molecules such as fibronectin in an active and pertussis toxin-sensitive fashion (Fox et al., 2003). This finding classifies ATX as a matricellular protein, i.e. a protein that mediates an intermediate adhesive state, and it suggests a supportive role of ATX, via its MORFO domain, on cellular remodeling (Murphy-Ullrich, 2001).

In agreement with the above, recent data have demonstrated that ATX's MORFO domain facilitates morphological maturation of post-migratory, premyelinating oligodendrocytes (Dennis et al., 2008). Post-migratory, premyelinating oligodendrocytes mature from cells that extend a few processes to cells that generate a highly complex process network, and it is this transition that is facilitated by ATX's MORFO domain (Dennis et al., 2008). The role of ATX in process outgrowth was found to be mediated in part via the EF hand-like motif located at the far C-terminal end of the MORFO domain.

LPA-mediated oligodendrocyte effects

The role of ATX on oligodendrocytes has only been investigated by our own laboratory but several other groups have studied LPA’s function in

oligodendrocytes (Weiner et al., 1998; Moller et al., 1999; Stankoff et al., 2002; Dawson et al., 2003; Yu et al., 2004).

Oligodendrocytes express LPA receptors and LPA has been shown to exert a variety of effects on them (Allard et al., 1998; Weiner et al., 1998; Moller et al., 1999; Handford et al., 2001; Stankoff et al., 2002; Dawson et al., 2003; Yu et al., 2004; Nogaroli et al., 2009). LPA1 was the first LPA receptor found and its expression correlates with neurogenesis during embryonic development and myelination postnatally (Allard et al., 1998). Postnatally, LPA1 is expressed in developing white matter tracks and co-expressed with the myelin proteins PLP and MBP (Weiner et al., 1998; Cervera et al., 2002). Other investigators have also reported expression of LPA1 in OPCs and oligodendrocytes (Handford et al., 2001; Stankoff et al., 2002; Dawson et al., 2003; Yu et al., 2004; Matsushita et al., 2005; Nogaroli et al., 2009), as well as LPA2 and LPA3 (Yu et al., 2004; Matsushita et al., 2005; Nogaroli et al., 2009) and its expression in OPCs increases as they differentiate (Dawson et al., 2003; Matsushita et al., 2005). Oligodendrocytes also express LPA2 and LPA3 but at a much lower level than LPA1 (Yu et al., 2004; Matsushita et al., 2005; Nogaroli et al., 2009). Along with receptor expression, the highest tissue concentration of LPA has been found in the brain (Das and Hajra, 1989) and so effects of LPA in the central nervous system have been investigated.

In cultured oligodendrocytes, LPA modulates calcium signals and activation of ERK1/2 (Moller et al., 1999; Stankoff et al., 2002; Yu et al., 2004). LPA also exerts cytoskeletal effects such as process retraction and inhibition of

process formation in OPCs but not in differentiated oligodendrocytes suggesting different roles for LPA in oligodendrocyte development and differentiation (Stankoff et al., 2002; Dawson et al., 2003). LPA stimulates astrocyte proliferation (Shano et al., 2008), promotes survival in Schwann cells and in an oligodendrocyte cell line but not in primary oligodendrocytes (Weiner and Chun, 1999; Stankoff et al., 2002; Li et al., 2003; Matsushita et al., 2005). Interestingly *jimpy* mice, which have a mutation in the PLP gene and increased oligodendrocyte apoptosis, exhibit lower expression levels of the LPA1 receptor (Weiner et al., 1998). These findings indicate that LPA responses can vary not only by cell type but also by developmental stage (at least in oligodendrocytes).

Due to the limited number of studies involving ATX and LPA function in oligodendrocytes and the observation that ATX's MORFO domain is important for oligodendrocyte differentiation, the next question was whether ATX's lysoPLD active site may also be involved in the regulation of oligodendrocyte differentiation. LPA has already been shown to promote differentiation in Schwann cells, cortical neuroblasts and in an oligodendrocyte cell line (Li et al., 2003; Matsushita et al., 2005; Fukushima et al., 2007). The findings in chapter two demonstrate that LPA, produced from ATX's lysoPLD domain, are important for differentiation of oligodendrocytes *in vitro* (Nogaroli et al., 2009).

Figure 1.1. **The oligodendrocyte lineage.** This figure depicts both the changes in morphology and gene expression that oligodendrocytes undergo as they differentiate. OPCs are generated in restricted regions of the central nervous system where they migrate from and proliferate extensively, populating the brain and spinal cord. Once they have reached their destination, they begin to develop a complex process network and eventually form membranous structures which wrap around axons *in vivo*. As changes are observed morphologically, oligodendrocytes also undergo changes in gene expression as shown underneath the pictures. The markers listed are used to identify different stages of the oligodendrocyte lineage: ganglioside (A2B5), platelet-derived growth factor receptor (PDGFαR), pro-oligodendrocyte surface antigen or sulfatide (O4), galactocerebroside (O1), 2,3-cyclic nucleotide 3-phosphodiesterase (CNP), myelin basic protein (MBP), proteolipid protein (PLP), myelin oligodendrocyte glycoprotein (MOG).

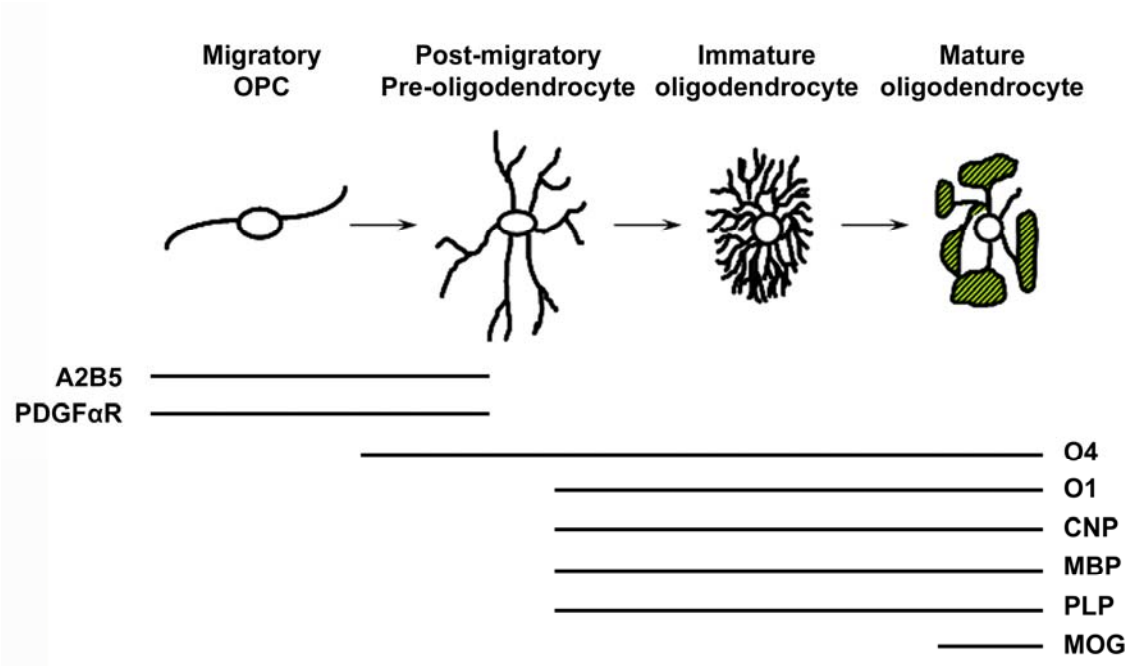
Migratory
OPC
Post-migratory
Pre-oligodendrocyte
Immature
oligodendrocyte
Mature
oligodendrocyte
A2B5
PDGFαR
O4
O1
CNP
MBP
PLP
MOG

Figure 1.2. **Scheme of the structure–function domains of ATX**. The N-terminal hydrophobic sequence of ATX is a signal peptide, thus resulting in the secretion of the protein. Two somatomedin B-like domains are located at the N-terminal end of the protein. So far, no functional properties have been assigned to these domains. The catalytic domain of ATX functions as lysoPLD thus generating LPA, which exerts its effects through binding to G-protein-coupled receptors (LPA1-5). Catalytic activity is dependent on the catalytic site residue T^{210}. At the C-terminal end, the *M*odulator of *O*ligodendrocyte *R*emodeling and *F*ocal adhesion *O*rganization (MORFO) domain entails the nuclease-like domain, which is probably enzymatically inactive. The functional properties of the MORFO domain are thought to be mediated via binding to a yet-to-be-identified cell surface receptor. The EF hand-like motif located at the far C-terminal end of the protein was found to contribute to the function of the MORFO domain. The most intensively characterized biological systems (Systems) and cellular molecular mechanisms (Mechanisms) for each of the functionally active sites of ATX are listed. Individual structure–function domains are depicted according to the gray scale scheme shown at the bottom.

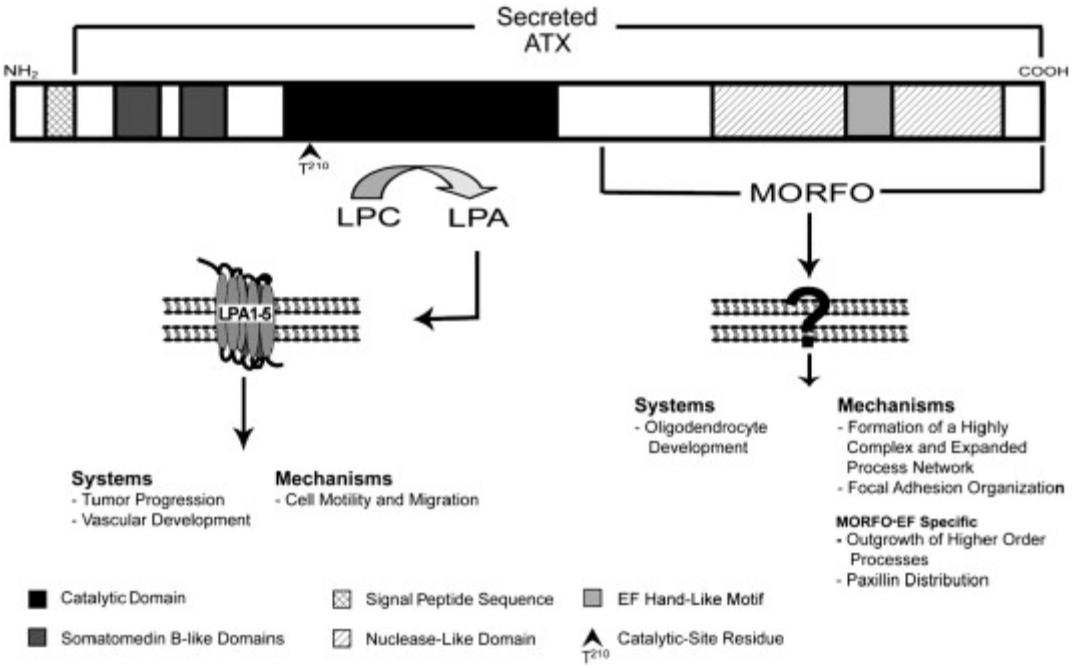
Secreted
ATX
NH2
COOH
T210
LPC
LPA
MORFO
LPA1-5
?
Systems
- Tumor Progression
- Vascular Development
Mechanisms
- Cell Motility and Migration
Systems
- Oligodendrocyte Development
Mechanisms
- Formation of a Highly Complex and Expanded Process Network
- Focal Adhesion Organization
MORFO-EF Specific
- Outgrowth of Higher Order Processes
- Paxillin Distribution
Catalytic Domain
Somatomedin B-like Domains
Signal Peptide Sequence
Nuclease-Like Domain
EF Hand-Like Motif
Catalytic-Site Residue
T210

CHAPTER 2

Lysophosphatidic acid can support the formation of membranous structures and an increase in MBP mRNA levels in differentiating oligodendrocytes

(*This chapter was accepted as a paper in Neurochemical Research in June of 2008. The work reported for this manuscript was performed with assistance from Dr. Luciana Nogaroli, Dr. Jameel Dennis and Karen Gorse. My own efforts on this paper include the MBP studies, LPA receptor mRNA expression and ATX enzymatic activity assay. The results are displayed in figures 2.1B and C, 2.2, 2.5A and B, 2.6A and B.)*

Introduction

Oligodendrocytes are the myelin-forming cells of the central nervous system (CNS). During development, they originate from progenitor cells that are generated in discrete areas of the CNS and migrate to their final destination to differentiate in a cell autonomous fashion into post-migratory, premyelinating oligodendrocytes (Miller, 2002; Richardson et al., 2006). At the prospective sites of myelination such post-migratory, premyelinating oligodendrocytes undergo distinct stages of maturation, which are defined by changes in morphology and gene expression pattern (see Fig.2.1A and (Kachar et al., 1986; Knapp et al., 1987; Pfeiffer et al., 1993; Hardy and Friedrich, 1996; Dugas et al., 2006)). In particular, cells first survey the environment for axonal segments to be myelinated by extending a large and complex network of fine processes. This step of extensive process outgrowth is followed by the transformation of cellular protrusions into membranous structures ultimately forming the myelin sheath and by the expression of proteins involved in the regulation of myelination such as myelin basic protein (MBP) and myelin oligodendrocyte glycoprotein. Despite the

well described characterization of these maturation stages, however, little is known about the signals that regulate their well coordinated progression (Baumann and Pham-Dinh, 2001).

One of the extracellular factors long suspected to play a critical role during the later stages of oligodendrocyte maturation is the lipid signaling molecule lysophosphatidic acid (LPA). Extracellular LPA exerts its physiological functions by activating specific G protein-coupled receptors (GPCRs; for review see:(Birgbauer and Chun, 2006; Meyer zu Heringdorf and Jakobs, 2007; Choi et al., 2008)). GPCRs of the endothelial differentiation gene family were the first to be recognized as LPA receptors, and they are designated LPA1 (Edg-2), LPA2 (Edg-4) and LPA3 (Edg-7). In addition to these classical LPA receptors three GPCRs of the purinergic family, GPR23/LPA4, GPR92/LPA5 and GPR87, have been recently identified to also mediate signaling via LPA (Noguchi et al., 2003; Lee et al., 2006; Tabata et al., 2007; Valentine et al., 2008). Out of the above, LPA1 and LPA3 have been described to be expressed by differentiating oligodendrocytes (Allard et al., 1998; Weiner et al., 1998; Allard et al., 1999; Handford et al., 2001; Yu et al., 2004). The *in vivo* expression pattern of LPA1 was found to coincide with myelination, and it was this observation that prompted a number of investigations into the role of LPA for oligodendrocyte differentiation and function (Moller et al., 1999; Cervera et al., 2002; Stankoff et al., 2002; Dawson et al., 2003). Somewhat disappointingly, no significant effects on morphology and/or gene expression were identified in these studies.

Differentiating oligodendrocytes express not only the receptors for extracellular LPA, but also the major enzyme responsible for the production of extracellular LPA, namely the lysophospholipaseD (lysoPLD) phosphodiesterase-Iα/autotaxin (PD-Iα/ATX) (Narita et al., 1994; Fuss et al., 1997; Tanaka et al., 2006; van Meeteren et al., 2006; Yuelling and Fuss, 2008). Our previous studies identified PD-Iα/ATX as an extracellular factor that is released by differentiating oligodendrocytes during the initial stages of myelination and that stimulates the establishment of a complex process network independently of its lysoPLD activity via a second functionally active domain, i.e. the modulator of oligodendrocyte remodeling and focal adhesion organization (MORFO) domain (Fox et al., 2003; Fox et al., 2004; Dennis et al., 2008). In addition, however, it is reasonable to assume that the presence of PD-Iα/ATX in the extracellular environment of differentiating oligodendrocytes results in the extracellular production of LPA and in the stimulation of LPA-mediated effects. Thus, the limited responses observed so far when adding LPA exogenously to differentiating oligodendrocytes may at least be in part due to PD-Iα/ATX precluding or masking the physiological effects of LPA.

In the present study we have, therefore, revisited the role of LPA on differentiating oligodendrocytes, and we have assessed its effects under conditions where the expression of PD-Iα/ATX was down-regulated. Under these conditions, exogenous application of LPA was found to support the formation of membranous structures and to stimulate an increase in mRNA levels coding for

MBP but not MOG. Taken together, these findings demonstrate that LPA can stimulate the later maturation steps of differentiating oligodendrocytes.

Experimental Procedures

Materials

Antibodies: Hybridoma clone A2B5 (ATCC, Manassas, VA), hybridoma clone O4 (gift from S.E. Pfeiffer (Sommer and Schachner, 1982; Bansal et al., 1989)), anti-LPA1 (Edg-2) antibodies (Abcam Inc., Cambridge, MA), anti-LPA2 (Edg-4) and anti-LPA3 (Edg-7) antibodies (Santa Cruz Biotechnology Inc., Santa Cruz, CA), anti-acetylated α-tubulin antibodies (Zymed Laboratories Inc., South San Francisco, CA), anti-MBP antibodies (Covance Berkeley, CA), secondary Alexa 488- and Alexa 594-conjugated antibodies (Invitrogen/Molecular Probes, Carlsbad, CA), secondary horseradish peroxidase (HRP)-conjugated antibodies (Vector Laboratories, Burlingame, CA). The tyramide signal amplification (TSA) Plus Cyanine 3 system was from Perkin Elmer (Waltham, MA). SMARTpool siRNA directed against rat PD-Iα/ATX and control non-targeting SMARTpool siRNA were obtained from Dharmacon Inc. (Lafayette, CO). Tissue culture and transfection reagents were from Invitrogen (Carlsbad, CA) unless stated otherwise. LPA (18:1-1-oleoyl-2-hydroxy-*sn*-glycero-3-phosphate) was purchased from Avanti Polar Lipids Inc. (Alabaster, AL) as a 54.5 mM stock solution prepared in chloroform. Oligonucleotide primers for PCR analysis were from MWG-BIOTECH Inc (High Point, NC). RNA purification and RT kits were obtained from Qiagen (Valencia, CA). The SYBR Green PCR mix was from

BioRad (Hercules, CA). All other reagents and supplies were from Fisher Scientific (Atlanta, GA) unless noted otherwise.

Animals

Sprague–Dawley female rats with early postnatal litters were obtained from Zivic Miller (Pittsburg, PA) and Harlan (Indianapolis, IN). All animal studies were approved by the Institutional Animal Care and Use Committee at Virginia Commonwealth University.

Cell Culture, siRNA and LPA Treatment

Primary cultures of differentiating oligodendrocytes were prepared from brains of postnatal day 4–5 rat pups as described previously (Barres et al., 1992; Fox et al., 2003). Briefly, cerebral hemispheres were dissected out and single cell suspensions were prepared by incubation in Hank's Balanced Salt Solution supplemented with 0.25% trypsin/1 μg/ml DNase (Sigma, St Louis, MO) and subsequent trituration. Differentiating oligodendrocytes where then isolated by O4 immunopanning. Isolated cells were placed on fibronectin (10 μg/ml)-coated coverslips and cultured in serum-free defined medium [Dulbeccos's Modified Eagle's Medium (DMEM) containing 40 ng/ml tri-iodo-thyronine (T3; Sigma, St Louis, MO) and 1× N2 supplement (DMEM/T3/N2)]. After 2 days in culture, cells were transfected with siRNA as described previously (Dennis et al., 2008). siPD-Iα/ATX- and siControl-treated cells were analyzed after an additional 48 h in culture. Knock-down of PD-Iα/ATX was assessed by real-time qRT-PCR. When

cells were treated with exogenous LPA, it was done for 2 h at a concentration of 1 μM (diluted in DMEM/N2). Immediately before use, the required aliquot of the LPA stock solution was dried down under sterile conditions, and the lipid film was resuspended by sonication in 0.4% fatty acid-free BSA (Sigma-Aldrich, St. Louis, MO) dissolved in tissue culture medium.

PD-Iα/ATX-lysoPLD Activity Assay

PD-Iα/ATX's lysoPLD activity was determined using the fluorogenic assay described by Ferguson et al. (Ferguson et al., 2006). Cell culture supernatants were incubated with 2.5 μM FS-3 substrate (Echelon Biosciences Inc., Salt Lake City, UT) in 140 mM NaCl, 5 mM KCl, 1 mM $CaCl_2$, 1 mM $MgCl_2$, 5 mM Tris/HCl (pH 8.0), 1 mg/ml fatty acid-free BSA (Sigma-Aldrich, St. Louis, MO) for 5.0 h at 37°C. Increase in fluorescence with time was measured at an excitation wavelength of 485 nm and an emission wavelength of 520 nm using a PHERAstar multimode microplate reader (BMG LABTECH Inc. Durham, NC).

Immunocytochemistry

For immunocytochemical detection of the O4 antigen as a marker for differentiating oligodendrocytes in combination with one of the three classical LPA receptors, cells were fixed in 4% paraformaldehyde dissolved in Phosphate Buffered Saline (PBS). Unspecific binding sites were blocked using DMEM/10% Fetal Calf Serum (FCS) and cells were incubated overnight at 4°C with O4 hybridoma supernatants (1:1 diluted in DMEM/10% FCS). Bound O4 antibodies

were detected using Alexa 488-conjugated secondary antibodies (1:250 diluted in PBS). Cells were then fixed again and incubated for 30 min in blocking/permeabilization solution (PBS containing 5% normal goat serum, 2% non fat dry milk and 0.05% Tween-20). Primary antibodies to each of the classical LPA receptors were applied at a concentration of 1:100 (in PBS containing 1% normal goat serum, 0.05% Tween-20) overnight at 4°C. Bound primary antibodies were detected using the TSA Plus Cyanine 3 system. The primary antibodies to the three classical LPA receptors used here have been employed successfully by others (e.g. (Horak et al., 2007; Park et al., 2007)). When tested for specificity by us using Western blot analysis of whole brain lysates, all three antibodies were found to react with a single band of approximately 40 kDa, which is consistent with the size of the receptor monomers (data not shown). Furthermore, all antibodies detected an additional band of approximately 80 kDa, likely representing previously described LPA receptor homo- and/or heterodimers (Zaslavsky et al., 2006).

For immunocytochemical detection of MBP, cells were fixed in 4% paraformaldehyde dissolved in PBS and permeabilized using 0.5% triton/0.4 M sucrose in PBS. Subsequently, cells were incubated for 30 min in DMEM/10% FCS and then overnight with anti-MBP antibodies (1:250 diluted in DMEM/10% FCS). Bound primary antibodies were detected using Alexa 488-conjugated secondary antibodies (1:250 diluted in PBS) and nuclei were stained using Hoechst (1 µg/ml; Calbiochem, San Diego, CA).

For immunocytochemical detection of the O4 antigen in combination with acetylated α-tubulin the treatment for O4 immunostaining was as described above. Bound O4 antibodies were detected using Alexa 594-conjugated secondary antibodies (1:250 diluted in PBS). Cells were then fixed again and permeabilized using 0.5% TRITO-X100 in PBS. Following permeabilization cells were incubated in DMEM/10% FCS and then overnight with anti-acetylated α-tubulin antibodies. Bound antibodies were detected using Alexa 488-conjugated secondary antibodies (1:250 diluted in PBS).

Cells were analyzed using an Olympus BX51 inverted fluorescent microscope (Olympus America Inc., Center Valley, PA) or a confocal laser scanning microscope (TCS SP2 AOBS, Leica Microsystems, Exton, PA or LSM 510 META, Carl Zeiss MicroImaging, Inc., Thornwood, NY).

Real-Time qRT-PCR Analysis

Total RNA was isolated from oligodendrocyte cultures using the RNeasy Micro Kit. Purified RNA samples were quantified by fiber optic spectrophotometry using the Nanodrop ND-1000 (Nanodrop Inc., Wilmington, DE) and their quality was assessed using Experion RNA HighSens Chips (BioRad, Hercules, CA). For real-time qRT-PCR, oligo(dT)-primed cDNAs were synthesized using the Sensiscript or Omniscript RT kit. PCR was performed on a Chromo 4 Four-Color Real-Time System (BioRad, Hercules, CA) using the iQ SYBR Green Supermix. The following primer pairs were used at the indicated annealing temperatures: PD-Iα/ATX: forward (5′-GACCCTAAAACCATTATTGCTAA-3′), reverse (5′-

GGGAAGGTGCTGTTTCATGT-3′), 60°C; MBP (exon 2 containing isoforms) forward (5′-ACTTGGCCACAGCAAGTACCATGGACC-3′), reverse (5′-TTGTACATGTGGCACAGCCCGGGAC-3′), 60°C; MOG: forward (5′-CTCATTGCCCTTGTGCCTAT-3′), reverse (5′-GCACGGAGTTTTCCTCTCAG-3′), 60°C; LPA1 (Edg-2): forward (5′-GACACCATGATGAGCCTTCTGA-3′), reverse (5′-CCCGGAGTCCAGCAGACA-3′), 65°C; LPA2 (Edg-4): forward (5′-CGCTCAGCCTAGTCAAGACA-3′), reverse (5′-TTGCAGGATTTACAGTCCAGAC-3′), 65°C; LPA3 (Edg-7): forward (5′-CACACGAGTGGCTCCATCAG-3′), reverse (5′-GGTCCAGCACACCACGAA-3′), 65°C. For normalization, amplification of 18S rRNA was performed: forward (5′-TTCGGAACTGAGGCCATGAT-3′), reverse (5′-TTTCGCTCTGGTCCGTCTTG-3′), 60 or 65°C. PCR conditions were as follows: 95°C for 15 min followed by 34 cycles at 94°C for 15 s, annealing temperature for 20 s, and 72°C for 20 s. For quantification of relative LPA receptor mRNA levels, the method described by Peirson et al. (Peirson et al., 2003) was used. For relative comparison of MBP and MOG mRNA levels in the presence of siPD-Iα/ATX or siControl, the ΔΔCT method was used (Livak and Schmittgen, 2001).

Oligodendrocyte Morphology Analysis

For morphology analysis, cells were immunostained using the O4 antibody and an anti-acetylated α-tubulin antibody. Images of approximately 40 cells were taken randomly for each treatment group in each experiment using an Olympus BX51 inverted fluorescent microscope (Olympus America Inc., Center Valley,

PA). IP Lab imaging software (BD Biosciences Bioimaging, Rockville, MD) was used to determine process index (total amount of O4-positive process surfaces per cell minus the cell body), network area (total area within the radius of the process network surrounding the cell body minus the cell body) and complexity index (1 minus process index divided by network area) as previously described (Dennis et al., 2008). In addition, a membrane index was defined as follows: [(O4 network area minus acetyl-tubulin network area) divided by the O4 network area]. A 1:1 correlation of network area to microtubule area yields values approaching 0, while a membranous network area considerably larger than the microtubule network area produces a membrane index approaching 1.

Cell Count Analysis (MBP-Positive Cells)

Composite images of MBP-positive cells were collected by tile scan using a Leica TCS SP2 AOBS confocal microscope (Leica Microsystems, Exton, PA). The total number of detectable nuclei and MBP-positive oligodendrocytes was determined using the particle count plugin (Wright Cell Imaging Facility) to the ImageJ software package (Abramoff et al., 2004) and the following parameters: nuclei (threshold size: 0–10, circularity: 0–1.0); MBP (threshold size: 0.5–5.0, circularity: 0–1.0).

Results

Differentiating Oligodendrocytes Express Enzymatically Active PD-Iα/ATX and all Three Classical LPA Receptors

Prior to analyzing the role of LPA on differentiating oligodendrocytes, studies were undertaken to confirm the enzymatic activity of secreted PD-Iα/ATX and the expression of LPA receptors in the culture system to be used. Differentiating oligodendrocytes were isolated from brains of 4 to 5 day-old rats by O4 immunopanning and allowed to mature for 4 days in vitro. The antigenic marker O4 has been previously demonstrated to be present on the membrane surface of oligodendrocytes that are considered post-migratory, premyelinating cells (Sommer and Schachner, 1981, 1982; Bansal et al., 1989; Warrington et al., 1992). In addition, such O4-positive oligodendrocytes release endogenous PD-Iα/ATX and start to express MBP and MOG (Fig. 2.1A and (Pfeiffer et al., 1993; Solly et al., 1996; Fox et al., 2003)). To determine lysoPLD activity of the secreted PD-Iα/ATX, cell culture supernatants were tested using a fluorogenic assay in which enzymatic activity is measured in a concentration and time dependent manner via an increase in fluorescence (Fig. 2.2 and (Ferguson et al., 2006)). Using this assay, cell culture supernatants of differentiating oligodendrocytes were found to contain significant amounts of enzymatically active PD-Iα/ATX (see Fig. 2.1B). This finding is in agreement with our previous data demonstrating an increase in PD-Iα/ATX expression levels during the initial stages of myelination (Fox et al., 2003). In contrast, oligodendrocyte progenitor cells were found to be negative for PD-Iα/ATX mRNA, and only low levels of PD-Iα/ATX mRNA were detected in oligodendrocytes present in the adult CNS (unpublished observations and (Fuss et al., 1997)).

To assess LPA receptor expression, RNA was isolated from differentiating oligodendrocyte cultures and analyzed using real-time qRT-PCR. Amplification products for all three classical LPA receptors were noted. Quantification of the mRNA expression levels revealed highest expression of LPA1 followed by LPA3 and LPA2 (Fig. 2.1C). The data related to LPA1 and LPA3 expression are consistent with previous findings (Stankoff et al., 2002; Yu et al., 2004). Expression of LPA2, however, may have been overlooked so far due to its very low expression levels. To further confirm the expression of the three classical LPA receptors by differentiating oligodendrocytes, we took advantage of the availability of specific antibodies. As shown in Fig. 2.1D all three receptors were detected in O4-positive cells of both simple and complex process morphology. In addition, a punctate distribution was noted that may be indicative of receptor localization to intracellular vesicles. Taken together, the above data confirm and extend the finding that differentiating oligodendrocytes secrete enzymatically active PD-Iα/ATX and express receptors known to mediate signaling by extracellular LPA.

Extracellular LPA can Support an Increase in Oligodendrocyte Network Area via Stimulation of the Formation of Membranous Structures

As introduced above, the presence of PD-Iα/ATX in the extracellular environment of differentiating oligodendrocytes may preclude and/or mask some of the physiologic effects of LPA when it is added exogenously and/or in excess. Thus, we analyzed the effect of exogenous LPA on the morphology of

differentiating oligodendrocytes under conditions where PD-Iα/ATX expression was down-regulated. Differentiating oligodendrocytes were isolated by O4 immunopanning from postnatal day 4 to 5 rat brains and treated with a siRNA pool specific to PD-Iα/ATX 2 days after plating. We have previously established that under these conditions PD-Iα/ATX mRNA and protein levels are reduced by at least 50% 48 h after siRNA treatment (Dennis et al., 2008). For LPA treatment a concentration of 1 μM was chosen. At this concentration significant effects on Ca^{2+} mobilization and ERK1/2 activation have been described by others (Moller et al., 1999; Stankoff et al., 2002; Yu et al., 2004). Furthermore, for the LPA-induced increase in pERK an EC_{50} of 1 μM has previously been established (Yu et al., 2004). LPA was added 48 h after siRNA treatment and its effects were evaluated 2 h after application. We first determined the network area as a measure for morphological changes (Fig. 2.3A). In agreement with previous studies, no effects were noted under control conditions (Fig. 2.3B and (Stankoff et al., 2002)). At reduced levels of PD-Iα/ATX mRNA and protein, however, the network area was significantly reduced, and addition of LPA led to an increase to almost control levels (Fig. 2.3B).

To further define the nature of the morphological changes observed in response to LPA, process and complexity indices were determined (see Experimental Procedures and (Dennis et al., 2008)). As shown in Fig. 2.4A, treatment of differentiating oligodendrocytes with a siRNA pool specific to PD-Iα/ATX resulted in a decrease in both process and complexity indices. Thus, siPD-Iα/ATX-treated cells displayed a simple process morphology (Fig. 2.4B;

upper panel). Upon addition of exogenous LPA to these cells, an increase in process but not complexity index was noted (Fig. 2.4A). Such an increase could either be due to an increase in long, unbranched processes or in membranous structures. When visually inspecting the cells, the latter appeared to be the case (an example of maximal effect is depicted in Fig. 2.4B; lower panel). To quantify this effect, cells were double stained for O4 and acetylated α-tubulin, a protein associated with stabilized microtubules (Piperno et al., 1987). In oligodendrocytes, stabilized microtubules are found in processes of differentiating cells but not within their membranous structures (Lunn et al., 1997; Richter-Landsberg, 2001; Liu et al., 2003; Lee et al., 2005; Li et al., 2007b). Thus, the differential in distribution of the O4 antigen versus acetylated α-tubulin allowed us to define a membrane index for which a value close to 1 is characteristic for cells extending large membranous areas while a lower value denotes the presence of fine processes (for details see Experimental Procedures). As shown in Fig. 2.4C, the membrane index remained unaffected when PD-Iα/ATX expression was down-regulated. This finding is in agreement with our previous studies, and it reflects a decrease in the number of cells extending a complex network of fine processes (Dennis et al., 2008). Application of LPA to these cells of relatively simple process morphology significantly increased the membrane index (Fig. 2.4C). Thus, LPA can induce an increase in the oligodendrocyte's network area by stimulating the formation of membranous structures.

Extracellular LPA can Support an Increase in the Number of MBP-Positive Cells via Stimulation of an Increase in MBP mRNA Levels

In an attempt to gain insight into potential molecular mechanisms underlying the above observed effect of LPA on the formation of membranous structures, the expression of the classic isoforms of the myelin protein MBP was analyzed (Figs. 2.5 and 2.6). These MBP isoforms are highly expressed during the active stages of myelination and are thought to have regulatory effects on the myelination program (Barbarese et al., 1978; Campagnoni et al., 1978; Staugaitis et al., 1996; Kimura et al., 1998; Campagnoni and Campagnoni, 2004; Boggs, 2006). As shown in Fig. 2.5, down-regulation of PD-Iα/ATX expression led to a decrease in the number of MBP-positive cells. Upon addition of LPA, the number of MBP-positive cells returned to at least control levels.

The observed increase in the number of MBP-positive cells could be mediated by stimulation of gene expression or by regulatory posttranscriptional events such as mRNA transport and/or translational regulation. To evaluate the contribution of an increase in mRNA levels, real-time qRT-PCR was performed. In these studies, mRNAs coding for the exon 2-containing classic isoforms of MBP were assayed since these are expressed more abundantly during the initial stages of myelination. In contrast, exon 2-deficient MBP isoforms have been implicated primarily in the regulation of myelin maintenance and/or compaction [*59*, *60*]. Cells treated with a siRNA pool specific to PD-Iα/ATX displayed a reduction in MBP mRNA levels that was similar to the reduction in the number of MBP-positive cells (compare Fig. 2.6A with Fig. 2.5B). In contrast to MBP, MOG,

which is specifically expressed by myelinating oligodendrocytes, was not affected by the alteration in PD-Iα/ATX expression (Fig. 2.6A and (Solly et al., 1996)). These findings demonstrate that a reduction in PD-Iα/ATX expression affects mRNA levels for some but not all myelin genes. Upon treatment with LPA, MBP mRNA levels were increased by a factor of 2.9, while MOG mRNA levels remained unchanged (Fig. 2.6B). Interestingly, MBP mRNA levels reached above control levels after LPA application. This enhancement in MBP mRNA levels could either reflect a more efficient direct effect of LPA on MBP under low PD-Iα/ATX expression conditions, or it could, in part, be a consequence of an indirect or off-target effect of the siPD-Iα/ATX-treatment on other LPA-responsive genes. Nevertheless, these data demonstrate that under certain conditions LPA can induce an increase in the mRNA levels encoding classic isoforms of MBP.

Discussion

The well coordinated sequence of events leading to the final maturation of differentiating oligodendrocytes is crucial for proper functioning of the CNS. Our data presented here indicate that the lipid signaling molecule LPA may play a crucial role in regulating these events. In particular, we found that LPA can promote an increase in the area occupied by the oligodendrocyte's process network by stimulating the extension of membranous structures. In addition, LPA can increase the appearance of MBP-positive cells via stimulation of an increase in MBP mRNA levels. mRNA levels for the later stage marker MOG, however, appeared unaffected. Increases in neither the network area nor the MBP mRNA

levels were observed under control conditions. Detection of these exogenous LPA-mediated effects required prior down-regulation of PD-Iα/ATX expression. Thus, our data demonstrate that under conditions where PD-Iα/ATX expression is down-regulated LPA can promote the transition from a network of fine processes to the formation of myelin sheets as well as an increase in MBP mRNA levels (Fig. 2.7).

In the studies presented in Fig. 2.4, the formation of membranous structures was induced by LPA in cells of simple process morphology. In vivo and under control in vitro conditions, however, membrane sheath formation is preceded by the extension of a complex process network (Knapp et al., 1987; Hardy and Friedrich, 1996). Thus, for earlier differentiation stages of oligodendrocytes with simple morphology LPA does not appear to exert a similar effect as the one observed here. These cells may lack components of the signaling pathway leading to membrane sheath formation and/or this pathway may be inhibited by the expression of “silencing” factors. In either case, down-regulation of PD-Iα/ATX does not seem to affect the crucial components of these pathways. In an extended interpretation, these findings suggest that down-regulation of PD-Iα/ATX does not block the entire differentiation program in maturing cells of the oligodendrocyte lineage.

LPA-mediated effects on oligodendrocyte network area and MBP mRNA levels were only revealed after down-regulation of PD-Iα/ATX expression. Interestingly, in the case of the membrane index, a slight increase was observed upon LPA application under control conditions, i.e. without prior down-regulation

of PD-Iα/ATX expression (data not shown). This effect was, however, not associated with a concomitant increase in network area (see Fig. 2.3). Thus, the increase in membrane index under control conditions appears primarily due to a decrease in acetylated α-tubulin that is likely associated with a rearrangement from fine and complex process networks to membranous structures. Myelin sheath formation has been recently suggested to involve destabilization of microtubules and deacetylation of α-tubulin (Southwood et al., 2007). Thus, the LPA-mediated effect on oligodendrocyte morphology may be associated with cytoskeletal rearrangements involved in the transition from process outgrowth to membrane sheath formation. In support of this idea, it has been previously shown that LPA induces rearrangements of microtubules during remodeling of neuronal processes (Sayas et al., 2002; Fukushima and Morita, 2006).

Down-regulation of PD-Iα/ATX was found here to negatively affect MBP expression. Subsequent application of LPA reverted this effect. These data point toward a role of LPA on the expression of certain genes known to be important for myelination. Up-regulation of gene expression within hours of LPA application has been previously reported to occur and to be mediated by signaling through LPA receptors (Lee et al., 2004; Cui et al., 2006; Lee et al., 2006b; Klemm et al., 2007). Accordingly, the LPA-mediated effects described here are thought to be mediated by signaling through one or more of the cell surface LPA receptors expressed by differentiating oligodendrocytes. Upon agonist stimulation, most GPCRs are rapidly internalized into cells through endocytic pathways. Indeed, LPA receptor activation has been associated with vesicle-mediated endocytosis

(Luttrell et al., 1997; Kranenburg et al., 1999; Murph et al., 2003; Urs et al., 2005). Our immunostaining for LPA1 through three revealed a punctate pattern indicative of LPA receptor localization to intracellular vesicles. Thus, LPA receptor activation is likely operative in cultures of primary oligodendroglial cells as utilized here. We consider it unlikely that the effects we observe are mediated via the recently discovered nuclear LPA receptor (PPARγ) since extracellular LPA has long been known to have access to the intracellular compartment only when applied in a carrier (albumin)-free manner (Tokumura et al., 1992; McIntyre et al., 2003). Knock-out mice for LPA receptors have so far not revealed any specific myelination defects (Contos et al., 2002; Yang et al., 2002; Ye et al., 2005). This observation, however, does not minimize the predicted importance of LPA receptor signaling for oligodendrocyte differentiation and myelination. The existence of an increasing number of LPA receptors and the redundancy of lysophospholipid-evoked cellular responses create a scenario of great complexity (Valentine et al., 2008). Thus, more sophisticated strategies may have to be employed to be able to dissect in vivo the physiological roles for each of the LPA receptors.

In summary, the data presented here reveal a potentially crucial role for LPA during the later stages of oligodendrocyte maturation. Due to the heterogeneity of the oligodendrocyte cultures with respect to their developmental stage, we cannot rule out the possibility that the LPA-mediated effects observed here are limited to a narrow developmental window. Nevertheless, these effects were only revealed after down-regulation of PD-Iα/ATX expression. In light of the

well established role of PD-Iα/ATX as the major enzyme generating exogenous LPA, it is, therefore, tempting to speculate that during normal development LPA is generated in the environment surrounding the maturing oligodendrocyte via PD-Iα/ATX's lysoPLD active site. This generation of exogenous LPA can, at the appropriate developmental time point, promote the transition from a highly branched network of fine processes to myelin sheath formation associated with an increase in MBP expression. Interestingly, the prior establishment of the complex network of fine processes is facilitated by PD-Iα/ATX's second functionally active site, the MORFO domain (Dennis et al., 2008). Thus, PD-Iα/ATX seems to promote oligodendrocyte maturation via the concerted action of its functionally active sites. Future studies will, however, be necessary to dissect the exact roles of PD-Iα/ATX for myelination during normal development and during myelin repair under pathological demyelinating conditions.

Acknowledgements The authors thank S. Pfeiffer for the hybridoma cell line O4 and S. Spiegel for helpful discussions and comments. Confocal and fluorescent microscopy was performed at VCU's Department of Neurobiology and Anatomy Microscopy Facility, which was supported, in part, through NIH-NINDS Center Core grant 5P30NS047463. This work was supported by grants from the National Institute of Health (B.F.), the National Multiple Sclerosis Society (B.F.), a postdoctoral fellowship award from the National Multiple Sclerosis Society (J.D.) and a predoctoral fellowship award from the Coordenação de Aperfeiçoamento de Pessoal de Nível Superior of the Brazilian Ministry of Education (L.N.)

Figure 2.1. **Differentiating oligodendrocytes secrete enzymatically active PD-Iα/ATX and express all three classical LPA receptors.** (A) Scheme of morphological and gene expression characteristics of differentiating oligodendrocytes. At all stages oligodendrocytes express the cell surface antigen O4 and the secreted protein phosphodiesterase-Iα/autotaxin (PD-Iα/ATX). The myelin proteins myelin basic protein (MBP) and myelin oligodendrocyte glycoprotein (Sato et al.) are expressed with increasing stages of maturation. (B) PD-Iα/ATX's lysoPLD activity was determined in tissue culture supernatants from O4 immunopanned oligodendrocytes (4 days after plating) using the fluorogenic assay described by Ferguson et al. [*37*]. Means ± SEM of three independent experiments done in triplicates are shown. Numbers on the *Y*-axis represent fluorescence increase as a measure for lysoPLD activity in arbitrary units. (C) Relative LPA receptor mRNA levels present in differentiating oligodendrocytes. mRNA levels were determined by real-time qRT-PCR [*41*] and are presented in % on a logarithmic scale. LPA1 mRNA levels were set to 100% and the levels for LPA3 and LPA2 calculated accordingly. Means ± SEM of three pooled samples run in triplicate are shown. (D) Immunocytochemistry of differentiating oligodendrocytes. Oligodendrocytes were isolated by O4 immunopanning and double-immunostained 4 days after plating for the O4 antigen and for LPA1, 2 or 3. Scale bar: 20 μm

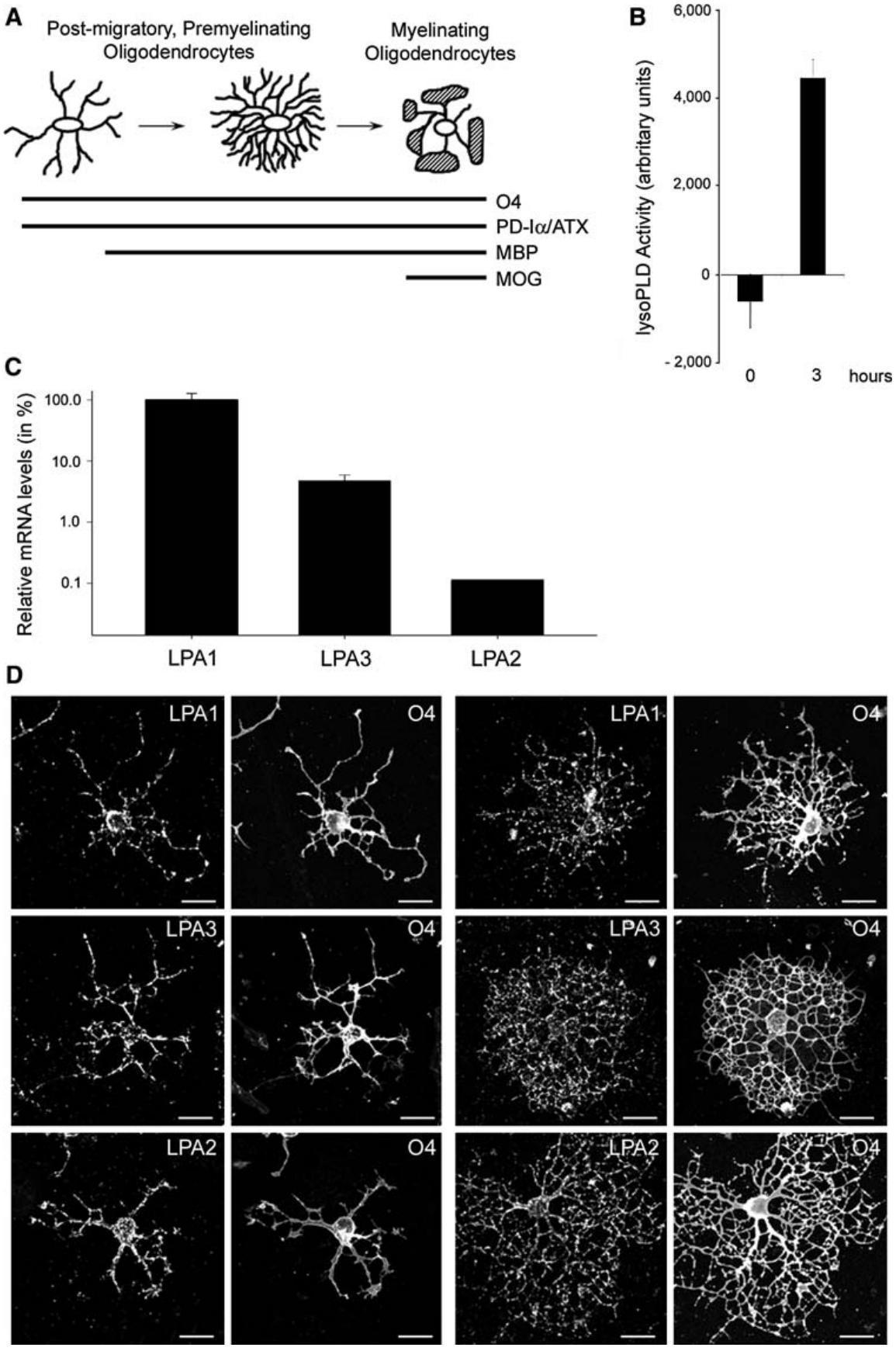
A
Post-migratory, Premyelinating Oligodendrocytes
Myelinating Oligodendrocytes
O4
PD-Iα/ATX
MBP
MOG
B
lysoPLD Activity (arbritary units)
6,000
4,000
2,000
0
- 2,000
0
3
hours
C
Relative mRNA levels (in %)
100.0
10.0
1.0
0.1
LPA1
LPA3
LPA2
D
LPA1
O4
LPA1
O4
LPA3
O4
LPA3
O4
LPA2
O4
LPA2
O4

Figure 2.2. **Time- and concentration-dependent measurement of PD-Iα/ATX's lysoPLD activity.** PD-Iα/ATX's lysoPLD activity was determined in tissue culture supernatants from O4 immunopanned oligodendrocytes (4 days after plating) using the fluorogenic assay described by Ferguson et al. (2006). Means ± SEM of a typical experiment done in triplicates is shown. Numbers on the Y-axis represent fluorescence increase as a measure for lysoPLD activity in arbitrary units. µg values represent amounts of input protein.

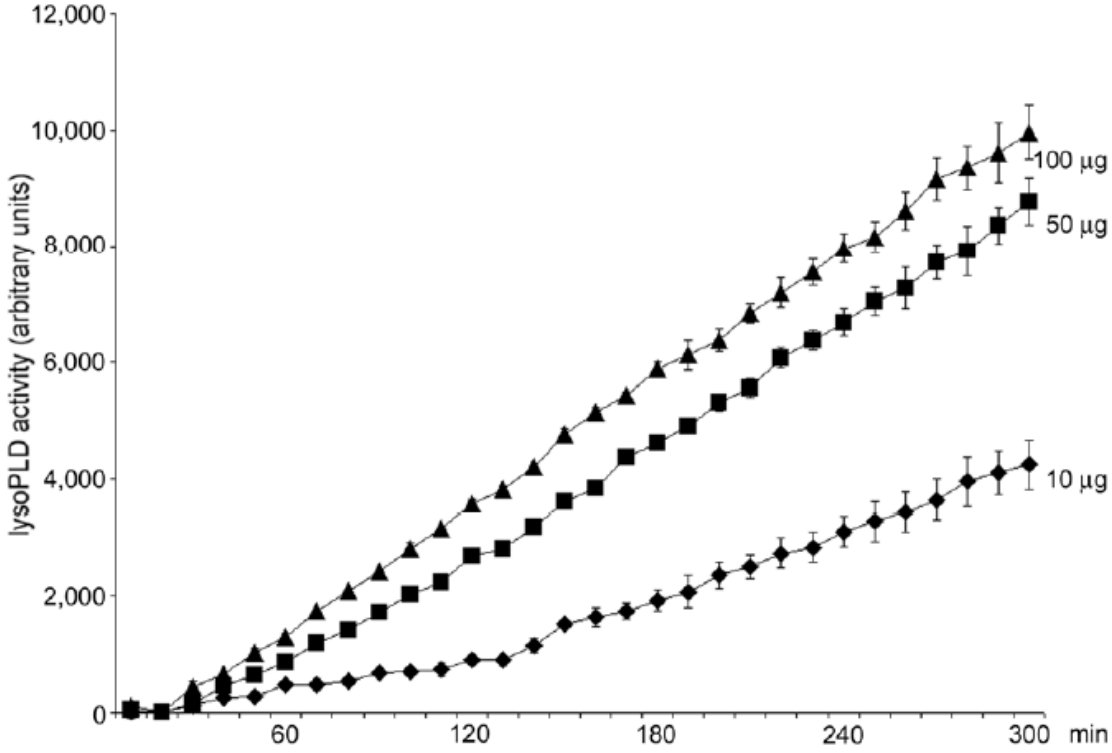
12,000
10,000
8,000
6,000
4,000
2,000
0
lysoPLD activity (arbitrary units)
60
120
180
240
300
min
100 µg
50 µg
10 µg

Figure 2.3. **LPA can induce an increase in network area under conditions where PD-Iα/ATX expression is down-regulated.** Differentiating O4-positive oligodendrocytes isolated from brains of 4 to 5 day-old rats were treated with a control (Control) or PD-Iα/ATX-specific (siPD-Iα/ATX) siRNA SMARTpool. 48 h after siRNA transfection, LPA was applied at a concentration of 1 μM for 2 h. Cells were then immunostained with the O4 antibody and the area covered by each cell's process network was determined. (A) Representative example of an oligodendrocyte labeled for the O4 antigen (left panel; confocal image representing a 2D maximum projection of stacks of 0.5 μm optical sections) and its network area (right panel). Scale bar: 20 μm. (B) Bar graph depicting the network area in % of control (mean of control = 100%). Means ± SEM of four independent experiments are shown. Stars indicate overall two-tailed significance levels of $P < 0.05$ as determined by Student's *t*-test

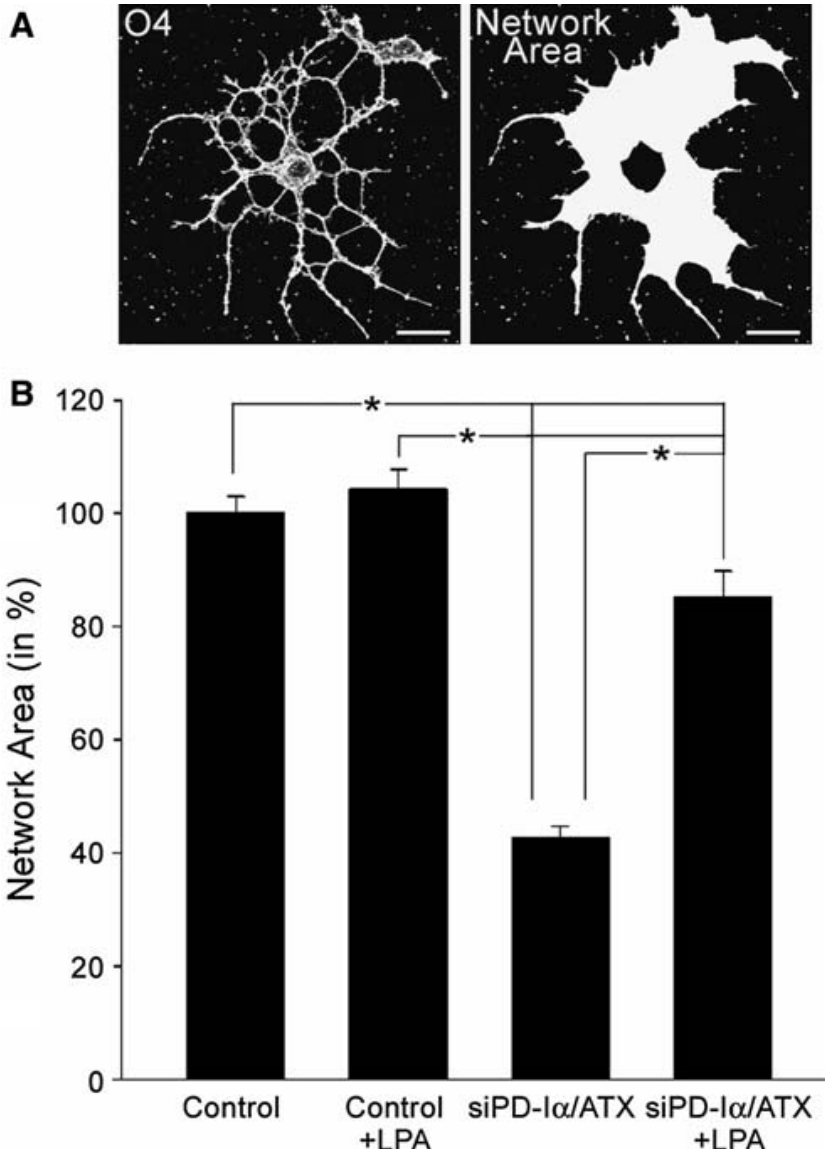
A
O4
Network
Area
B
Network Area (in %)
120
100
80
60
40
20
0
*
*
*
Control
Control
+LPA
siPD-Iα/ATX
siPD-Iα/ATX
+LPA

Figure 2.4. **LPA-induced increase in network area is due to an increase in the establishment of membranous structures.** Differentiating oligodendrocytes were isolated and treated as described in Fig. 2. (A) Normalized values of the cells' process indices were plotted against normalized values of their complexity indices on logarithmic scales (mean control values = 50; see dashed lines). The numbers in each of the quadrants represent % cells. Four independent experiments with at least 30 cells per condition are shown. (B) Upper panel: representative example of a siPD-Iα/ATX-treated cell that is characterized by a low membrane index. Lower panel: representative example of a siPD-Iα/ATX plus LPA-treated cell that is characterized by a high membrane index. Images were obtained by confocal microscopy and represent 2D maximum projections of stacks of 0.5 µm optical sections. Scale bar: 20 µm. (C) Bar graph depicting membrane indices. Means ± SEM of two independent experiments are shown. Stars indicate overall two-tailed significance levels of $P < 0.05$ as determined by Student's *t*-test

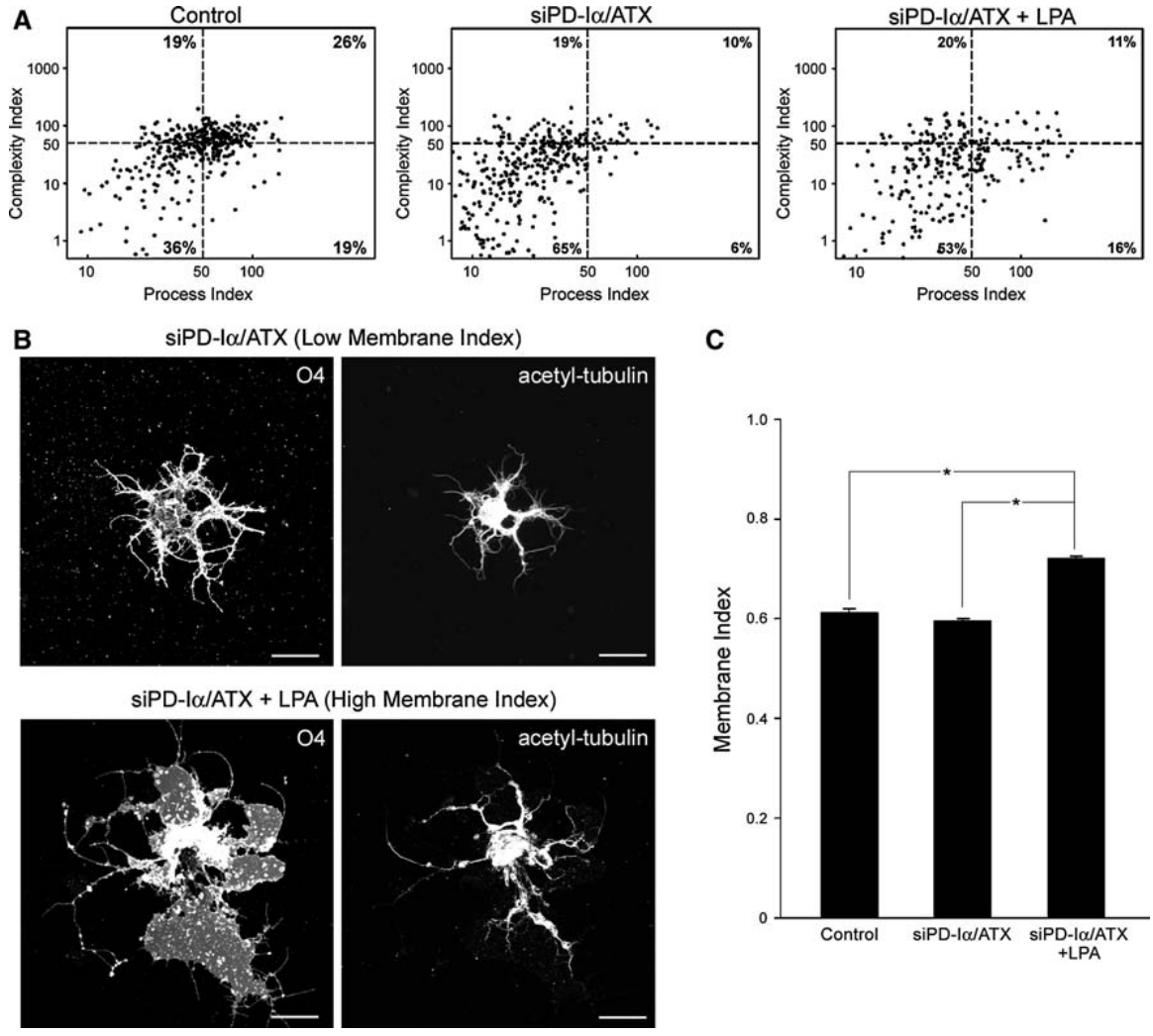
A
Control
siPD-Iα/ATX
siPD-Iα/ATX + LPA
19%
26%
36%
19%
19%
10%
65%
6%
20%
11%
53%
16%
Complexity Index
Process Index
1000
100
50
10
1
10
50
100
B
siPD-Iα/ATX (Low Membrane Index)
siPD-Iα/ATX + LPA (High Membrane Index)
O4
acetyl-tubulin
C
Membrane Index
1.0
0.8
0.6
0.4
0.2
0
Control
siPD-Iα/ATX
siPD-Iα/ATX +LPA
*
*

Figure 2.5. **LPA can induce an increase in the number of MBP-positive cells under conditions where PD-Iα/ATX expression is down-regulated.** Differentiating oligodendrocytes were isolated and treated as described in Fig. 2. (A) Representative images of cultures of differentiating oligodendrocytes treated with siPD-Iα/ATX (upper panel) or siPD-Iα/ATX plus LPA (lower panel). Cells expressing the classic isoforms of MBP were visualized by immunocytochemistry and nuclei were detected by Hoechst staining. Images were obtained by confocal microscopy and represent 2D maximum projections of stacks of 0.5 µm optical sections. Scale bar: 75 µm. (B) Bar graph depicting the number of MBP-positive cells as % of control. Control values were set to 100%. Means ± SEM of three independent experiments are shown. Stars indicate overall two-tailed significance levels of $P < 0.05$ as determined by Student's *t*-test

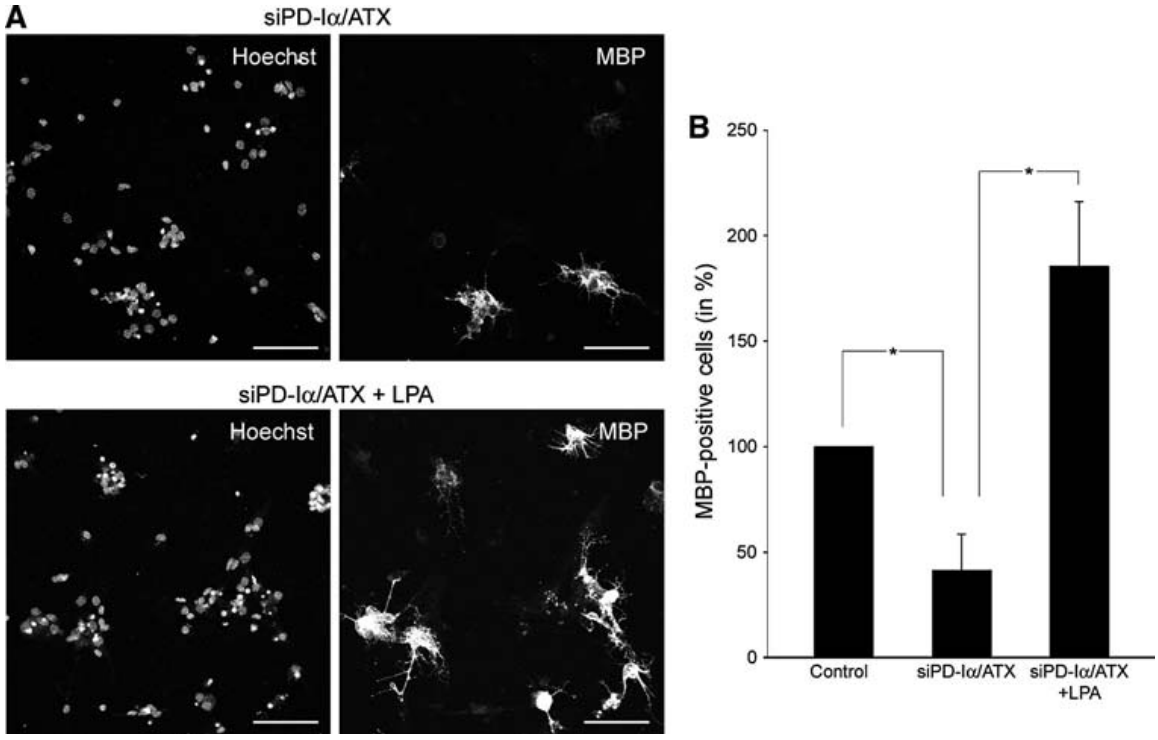
A
siPD-Iα/ATX
Hoechst
MBP
siPD-Iα/ATX + LPA
Hoechst
MBP
B
MBP-positive cells (in %)
250
200
150
100
50
0
*
*
Control
siPD-Iα/ATX
siPD-Iα/ATX
+LPA

Figure 2.6. **LPA-induced increase in the number of MBP-positive cells is due to an increase in MBP mRNA levels.** Differentiating oligodendrocytes were isolated and treated as described in Fig. 2. mRNA levels for MBP and MOG were determined by real-time qRT-PCR [*42*]. 18S rRNA was used for normalization. (A) Bar graph depicting mRNA levels as % of control (control levels were set to 100%). (B) Bar graph illustrating the fold increase in mRNA levels upon LPA treatment (mRNA levels under siPD-Iα/ATX conditions were set to 1; see dotted line). For both graphs, means ± SEM of three independent experiments done in duplicates are shown. Stars indicate an overall two-tailed significance level of $P < 0.05$ as determined by Student's *t*-test.

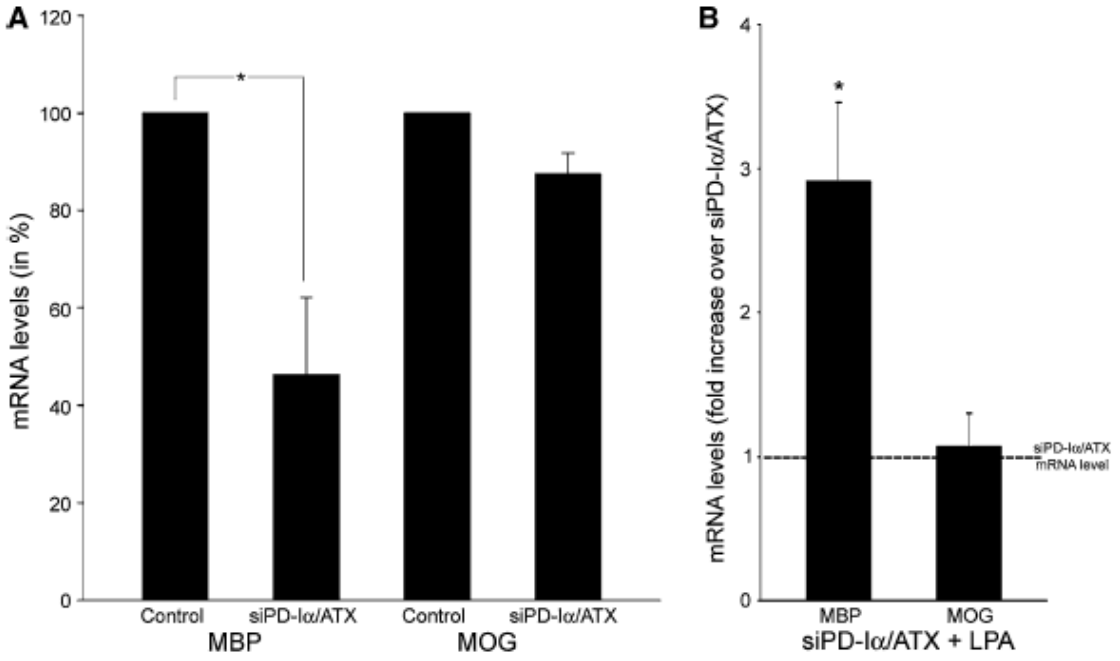
A
120
100
80
60
40
20
0
mRNA levels (in %)
*
Control
siPD-Iα/ATX
Control
siPD-Iα/ATX
MBP
MOG
B
4
3
2
1
0
mRNA levels (fold increase over siPD-Iα/ATX)
*
siPD-Iα/ATX mRNA level
MBP
MOG
siPD-Iα/ATX + LPA

Figure 2.7 **Potential effects of LPA on differentiating oligodendrocytes.** Our data presented here demonstrate that extracellular LPA can stimulate the formation of membranous structures and an increase in mRNA levels encoding classic isoforms of MBP at least under conditions where PD-Iα/ATX expression is down-regulated.

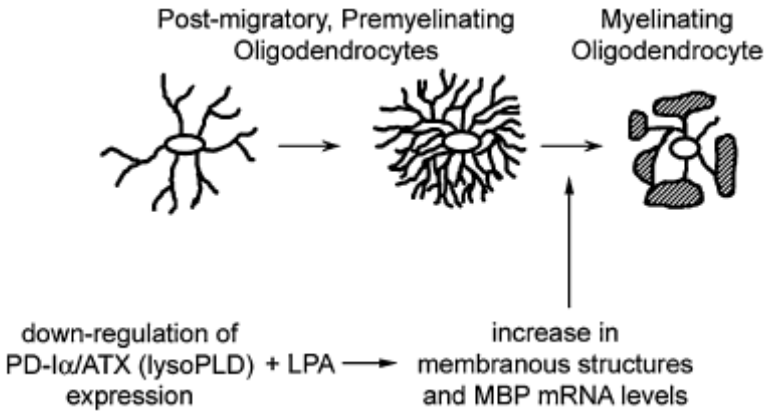
Post-migratory, Premyelinating Oligodendrocytes
Myelinating Oligodendrocyte
down-regulation of PD-Iα/ATX (lysoPLD) expression
+ LPA
increase in membranous structures and MBP mRNA levels

CHAPTER 3

Introduction to zebrafish oligodendrocyte development and myelination

During the last 20 years, the zebrafish has emerged as a model system for the study of vertebrate development. In the early 1970's, George Streisinger at the University of Oregon discovered this potential in the zebrafish and is considered the founding father of zebrafish research. The work done by his group stimulated interest in other laboratories and led to the validation of the zebrafish as an important developmental and genetic model.

Zebrafish

The zebrafish, *Danio rerio*, is a freshwater fish found naturally around the Ganges and Brahmaptura river basins in northeastern India, Bangladesh and Nepal. The name Danio is derived from the Bengali name "dhani" meaning "of the rice field" (Talwar and Jhingran, 1991).

Fishes are a very large and diverse group of vertebrates. They include the jawless fishes (hagfish and lampreys), cartilaginous fishes (sharks, rays and skates) and bony fishes (ray-finned and lobe-finned fishes). The ray-finned fishes (Class Actinopterygii) have more than 23,500 different species and make up more than 95% of all fish species and about half of all non-extinct vertebrate species. Zebrafish belong to the teleost infraclass of the actinopterygians which make up about 99.8% of all ray-finned fishes. Other examples of teleosts used in

research include the rainbow trout, Atlantic salmon and the well-studied Japanese medaka (Volff, 2005).

Teleost fish are the most diverse and species-rich vertebrate group likely because of duplication events that have occurred in their genome (Ohno, 1970; Postlethwait et al., 2004; Volff, 2005). Duplicate pairs of genes generated by this event have been maintained over hundreds of millions of years of evolution (Volff, 2005). Also many genes present in higher vertebrates are present in the zebrafish genome (Barbazuk et al., 2000). These homologous genes can be referred to as either paralogs (separated by a speciation event) or orthologs (separated by a genome duplication event).

Tetrapods, land dwelling vertebrates with four limbs (amphibians, reptiles, birds and mammals), have been considered to be descendants of lobe-finned fishes. Bony fishes are more related to lobe-finned fishes than evolutionarily older jawless and cartilaginous fishes and are therefore are more related to tetrapods, suggesting that teleosts share a common fish ancestor with tetrapods allowing the use of fish for the study tetrapodal processes (Volff, 2005). Because of this potential and the advantages described below, the zebrafish has become an important vertebrate model in developmental biology. Many favorable characteristics of zebrafish for study in the laboratory include their small size and robustness and relatively cheap maintenance. They can breed throughout the year, two to three times a week, with clutch sizes around a couple of hundred eggs. Fertilization is external and embryos are optically clear allowing for easy manipulation and visualization under a microscope. Their embryos are smaller

and have less numbers of cells than tetrapod embryos, making it easy to trace the development of individual cells. Embryogenesis is rapid and complete by 3 days post fertilization (dpf) with a full body axis and major neurons being laid down by 24 hours post fertilization (hpf) and precursors to major organs developed by 36 hpf (Kimmel et. al., 1995). Developmental staging of zebrafish has also been very well characterized (Kimmel et al., 1995) and orthologs for most human genes can be found and studied in zebrafish (Barbazuk et al., 2000; Postlethwait et al., 2000).

Many methods are available for the study of developmental processes in the zebrafish. Visualizing cells within a whole embryo can be carried out using whole mount *in situ* hybridization or whole mount immunohistochemistry. Also, transgenic zebrafish with tissue-specific promoters that drive fluorescent protein expression allow the visualization of cells in living zebrafish. Knock down technologies such as the use of antisense morpholino oligonucleotides allow easy manipulation of gene function in developing embryos.

These methods as well as similarities in central nervous system development, including oligodendrocyte development, between zebrafish and mammals described below allow us to undertake studies of ATX in this model.

CNS development in the zebrafish - overview

The neural tube of zebrafish embryos is like that of other vertebrates in that it is highly polarized along its dorsoventral axis. In the spinal cord, sensory neurons form at the dorsal locations while motor neurons and oligodendrocytes

develop at ventrolateral regions. The floor plate develops at ventral regions and interneurons occupy the intermediate regions (Blader and Strahle, 2000).

The first neurons become post mitotic shortly after gastrulation and by the end of the first day post fertilization embryos generate movements by spontaneous twitching. During the second day post fertilization, embryos can respond to touch because of the presence of differentiated neurons and pioneering axons. This is important for a startle response required for escape in the wild (Blader and Strahle, 2000).

Oligodendrocyte specification/early development

Oligodendrocyte development and differentiation occur later in development than neurons as in the mammalian system. Oligodendrocytes also share cell lineage similarities with mammalian oligodendrocytes, including specification, development and myelination as well as many of the genes involved in these processes (Buckley et al., 2008). Unless otherwise noted, the mechanisms described in this chapter are conserved between zebrafish and mammals.

Oligodendrocytes are reported to first arise between 24hpf to 36hpf in the midbrain and hindbrain and from 36hpf to 48hpf in the spinal cord of the developing zebrafish (Park et al., 2002; Kirby et al., 2006; Li et al., 2007a; Schebesta and Serluca, 2009).

The majority of information known for oligodendrocyte specification has been gained from study in the developing spinal cord therefore the descriptions below are limited to spinal cord-derived oligodendrocytes.

In order for oligodendrocytes to be specified in the spinal cord, the notochord must first develop. The notochord is a transient, embryonic midline structure in vertebrates important for fate determination of surrounding tissues (Stemple, 2005). In the central nervous system, it is required for the formation of the dorsal-ventral axis of the overlying neural tube, including specification of the floor plate, the ventral-most portion of the spinal cord (van Straaten et al., 1989; Placzek et al., 1990; van Straaten and Hekking, 1991; Dodd et al., 1998). This dorsoventral patterning of the developing neural tube is dependent on the notochord-derived glycoprotein sonic hedgehog (SHH) in a high to low concentration dependent manner (Fig. 3.1) (Tanabe and Jessell, 1996; Ericson et al., 1997; Wilson and Maden, 2005; (Ericson et al., 1995).

OPCs are generated adjacent to the floor plate in the same location that gives rise to motor neurons, the motor neuron progenitor domain (Fig. 3.1) (Warf et al., 1991; Noll and Miller, 1993; Pringle and Richardson, 1993; Yu et al., 1994) and their specification begins when motor neuron production has ended (Richardson et al., 2000; Zhou and Anderson, 2002; Park et al., 2004).

After the floor plate is induced, it also releases SHH, important for OPC specification (Poncet et al., 1996; Pringle et al., 1996; Orentas et al., 1999; Park et al., 2002; Park et al., 2004). SHH is also important for specification of motor neurons and interneurons in a high to low (ventral to dorsal) concentration

gradient, where motor neurons and oligodendrocytes require the same concentration (Pringle et al., 1996; Ericson et al., 1997; Orentas et al., 1999).

Transcriptional regulation is very important for the timely and proper development and differentiation of oligodendrocytes. Shh regulates the expression of many transcription factors, including genes known to be expressed early during oligodendrocyte lineage progression (*olig1* and o*lig2*), which encode basic helix-loop-helix transcription factors. They were first identified in areas of the neuroepithelium where oligodendrocytes arise (Lu et al., 2000; Zhou et al., 2000; Park et al., 2002b). More specifically, *olig1* and *olig2* are expressed in cells of the motor neuron domain, where oligodendrocytes and motor neurons are generated (Zhou et al., 2000).

Olig2 is necessary for the specification of both motor neurons and oligodendrocytes as mice and zebrafish lacking *olig2* display an absence of both cell types (Lu et al., 2002; Takebayashi et al., 2002; Zhou and Anderson, 2002; (Park et al., 2002).

o*lig1* null mice reveal that *olig1* is necessary for oligodendrocyte maturation and not specification (Lu et al., 2002; Xin et al., 2005). *olig1* is important during oligodendrocyte development in the brain only in the absence of *olig2* suggesting that, at least in restricted areas, *olig1* expression is sufficient for oligodendrocyte development (Lu et al., 2002). This observation was also confirmed by a complete lack of oligodendrocyte generation in *olig1/olig2* double-null mice (Zhou and Anderson, 2002). Consistent with *olig1*'s role in oligodendrocyte maturation, other studies have shown its importance in

oligodendrocyte differentiation by regulating transcription of the major myelin-specific genes, *mbp*, *plp* and *mag*, as well as in myelinogenesis (Xin et al., 2005) and during remyelination in a demyelination model (Arnett et al., 2004). In the zebrafish, o*lig1* is expressed by oligodendrocytes (Li et al., 2007a; Schebesta and Serluca, 2009; Tiso et al., 2009) and is also important in their differentiation as it can activate MBP transcription as in the mouse (Xin et al., 2005; Li et al., 2007a).

Due to the importance of *olig2* in the generation of both motor neurons and oligodendrocytes, it has been proposed that these cell types are generated from the same precursor cell population in the spinal cord. Fate-mapping studies in the zebrafish demonstrated that oligodendrocytes are generated from the same *olig2*-expressing precursors as earlier-derived motor neurons (Park et al., 2002). Studies in the rodent system also suggest a common lineage-restricted precursor cell population although it is still under debate (Richardson et al., 1997; Richardson et al., 2000; Lu et al., 2002; Zhou and Anderson, 2002; Wu et al., 2006).

Floor plate

The floor plate is a ventral midline structure made of up cuboidal epithelial cells that extends through the spinal cord, hindbrain, midbrain and posterior diencephalon (Jessell et al., 1989; Wilson and Houart, 2004). The floor plate has not yet been identified in the forebrain where patterning is the least understood. Once the floor plate is specified, it will then begin to express *shh* (Fig. 3.1) (Marti

et al., 1995; Roelink et al., 1995; Chiang et al., 1996; Goodrich et al., 1997; Ding et al., 1998) necessary for the specification for oligodendrocytes as described above.

In the zebrafish, the floor plate in the spinal cord is three to four cells wide, comprised of one row of medial floor plate cells flanked by two rows of lateral floor plate cells (Fig. 3.1), while in the brain, there are six to seven rows (Odenthal et al., 2000). These different populations of cells can be distinguished via the expression of specific genes (Placzek et al., 1993; Roelink et al., 1995; Yamada et al., 1991; Ang et al., 1993; Monaghan et al., 1993; Sasaki and Hogan, 1993). The *shh* gene is duplicated in zebrafish, one named *shh* and the other *twhh* (Ekker et al., 1995; Zardoya et al., 1996). They vary in expression whereby they are both expressed in the medial floor plate but *shh* is also expressed in the notochord (Krauss et al., 1993; Ekker et al., 1995; Etheridge et al., 2001). Along with the *shh* paralogs, cells of the medial floor plate also express members of the *foxa* subfamily of winged-helix/fork head box (*fox*) transcription factor genes, *fkd4* (*foxa*), *fkd7* (*foxa1*) (Odenthal and Nusslein-Volhard, 1998), and *axial* (*foxa2*) (Strahle et al., 1993; Odenthal and Nusslein-Volhard, 1998). In addition to expression in the medial floor plate, cells of the lateral floor plate also express *fkd4* (*foxa*) and *axial* (*foxa2*) (Odenthal et al., 2000)..

Along with different populations of floor plate cells existing along the mediolateral axis, there has also been evidence for distinct populations of medial floor plate cells along the anterioposterior axis. These populations differ

morphologically and molecularly. They also arise from separate embryonic origins and require distinctive inductive processes. There has also been evidence for floor plate cells beyond the caudal diencephalon. It is currently unknown if these different populations of cells also function differently (Placzek and Briscoe, 2005).

Myelin genes

After OPCs are specified, they proliferate and migrate away from their restricted locations to populate the brain and spinal cord (Park et al., 2002; Park et al., 2007; Schebesta and Serluca, 2009; Buckley et al., 2010). Along with genes regulating oligodendrocyte specification and early stages of differentiation as mentioned earlier in this chapter, oligodendrocytes also express genes important for later stages of oligodendrocyte differentiation and myelination including the mammalian orthologs of *mbp*, *dm20* (*plp1b*) and *p0* (Brosamle and Halpern, 2002; Buckley et al., 2010).

Expression of these three genes begins at 48hpf in a few cells in the ventral medial hindbrain and at 72hpf in the spinal cord (Brosamle and Halpern, 2002). By 4dpf, a small number of oligodendrocytes express these genes in the midbrain while large numbers are positive in the hindbrain along the ventral hindbrain bundle and in the spinal cord along the ventral midline. In the optic nerve, expression was detectable by 4dpf in very few oligodendrocytes, while the number of cells continued to increase by 7dpf and 10dpf (Brosamle and Halpern, 2002).

mbp is also expressed in Schwann cells of the lateral line system, a mechanosensory organ of fish and amphibians used to detect motion in the water (Montgomery et al., 2000). It is composed of two major branches, the anterior lateral line located on either side of the head and the posterior lateral line that runs lengthwise down both sides of the trunk and tail (Ma and Raible, 2009). *Mbp* was first detected in the posterior lateral line of the trunk at 48hpf, and by 4dpf, *mbp* was expressed by both the anterior and posterior lateral lines (Brosamle and Halpern, 2002).

The function of these three genes have not yet been studied in detail but due to conservation of their predicted protein sequences with the mammalian sequences and the fact that they are expressed prior to myelination, it is very likely functions are conserved between zebrafish and mammals (Brosamle and Halpern, 2002; Buckley et al., 2008; Buckley et al., 2010).

Myelin basic proteins are common to the myelin of nearly all vertebrate fish and are expressed in the central and peripheral nervous systems. In zebrafish, the *mbp* gene may also be alternatively spliced as demonstrated in mammals but low sequence similarity has made it difficult to relate the sequence to individual exons of mammalian *mbp*, but exons I, 3, and part of 4 seem to exhibit the greatest similarity (Brosamle and Halpern, 2002). Three predicted variants have been identified thus far (Buckley et al., 2010) but no exon-specific functions have been characterized.

Mbp mRNA is also localized to oligodendrocyte processes in zebrafish and sequence analysis revealed a RNA transportation signal in the 3′

untranslated region of the transcript important for packaging of *mbp* mRNA to transport vesicles (Brosamle and Halpern, 2002). *mbp* mRNA is not transported into cell processes of the shark (Smith et al., 2001), indicating that this way of MBP targeting may have evolved later.

Methods have become available for accurate, rapid assessment of relative levels of myelination in zebrafish by the use of *mbp* mRNA quantification and MBP immunohistochemistry, indicating the importance of MBP in myelin of zebrafish (Buckley et al., 2010).

In addition to MBP, oligodendrocytes express PLP-splice variant DM20. Fish contain the DM20 variant while tetrapods contain both DM20 and PLP. The reason for this is because in the beginning of tetrapod evolution after their divergence from lungfishes, the DM20 gene acquired a splice donor site for inclusion of exon 3B, which encodes the PLP-specific domain of the third cytosolic loop (Nave et al., 1987; Schliess and Stoffel, 1991; Yoshida and Colman, 1996). Zebrafish only express the DM20 isoform of *plp* (Brosamle and Halpern, 2002) and there has been conflicting data on whether DM20 can functionally replace PLP in mammalian central nervous system myelin (Stecca et al., 2000; Sporkel et al., 2002).

PLP is a member of the lipophilin family which includes two other members, M6A and M6B (Yan et al., 1993; Gow, 1997). M6a and M6b mRNA is localized to neurons and not oligodendrocytes (Yan et al., 1993). The orthologous gene names in fish are DMα (PLP), DMβ (M6A) and DMγ (M6B). These three genes were duplicated as a result of genome-wide duplication

events and named: *dmα1*, *dmα2*, *dmβ1, dmβ2*, *dmγ1*, *dmγ2* (Schweitzer et al., 2006). The d*mα2* gene is the closest relative of mammalian *dm20* and is expressed by oligodendrocytes and present in central nervous system myelin of fish (Yoshida and Colman, 1996; Brosamle and Halpern, 2002; Schweitzer et al., 2003; Morris et al., 2004). Many published studies, including chapter 4, refer to this gene as *plp1b* instead of d*mα2*.

PLP's counterpart in the myelin of the PNS is myelin protein zero (P_0), the most abundant protein in Schwann cells of mammals. P_0 is a glycosylated cell adhesion molecule of the immunoglobulin superfamily (Lemke and Axel, 1985; Williams and Barclay, 1988) and is important for adhesion and compaction of extracellular myelin layers in mammals (D'Urso et al., 1990; Filbin et al., 1990; Schneider-Schaulies et al., 1990; Lanwert and Jeserich, 2001). In phylogenetically older vertebrate classes, such as fishes, P_0 and P_0–like protein genes are expressed in the peripheral nervous system as in mammals, but are predominantly expressed in the central nervous system which marks one of the largest biochemical differences between oligodendrocytes in fish versus mammals (Franz et al., 1981; Lanwert and Jeserich, 2001; Brosamle and Halpern, 2002; Schweitzer et al., 2003; Schweigreiter et al., 2006; Avila et al., 2007). Its function has not yet been characterized in the zebrafish but its adhesive properties have been demonstrated *in vitro* showing similarity with the mammalian proteins (Lanwert and Jeserich, 2001).

Since P_0 is predominantly expressed by fish oligodendrocytes and PLP is expressed by mammalian oligodendrocytes, it has been suggested that there

was likely an evolutionary shift from P_0 to PLP in terrestrial vertebrates. The appearance of PLP was thought to occur after the divergence of bony fishes, and through millions of years thereafter, while it was still co-expressed with P_0, it underwent a high mutational rate ultimately leading to the evolution of its function. Shortly after, P_0 silently dropped out of central nervous system myelin (Yoshida and Colman, 1996). Supporting the idea of a P_0 to PLP switch in myelin of the central nervous system, the zebrafish P_0 promoter shares greater sequence homology with the mammalian *plp* promoter than with the mammalian p_0 promoter (Jeserich et al., 1997; Jeserich et al., 2008) suggesting that they may be regulated in a similar manner. In support of this idea, the mouse *plp* promoter is able to drive expression of enhanced green fluorescent protein in oligodendrocytes of transgenic zebrafish (Yoshida and Macklin, 2005).

A microarray screen on cells sorted from transgenic zebrafish has recently identified additional genes expressed by oligodendrocytes, including claudink, a tight junction associated protein expressed only in oligodendrocytes and Schwann cells (Takada and Appel, 2010). Its expression timeline is similar to the one found for *mbp* as it begins at 48hpf in the ventral medial hindbrain and by 72hpf expression is more prominent in the brain as well as in the anterior and posterior lateral lines (C. Brösamle, personal communication). No functions have been reported yet in zebrafish but its related mammalian protein, Claudin-11/Osp, is expressed by mammalian oligodendrocytes (Morita et al., 1999) and Claudin-11 null mice exhibit slowed nerve conduction and hind limb paralysis (Gow et al., 1999).

Myelination

After the above-described genes are properly expressed, myelination occurs in a caudal to rostral fashion in the zebrafish, beginning in the spinal cord at 3dpf, in the hindbrain at 4dpf and at 7dpf in the optic nerve (Brosamle and Halpern, 2002; Kirby et al., 2006; Buckley et al., 2010). Myelin compaction begins at 4dpf in the spinal cord, 7dpf in the hindbrain and by 10dpf in the optic nerve (Brosamle and Halpern, 2002; Buckley et al., 2010).

Structural similarities are shared between the myelin of zebrafish and mammals except that the periodicity differs slightly (Avila et al., 2007). The nodes of Ranvier have similar ultrastructure and protein composition (Woods et al., 2006; Voas et al., 2007). Thus, the properties of vertebrate myelin are evolutionarily highly conserved.

Figure 3.1. **Cross section of the developing spinal cord.** The floor plate is composed to two populations of cells: medial floor plate (M) and lateral floor plate (L). The floor plate is present in the ventral developing spinal cord, hindbrain, midbrain and posterior diencephalon (spinal cord depicted here) and lies directly above the notochord (N). It secretes the signaling molecule SHH which specifies dorsal to ventral fates including motor neurons and oligodendrocytes from the motor neuron progenitor domain (pMN). Dorsal is to the top.

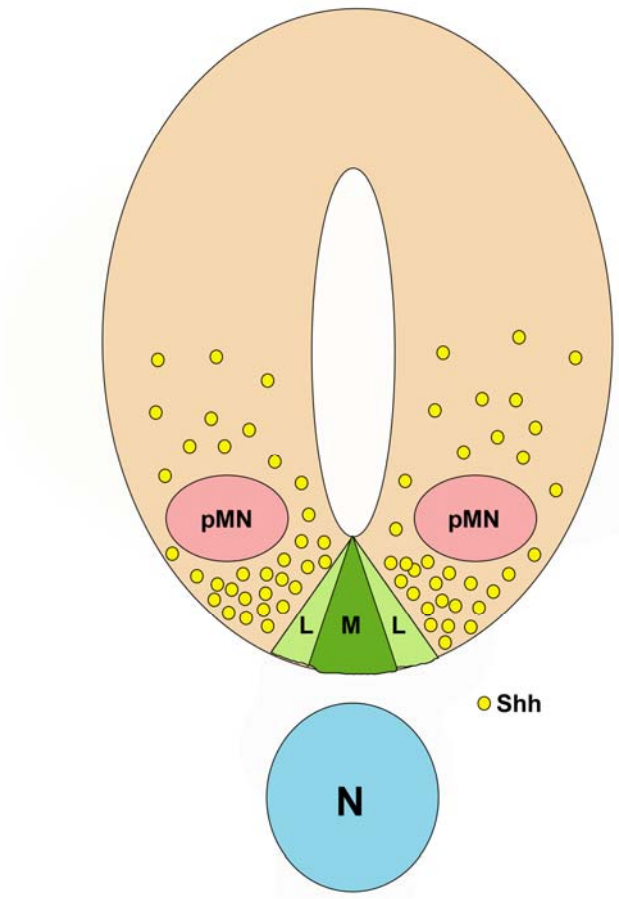
pMN
pMN
L
M
L
Shh
N

CHAPTER 4

Autotaxin regulates the presence of differentiating oligodendrocytes in the developing CNS of the zebrafish

(*This chapter is in preparation for submission to the Journal of Neuroscience or Glia. The work reported for this manuscript is based primarily on my own efforts. Assistance was provided by Dr. James Lister (collaboration and training in zebrafish-related techniques), Sati Afshari (western blots in Fig 4.4a), Christopher Waggener (cryosectioning for Fig. 4.2B) and Jessicka Hall (counting of olig1-positive oligodendrocytes in Fig 4.8c). Due to different conventions related to the nomenclature of genes, mRNAs and proteins in different species, I would like to clarify that throughout this manuscript the zebrafish conventions were used.)*

Introduction

Autotaxin (Atx), also referred to as phosphodiesterase I-α/Atx (PDI-α/Atx) or ENPP2, was originally identified as an autocrine tumor motility stimulating factor in melanoma cell supernatants (Stracke et al., 1992). The majority of functions relating to Atx have been attributed to the generation of the lipid signaling molecule, lysophosphatidic acid (LPA), via Atx's lysophospholipaseD (lysoPLD) enzymatic activity (Tokumura et al., 2002; Umezu-Goto et al., 2002). Atx is secreted by a variety of cell types and has been implicated in both disease and normal development (Moolenaar et al., 2004; van Meeteren and Moolenaar, 2007; Yuelling and Fuss, 2008; Nakanaga et al., 2010).

One of the cell types that express and secrete Atx are oligodendrocytes, the myelinating cells of the central nervous system (Fuss et al., 1997; Fox et al., 2003). Oligodendrocytes develop from oligodendrocyte progenitor cells (OPCs) that are specified in restricted regions of the central nervous system followed by extensive proliferation and migration to their prospective destinations throughout

the brain and spinal cord. *In vitro* data in rodents indicate that as oligodendrocytes develop, they undergo coordinated changes in morphology and gene expression necessary for their differentiation into mature myelinating oligodendrocytes. During this differentiation process, they transition from having a bipolar morphology into a cell with a complex network of multiple, branching processes which will eventually result in the establishment of membranous structures that wrap axons, if present. As oligodendrocytes differentiate, their gene expression profile also changes. Transcription factors of the basic helix-loop-helix family, Olig1 and Olig2 regulate oligodendrocyte specification and early differentiation, respectively, while myelin basic protein (Mbp) and proteolipid protein (Plp) are expressed during later stages of differentiation (Miller, 2002).

Previous studies from our laboratory have demonstrated that Atx and its product, LPA, are involved in regulating the differentiation of oligodendrocytes (Fuss et al., 1997; Fox et al., 2003; Fox et al., 2004; Dennis et al., 2008; Nogaroli et al., 2009). More specifically, our previous *in vitro* data suggest that LPA, likely generated via Atx's lysoPLD enzymatic site, regulates the expression of *mbp* and formation of membranous structures, while a newly identified functional domain of ATX, the MORFO domain (modulator of oligodendrocyte remodeling and focal adhesion organization) facilitates process remodeling and the development of a complex process network (Fox et al., 2003; Dennis et al., 2008; Nogaroli et al., 2009). In order for oligodendrocytes to develop into fully mature, functionally myelinating cells, they must undergo timely changes in both gene expression and

morphology. Atx, regulating both of these processes, has been identified as an important molecular player during oligodendrocyte development.

The results obtained in our previous studies were found using an *in vitro* paradigm. Thus, Atx's role in regulating oligodendrocyte development *in vivo* is still unresolved. Knockout mice for Atx die at midgestation due to severe vascular defects in the yolk and embryo proper (Tanaka et al., 2006; van Meeteren et al., 2006) preventing the study of later processes such as oligodendrocyte development and myelination.

Zebrafish are a powerful *in vivo* model in genetics and developmental biology and can be used for a large range of applications related to human disease (Lieschke and Currie, 2007). High fertility, rapidly developing and transparent embryos as well as external fertilization allow for easy manipulation and observation of many developmental processes including oligodendrocyte development and myelination in the central nervous system. Oligodendrocyte specification, differentiation and myelination, as well as many of the genes regulating these processes, have been found to be evolutionarily conserved in all vertebrates analyzed thus far, including zebrafish (Brosamle and Halpern, 2002; Park et al., 2002; Park et al., 2004; Kirby et al., 2006; Woods et al., 2006; Avila et al., 2007; Li et al., 2007a; Voas et al., 2007; Buckley et al., 2008; Buckley et al., 2010). Thus, zebrafish provide an excellent model to investigate the *in vivo* role of Atx for oligodendrocyte development. In addition, zebrafish can overcome potential vascular defects as those reported to occur in *atx* knockout mice because of their ability to survive for up to seven days without a functional

vascular system (Ny et al., 2006). This time frame of independence from a fully functional vascular system is sufficient for investigating oligodendrocyte development, which occurs within the first three to four days of development (Brosamle and Halpern, 2002; Park et al., 2002; Kirby et al., 2006; Schebesta and Serluca, 2009; Buckley et al., 2010).

In this study, we have identified the zebrafish ortholog to mammalian *atx* and characterized its expression pattern in the developing zebrafish. Using morpholino-mediated knockdown of Atx, we discovered a novel functional role for Atx during early stages of oligodendrocyte development and by doing so, have demonstrated for the first time that Atx is important for oligodendrocyte development *in vivo*. We also found that Atx can regulate later stages of differentiation in agreement with our previous *in vitro* studies. The results presented here therefore indicate that ATX is necessary for both early and late stages of oligodendrocyte development

Materials and Methods

Zebrafish strains and care

Embryos of the wild type AB strain were obtained through natural matings, raised at 28.5 °C or 24 °C, and staged according to morphological criteria and hours post fertilization (hpf) (Kimmel et al., 1995). To prevent pigmentation, embryos were raised in egg water and treated with 0.003% phenylthiourea after gastrulation.

Sequence analysis

Due to different conventions related to the nomenclature of genes, mRNAs and proteins in different species, we would like to clarify that throughout this manuscript the zebrafish conventions were used. Sequence data for *atx* were originally obtained by BLAST searches on the NCBI database (Sayers et al., 2009). Amino acid alignments and phylogenic tree analyses were performed using the Vector NTI software package (Invitrogen, Carlsbad, CA).

Cloning of cDNAs

For the *atx in situ* probe, a partial coding sequence was obtained using Not1 and EcoR1 restriction sites from the ATX ORF (clone ID 3816628; Open Biosystems, Huntsville, AL) and cloned into the pBS vector. For cloning of a partial coding sequence of *olig1* for an *in situ* probe, we performed RT-PCR on RNA isolated from 3dpf embryos using the following primers: forward (5'-ATACAGAGAGCAGGGCGAAA-3'), reverse (5'-AAACGCATGGCTGGATTAAC-3') and cloned the PCR product into the pBS vector. An *in situ* probe for *twhh* was obtained with PCR amplification of the partial coding sequence in the pDNR-LIB vector (ATCC, Manassas, Va) with the following primers: forward (5'-TGGATAACCGTATTACCGCC-3'), reverse (5'-CGCGCAATTAACCCTCACTAAAGCACTAGTCATACCAGGATC-3').

in situ hybridization

Digoxigenin- or fluorescein-labeled anti-sense cRNA probes were synthesized using T3 or T7 RNA polymerase. The following cRNA probes were used: *atx*, *mbp* (Brosamle and Halpern, 2002), *olig1*, *foxa1* (Odenthal and Nusslein-Volhard, 1998), *foxa2* (Strahle et al., 1993) and *twhh* (ATCC, Manassas, VA). *In situ* hybridizations were performed as previously described (Thisse and Thisse, 2008) with the following modification: embryos were permeabilized in proteinase K at 5ug/mL for 0.5min per hpf at 37°C followed by additional permeabilization in acetone for 8 minutes at -20C. For colorimetric *in situ* hybridizations, digoxigenin-labeled cRNA probes were used and bound cRNAs were detected using alkaline phosphatase-conjugated anti-digoxigenin antibodies and NBT/BCIP (Roche Diagnostics, Indianapolis, IN) as substrate.

Dual fluorescent *in situ* hybridizations were conducted using digoxigenin- and fluorescein-labeled cRNA probes. Bound cRNA probes were detected using peroxidase-conjugated anti-digoxigenin or anti-fluorescein antibodies (Roche Diagnostics, Indianapolis, IN) in combination with tyramide fluorochrome (Cy3 or Fluorescein) derivatives (Perkin Elmer, Waltham, MA) as previously described (Julich et al., 2005; Brend and Holley, 2009). The following parameters were modified: embryos were permeabilized in 10ug/mL proteinase K for 30min at RT and were not dehydrated in between antibody incubations.

After *in situ* RNA hybridization, embryos were either imaged as whole mounts or cryosectioned. Embryos for sectioning were sucrose cryoprotected (30% sucrose/PBS), embedded in Tissue-Tek O.C.T. compound (Sakura

Finetek, Torrance, CA), then frozen and stored at −80°C until use. Cryostat sections (20 μm) were obtained with a Shandon cryostat microtome (GMI, Ramsey, MN). Embryos and sections of colorimetric *in situ* hybridizations were mounted in 90% glycerol/PBS, while fluorescent *in situ*s were mounted in Vectashield® mounting medium (Vector laboratories, Burlingame, CA).

Immunohistochemistry

Zebrafish embryos were permeabilized using 0.25% trypsin in PBS/0.1% Tween-20 then blocked in 10% normal goat serum in PBS/0.1% Tween-20. Embryos were then incubated with primary antibodies: anti-acetylated α-tubulin (1:1000; Sigma-Aldrich, St. Louis, MO) or anti-caspase (1:50; BD Biosciences, Franklin Lakes, NJ) in blocking buffer overnight at 4°C. Secondary antibodies used were goat anti-mouse Alexa 488 (for anti-acetylated α-tubulin; Invitrogen, Carlsbad, CA) or goat-anti-rabbit Alexa 568 (for anti-caspase; Invitrogen, Carlsbad, CA).

Image analysis

Embryos and sections of colorimetric *in situ* hybridizations were mounted in 90% glycerol/PBS. Whole mount images were acquired on an Axio Observer Z.1 microscope or a Discovery.V20 stereoscope with an AxioCam MRc camera using the extended focus module of the axiovision software package (Carl Zeiss MicroImaging, Inc., Thornwood, NY). Images of MBP stained embryos were acquired on an Olympus SZX12 stereomicroscope with a DP70 digital camera

(Olympus, Center Valley, PA). Fluorescent *in situ* hybridized and antibody stained embryos were mounted in Vectashield® mounting medium (Vector laboratories, Burlingame, CA). Images were obtained using confocal laser scanning microscopy (TCS SP2 AOBS, Leica Microsystems, Exton, PA or LSM 510 META, Carl Zeiss MicroImaging, Inc., Thornwood, NY). Once captured, images were imported into Adobe Photoshop and adjustments were limited to contrast, levels, color matching settings and cropping.

Olig1-positive cell numbers were determined using the particle count plugin (Wright Cell Imaging Facility) to the ImageJ software package (Abramoff et al., 2004). Cells expressing *mbp* mRNA were visualized with a dissecting microscope and manually counted. Numbers of cells stained for *olig1* and *mbp* in the brain were counted, averaged and set as percentage of control.

Morpholino injections

Morpholino anti-sense oligonucleotides (MOs) were designed and synthesized by GeneTools (Philomath, OR) in accordance with the published zebrafish genome data (ensemble entry ENSDART00000047920). Two *atx* MOs were used: Translation blocking (5'-TGCGTCTGGTGGCTCTCTTCCACAC-3') and splice-blocking (5'-AAGAAGCATCCTACTTTTTGAGAGC-3'). As controls, 5 base pair mismatch MOs were used: translation blocking control: (5'-TGCGTGTGGTGCCTGTCTTGCAGAC-3') and splice-blocking control: (5'-AACAAGGATCGTACTTTTTGACACC-3'). MOs were reconstituted in ddH2O and quantified by fiber optic spectrophotometry using the Nanodrop ND-1000

(Nanodrop Inc., Wilmington, DE) as previously described (Arbogast, 2007). MOs were then diluted in Danieau buffer (Westerfield, 1993) and 1nL was injected at the 1 to 4-cell stage. The *atx* translation-blocking MO and its control were injected at a concentration of 1mg/mL, while the *atx* splice-blocking MO and its control were used at a concentration of 10mg/mL.

Western blot analysis

Embryos were deyolked as previously described (Westerfield, 2000). Briefly, embryos were anesthetized with Tricaine, resuspended in cold Ringer's solution containing 1mM EDTA and cOmplete mini protease inhibitor cocktail (Roche Diagnostics, Indianapolis, IN) and triturated with a 1-200µL pipette tip. Embryos were washed twice in Ringer's solution, homogenized in 40mM HEPES; 40mM NaCl; 10mM EDTA; 1% Triton; 0.1% SDS with cOmplete mini protease inhibitor cocktail and centrifuged at 10,000rpm for 3 min. Supernatants were collected and used for further analysis

Supernatants of whole, deyolked embryos were separated on 7.5% precast acrylamide gels (MiniProtean TGX precast gel; BioRad, Hercules, CA), and proteins were transferred onto immobilon-P membranes (Millipore, Billerica, MA). Membranes were blocked in 5% milk/PBS/0.1% Tween-20 for 30 min and incubated with primary antibodies overnight at 4°C. The following antibodies were used: zebrafish-specific anti-Atx (1:750; EZBiolab, Carmel, IN) and anti-actin (1:500; Sigma-Aldrich, St. Louis, MO). The zebrafish-specific anti-Atx antibody was generated against a peptide by EZbiolab and is not available

commercially. In antibody blocking experiments, anti-ATX antibodies were preincubated in a 1:2 dilution of antigenic peptide for 30 min. For detection of bound primary antibodies, membranes were incubated with a HRP-conjugated goat anti-rabbit IgG secondary antibody (1:10,000; Vector Laboratories, Burlingame, CA) for 30 min. Bound antibody complexes were detected using Amersham ECL plus western blot detection reagents (GE Healthcare, Piscataway, NJ). Chemiluminescent signals were detected using a Futura 2000K developer (Fisher Scientific, Pittsburgh, PA). For densitometric analysis the ImageJ software package was used (Abramoff et al., 2004).

qRT-PCR

Total RNA was isolated from embryos using Trizol (Invitrogen, Carlsbad, CA) and RNA samples were treated with DNase using the DNA-Free kit (Applied Biosystems, Austin, TX). RNA was quantified by fiber optic spectrophotometry using the Nanodrop ND-1000 (Nanodrop Inc., Wilmington, DE). For qRT-PCR, oligo (dT)-primed cDNAs were synthesized using the Superscript II RT kit (Invitrogen, Carlsbad, CA). PCR was performed on a Chromo 4 Four-Color Real-Time or a CFX96 system (BioRad, Hercules, CA) using the iQ SYBR Green Supermix (BioRad, Hercules, CA). The following primer pairs were used at an annealing temperature of 58°C: mbp (Buckley et al., 2010); plp1b: forward (5'-TGCCATGCCAGGGGTTGTTTGTGGA-3'), reverse (5' TGGCGACCATGTAAACGAACAGGGC-3'); cldnk: forward (5'-TGGCATTTCGGCTCAAGCTCTGGA-3'), reverse (5'-

GGTACAGACTGGGCAATGGACCTGA-3'); olig1: forward: (5'-CCGGTGTAGGGGGAGCACTGCA-3'), reverse (5-'TCCGAGCCAGCACCAGTGTCGAG-3'). β-actin (Buckley et al., 2010) and EF1α: forward (5'-GTACTACTCTTCTTGATGCCC-3'), reverse (5'-GTACAGTTCCAATACCTCCA-3') were also amplified and their geometric averages were used for normalization (Vandesompele et al., 2002).

PCR conditions were as follows: 95°C for 3 min followed by 39 cycles at 94°C for 15 s, annealing temperature for 20 s, and 72°C for 20 s. For relative comparison of mbp, olig1, plp1b and cldnk mRNA levels present in atx TL MO or atx E2I2 MO-treated embryos compared to their respective controls, the ΔΔCT method was used (Livak and Schmittgen, 2001).

Results

Atx is expressed in the zebrafish

The expression of *atx* has been described in a number of vertebrate species, including human, rat, mouse, chicken and frog, thus suggesting that *atx* represents an evolutionary conserved gene in vertebrates including the zebrafish (Murata et al., 1994; Narita et al., 1994; Bachner et al., 1999; Ohuchi et al., 2007; Masse et al., 2010). To identify the *atx* ortholog in zebrafish, BLAST searches were performed using the zebrafish genome database (http://www.zfin.org) and the rat and human *atx* mRNA sequences. A single entry (NM_200603.1) with high homology to the existing *atx* sequences was identified (Fig. 4.1). The sequence identity of zebrafish *atx* with its orthologs is similar to what has been

described for other zebrafish genes (Brosamle and Halpern, 2002). Amino acid sequence alignments further confirmed the presence of conserved functional domains within zebrafish Atx, including the enzymatically active lysoPLD site that is critically dependent on the presence of the tyrosine-residue located at position 210 in the human sequence (Fig. 4.1C; (Clair et al., 1997; Gijsbers et al., 2003; Koh et al., 2003; Masse et al., 2010).

The human and mouse *atx* genes span 27 exons and give rise to three known protein isoforms, Atxα, Atxβ and Atxγ, due to alternative splicing of exons 12 and 21 (Giganti et al., 2008). Out of the known Atx protein isoforms, Atxβ, which lacks exons 12 and 21, appears to be the evolutionary oldest form, since it is present in all species so far characterized. Atxγ has been identified in the rat but not in chicken or zebrafish (data not shown and (Narita et al., 1994; Fuss et al., 1997).

In the teleost fish lineage, whole-genome duplication occurred subsequent to its divergence from mammals, thus generating co-orthologs to many single mammalian genes (Ohno, 1970; Taylor et al., 2003; Postlethwait et al., 2004). Two zebrafish *atx* genes with almost identical coding sequences with 99.6% identity have so far been identified. These two *atx* genes are located next to each other, and they are transcribed in the same direction. Due to the fact that both genes are located right next to each other and not on different linkage groups, they are likely a result of a tandem rather than a large scale genome duplication event.

To assess the extent to which *atx* is expressed in the developing zebrafish in a similar pattern as described for the other vertebrate species, we performed *in situ* hybridizations. In these studies, a*tx* mRNA was first detected at 36hpf. At all developmental stages analyzed (36-72hpf), *atx* mRNA was found to be present in the pectoral fin buds, the anterior pharyngeal arches (mandibular and hyoid) and the developing vasculature (posterior cardinal vein and head vessels) (Fig. 4.2A). Up to 72hpf, *atx* mRNA was additionally found in the hypochord and the cephalic floor plate. Both of these are transient structures that are no longer present at older ages (Altman and Bayer, 1984; Eriksson and Lofberg, 2000). Furthermore, *atx* mRNA could be detected in the posterior lateral line with mRNA levels decreasing with age. From lateral views, *atx* mRNA was also detectable in a structure resembling the trabecula cranii, a component of the neurocranium. *Atx* mRNA localization in the developing vasculature and the cephalic floor plate was further confirmed by comparative *in situ* hybridization using cRNA probes to genes known to be expressed in the vasculature (*fli1a*) or the floor plate (*foxa1*, *foxa2* and *twhh*) (Brown et al., 2000) (data not shown and Fig. 4.2B).

Detailed *atx* expression profiles during development have so far only been described for mouse, chick and frog (Bachner et al., 1999; Ohuchi et al., 2007; Masse et al., 2010). In these studies and similar to the zebrafish, *atx* was found expressed in the developing extremities (fin or limb buds) and jaw (pharyngeal arches). *Atx* expression in the developing vasculature, however, appears to be a feature restricted to lower vertebrates, the chick, frog and zebrafish. Nonetheless, Atx has been functionally implicated in regulating blood vessel

formation during development in the mouse. Thus, despite differences in the pattern of expression, Atx likely plays a functionally conserved role in regulating the formation and/or maintenance of the vasculature. *Atx* expression in the floor plate and/or ventral spinal cord was observed in all species analyzed with the exception of the chick. So far, the only structure in which *atx* appears to be expressed in a zebrafish-unique fashion is the hypochord, a structure that only exists in anamniotes and that has no homolog in mammals.

Taken together, the above data demonstrate that *atx* is a gene whose sequence is evolutionarily conserved within vertebrates. In addition, conserved features can be identified in *atx*'s developmental expression pattern. Thus, it is likely that ATX's functional properties are, at least in part, also evolutionarily conserved within vertebrates.

atx is expressed by differentiating oligodendrocytes in the developing zebrafish

Our previous studies identified ATX as a protein that is expressed and released by developing oligodendrocytes during the developmental period of active myelination (Fuss et al., 1997; Fox et al., 2003). Active myelination in the zebrafish has been described to occur between 48hpf and 96hpf in the developing hindbrain (Brosamle and Halpern, 2002; Buckley et al., 2010). Thus, to assess the extent to which *atx* is expressed by differentiating oligodendrocytes, we performed double-fluorescent *in situ* hybridizations of zebrafish embryos staged at 72hpf, a time point at which premyelinating and

actively myelinating oligodendrocytes are present, and *atx* was found expressed in the hindbrain (Fig. 4.2). To be able to unequivocally identify differentiating oligodendrocytes, we used cRNA probes specific for *mbp* and *plp1b* (Brosamle and Halpern, 2002). As shown in Fig. 4.3., *plp1b*-positive cells located in the developing hindbrain were also positive for *atx*. Similar results were obtained for *mbp*-positive cells (data not shown). Interestingly, we could not detect expression of *atx* in either *mbp*- or *plp1b*-positive cells at 60hpf, suggesting that *atx* expression may be restricted to the later stages of the oligodendrocyte lineage or very low and thus below the detection limit at the earlier stages analyzed.

The above data demonstrate that at least in the developing hindbrain of the zebrafish oligodendrocytes, similar to what has been observed in the rat, express *atx* during a time period when active myelination occurs.

Down-regulation of atx expression inhibits and/or delays the appearance of mbp-positive oligodendrocytes in the developing zebrafish hindbrain without significantly affecting the establishment and/or maintenance of axonal tracts

In vitro studies from our laboratory demonstrated that *atx'*s expression by differentiating oligodendrocytes is important for coordinating their timely development (Fuss et al., 1997; Fox et al., 2003; Fox et al., 2004; Dennis et al., 2005; Dennis et al., 2008; Yuelling and Fuss, 2008; Nogaroli et al., 2009). To determine the extent to which *atx* expression may be regulating oligodendrocyte development *in vivo* in the zebrafish, a translation-blocking morpholino (*atx* TL

MO) was used to knock-down *atx* expression. To assess the efficiency of this morpholino, western blot analyses were performed. As shown in Fig. 4.4A, injection of the *atx* TL MO resulted in reduced Atx protein levels. Interestingly, antibodies against zebrafish Atx recognized two molecular weight forms in whole zebrafish homogenates. The appearance of both molecular weight forms can be inhibited by pre-incubation with the peptide used to generate the zebrafish-specific antibodies. The nature of these two molecular weight forms is not entirely clear. It is most likely that they reflect differences in posttranslational modifications, such as glycosylations (Pradere et al., 2007). Both forms were included for quantification via densitometry.

After having verified that injection of the *atx* TL MO leads to significantly decreased Atx protein levels, developing zebrafish embryos staged at 66hpf were assessed for the presence of differentiating oligodendrocytes. For this purpose, *in situ* hybridizations using a cRNA probe specific for *mbp* were performed. As shown in Fig. 4.5A-C and F, there was a significantly reduced number of *mbp*-positive cells detectable in the hindbrain of *atx* TL MO-injected zebrafish embryos. This effect on the presence of mbp-positive cells in the CNS was much more dramatic than any effect noticed in the PNS. To further confirm the specificity of the effect of a reduction in *atx* expression on the timely appearance of mbp-positive cells, a splice blocking morpholino was used (*atx* E2I2 MO). RT-PCR analysis demonstrated that injection of the *atx* E2I2 MO led to an altered splice pattern and efficient elimination of atx's exon 2. The control

MO did not have such an effect (Fig. 4.4B). Elimination of exon 2 leads to premature termination of translation, due to the creation of a frame shift stop codon, and thus to reduced levels of full length Atx. As shown in Fig. 4.5.E, injection of the *atx* E2I2 MO led to a similar reduction in the number of zebrafish embryos expressing normal (untreated) levels of *mbp* mRNA as seen for the *atx* TL MO. To further substantiate these data, quantitative RT-PCR analysis was performed. As shown in Fig. 4.5G and E, injection of either *atx* MO led to a significant reduction in the levels of *mbp* RNA.

Due to the presence of early CNS defects in *atx* knock-out mice (Tanaka et al., 2006; van Meeteren et al., 2006; Fotopoulou et al., 2010), we wanted to ensure that the observed effects on oligodendrocytes were not secondary to gross effects on the axonal network. To assess the integrity of axonal projections, control and *atx* TL MO-injected embryos were immunostained with an anti-acetylated α-tubulin antibody. No significant differences were noted (Fig. 4.6).

Taken together, these data demonstrate that a reduction in the expression of *atx* inhibits and/or delays the appearance of *mbp*-positive oligodendrocytes in the developing zebrafish hindbrain without significantly affecting the establishment and/or maintenance of axonal tracts.

Down-regulation of atx expression inhibits and/or delays the appearance of the later stages of the oligodendrocyte lineage in the developing zebrafish hindbrain

The reduced number of *mbp*-positive cells seen upon atx MO injection could either be due to a specific effect on *mbp* expression or to an inhibition/delay of oligodendrocyte differentiation. To address this question, we performed in situ hybridizations using cRNA probes specific for two additional genes known to be expressed by differentiating oligodendrocytes just prior to or during myelination, namely *plp1b* and *claudinK* (Brosamle and Halpern, 2002; Takada and Appel, 2010). Injection of either *atx* MO led to a decrease in both *plp1b* and *claudinK* mRNA levels.

These data indicate that in the developing zebrafish hindbrain *atx* is an important regulator of oligodendrocyte differentiation at least at the later stages of the lineage.

Down-regulation of atx expression inhibits and/or delays the appearance of very early stages of the oligodendrocyte lineage in the developing zebrafish hindbrain

The above findings related to a role of Atx in regulating the differentiation of later stages of the oligodendrocyte lineage, similar to what has been described for differentiating rodent oligodendrocytes in culture (Nogaroli et al., 2009). In the cell culture studies, the effect of Atx was mediated by an autocrine mechanism via the secretion of Atx by differentiating oligodendrocytes. It is thus likely that

such an autocrine mechanism also contributes to the effects seen in the zebrafish. However, prior to the time of analysis, namely 66hpf, zebrafish oligodendrocytes appear to only express very low levels of *atx*. The major source of Atx release into the hindbrain at these earlier ages is the cephalic floorplate. Thus, Atx may be present in the developing hindbrain at very early stages during oligodendrocyte development. To assess the extent to which such an early developmental presence of Atx may influence oligodendrocyte differentiation, *in situ* hybridizations were performed using a cRNA probe specific for one of the earliest known genes specifically expressed in cells of the oligodendrocyte lineage in the zebrafish (Li et al., 2007a; Schebesta and Serluca, 2009). As shown in Fig. 4.8, upon injection of the *atx* TL MO the number of *olig1*-positive cells was found significantly reduced in the hindbrain of the developing zebrafish. Similarly, *olig1* mRNA levels were significantly lower compared to controls. This reduction in the number of *olig1*-positive cells was not found associated with a drastic increase in cell death as assessed by the presence of activated caspase 3 (data not shown).

Taken together, these data demonstrate that Atx *in vivo* in the developing zebrafish regulates the differentiation and/or specification of early stages of the oligodendrocyte lineage. In addition, our data suggest that this novel role of Atx during early oligodendrocyte development occurs by a paracrine mechanism via the secretion of Atx by cells of the cephalic floor plate.

Discussion

The data presented here demonstrate that *atx* is expressed in the zebrafish in a similar pattern as seen in other vertebrates and is necessary for regulating the later stages of oligodendrocyte development confirming our *in vitro* data (Nogaroli et al., 2009). We have also identified a novel function of ATX during early stages of oligodendrocyte development when specification and early differentiation is occurring.

Our expression analysis is the first complete developmental study of *atx* expression in the zebrafish embryo. Similar developmental studies have been conducted in mouse, chick and frog (Bachner et al., 1999; Ohuchi et al., 2007; Masse et al., 2010) reporting similar expression patterns and confirming evolutionary conservation of *atx's* expression pattern. Expression of *atx* in the floor plate is consistent with the mouse and potentially the frog where they describe expression in the ventral spinal cord (Bachner et al., 1999; Ohuchi et al., 2007; Masse et al., 2010). Before this study, *atx* expression by oligodendrocytes has only been reported for rodents (Fuss et al., 1997; Fox et al., 2003).

In the search for the function of Atx *in vivo*, ubiquitous deletion of *atx* in mice led to embryonic lethality due to vascular defects (Tanaka et al., 2006; van Meeteren et al., 2006; Fotopoulou et al., 2010). Before their death, *atx*-null mice display early central nervous system defects including failure of neural tube closure and increased cell death while heterozygous mice showed no phenotypic abnormalities (Fotopoulou et al., 2010). In order to study oligodendrocyte

developmental processes without affecting overall zebrafish development, especially central nervous system abnormalities, careful titration of our morpholinos was necessary. Titration of the morpholinos resulted in a reduction in Atx levels to 50% of control, which was sufficient for studying oligodendrocyte development in this system without major central nervous system defects. In agreement with this observation, phenotypically normal heterozygous mice have 50% Atx protein levels at least in the blood (van Meeteren et al., 2006) and our previous *in vitro* observations were also observed under conditions with 50% Atx protein levels (Nogaroli et al., 2009) indicating that functions of Atx during oligodendrocyte development do not require complete down-regulation of the protein allowing our analyses to be conducted without major gross abnormalities.

Upon down-regulation of Atx, we observed embryos with less *olig1*-expressing oligodendrocytes compared to controls. *olig1* is expressed by oligodendrocytes early during their development, shortly after they are specified, preceded by the expression of *olig2* (Park et al., 2002; Li et al., 2007a; Schebesta and Serluca, 2009). In order for oligodendrocytes to perform their ultimate function in myelination, they must first be specified at appropriate times then undergo tightly controlled, distinct stages of differentiation. It is unclear at this time what mechanisms are affected resulting in the phenotype observed here, but it is possible that the numbers of oligodendrocytes are reduced due to deficits in oligodendrocyte specification or proliferation. LPA has been shown to induce differentiation of oligodendrocytes from neuroepithelial precursor cells (Cui and Qiao, 2007) and proliferation in cell types other than oligodendrocytes

(Li et al., 2003; Yan et al., 2003; Shano et al., 2008). Signals released from the floor plate, including the glycoprotein SHH as described in chapter three, have the ability to regulate the expression of transcription factors important for the specification and differentiation of oligodendrocytes including *olig1* and *olig2* which are necessary for oligodendrocyte specification and differentiation, respectively (Park et al., 2002; Schebesta and Serluca, 2009). It was found in the mouse that ATX cannot regulate *shh* expression (Fotopoulou et al., 2010) making it unlikely to occur in the zebrafish and indicating that the changes we see are not indirectly due to a modulation of *shh* expression. In further support of this idea, *atx* is expressed in the floor plate during the time when oligodendrocytes are being specified and during their early development (Park et al., 2002; Schebesta and Serluca, 2009).

mRNA levels of the later stage oligodendrocyte markers, *mbp*, *plp1b* and *cldnk* were also found to be reduced along with *olig1*. In order to determine if the reduction in later stage mRNA levels were a result of Atx affecting later stages of differentiation or simply a result of fewer *olig1*-positive oligodendrocytes, we counted the number of *mbp*-positive oligodendrocytes. We found significantly fewer *mbp*-positive oligodendrocytes in relation to the number of *olig1*-positive oligodendrocytes when Atx levels were reduced. This indicates that the reduced number of *mbp*-positive oligodendrocytes is not solely a result of the reduction in *olig1*-positive oligodendrocytes, but because of Atx affecting *mbp* expression during later stages of differentiation, which is in agreement with our previous *in vitro* studies described in chapter two (Nogaroli et al., 2009). Despite the

differences observed in *olig1*- and *mbp*-oligodendrocyte cell numbers, we did not see differences in their mRNA levels. This is likely because Atx may also affect *mbp* expression in Schwann cells. Unfortunately, we were unable to count the number of *mbp*-positive Schwann cells in order to figure out this discrepancy because individual cells cannot be visualized at the time of our analysis. Expression of *mbp* by Schwann cells could therefore be masking the actual mRNA levels expressed in oligodendrocytes leading to no differences between *mbp* and *olig1* overall mRNA levels. Since *cldnk* is also expressed by both oligodendrocytes and Schwann cells (Takada and Appel, 2010), we would then suspect the same reduction in *cldnk* cell numbers. *Plp1b* mRNA levels were also not significantly different than *olig1* levels and because *plp1b* is only expressed by oligodendrocytes (Brosamle and Halpern, 2002), Atx down-regulation did not affect its expression suggesting that Atx may mediate the expression of specific genes.

The role for Atx in regulating *mbp* expression during zebrafish oligodendrocyte development is likely attributable to LPA generated from Atx's lysoPLD enzymatic site and not the recently identified MORFO domain (Dennis et al., 2008) based on our previous *in vitro* data (Nogaroli et al., 2009) and unpublished findings from our laboratory. LPA receptors are expressed by oligodendrocytes in the rodent (Stankoff et al., 2002; Nogaroli et al., 2009) and so far, one LPA receptor (LPA1) has been identified in the zebrafish (Lee et al., 2008). Whether LPA receptors are expressed in oligodendrocytes of the zebrafish and if LPA directly functions in this system has yet to be determined.

Expression of *mbp* has been shown to be a reliable method for quantifying myelin as well as myelination (Buckley et al., 2010). The decreased *mbp* mRNA levels observed upon down-regulation of Atx could potentially have functional consequences on myelination. We have not investigated whether reduced Atx levels will ultimately affect the myelination process. The timing of myelination (Brosamle and Halpern, 2002; Buckley et al., 2010) occurs near the outer limits of morpholino functionality. Thus, it may not be possible to investigate Atx's role on myelination with the methods available at this time.

atx expression in the floor plate begins to diminish when expression by oligodendrocytes begins. This could indicate a "switch" in expression between the floor plate and oligodendrocytes. As oligodendrocytes mature, they migrate away from the floor plate to populate the brain and spinal cord. Due to the distance that differentiating oligodendrocytes reside from the floor plate, and because the floor plate is a transient structure (Altman and Bayer, 1984), it may be crucial that oligodendrocytes generate *atx* themselves in order to promote their further differentiation. The use of new methods, such as caged morpholinos (Deiters et al., 2010), which have the ability to allow for temporal regulation of gene down-regulation, could aid in looking further into ATX's role during later stages of differentiation as a more comparable study to the *in vitro* data described in chapter two (Nogaroli et al., 2009).

All of the effects reported in this study are likely due to reduced expression of *atx* located in the floor plate, before we could detect expression in oligodendrocytes, indicating that Atx-mediated regulation may be via a paracrine

mechanism and not solely by an autocrine mechanism as previously thought by us and others (Stracke et al., 1992; Fuss et al., 1997; Fox et al., 2003; Fox et al., 2004; Dennis et al., 2008; Nogaroli et al., 2009). We cannot rule out the possibility that an autocrine mechanism is also involved during this time due to limits of the detection methods in oligodendrocytes. This is therefore the first study to suggest that Atx secreted from a separate non-oligodendroglial source regulates in particular the early stages of oligodendrocyte development.

Taken together, the data presented in this manuscript suggest that Atx is crucial for the timely appearance of differentiating oligodendrocytes prior to them becoming myelinating cells. Atx regulates this process during early stages of their development and continues to have a regulatory role through later stages of their development. Future studies will be necessary to dissect the exact mechanisms by which Atx regulates the biology of cells of the oligodendrocyte lineage.

Acknowledgements:

The authors would like to thank Bruce Appel for reagents and helpful discussions and Cynthia Cornelissen for use of instrumentation. Confocal and brightfield microscopy was performed at VCU's Department of Neurobiology and Anatomy Microscopy Facility, which was supported, in part, through NIH-NINDS Center Core grant 5P30NS047463. This work was supported by grants from the National Institute of Health (B.F.) and the National Multiple Sclerosis Society (B.F.).

Figure 4.1. **Zebrafish ATX amino acid identity is conserved with human, rat, mouse and chick ATX.** Sequences were obtained from the NCBI, ensembl or ZFIN database and cluster-aligned using the AlignX Software module of the Vector NTI software package (Invitrogen, Carlsbad, CA). (A and B). Phylogenetic tree and amino acid sequence identity percentages. (C) Amino acid sequence alignment. All letters are black and are distinguished by background color. Amino acids identical in all sequences are represented in yellow. The degree of conservation is color coded (light blue>magenta>white). Blocks of similar amino acids are represented in green. The T residue required for enzymatic activity, is marked by white letters on a dark blue background. The lyso-phospholipase D-active site is single underlined; nuclease-like domain is double-underlined, the MORFO domain overlaps with the nuclease domain and extra amino acids in MORFO are indicated by a dotted line. The somatomedin B domains are marked by a wavy line.

A

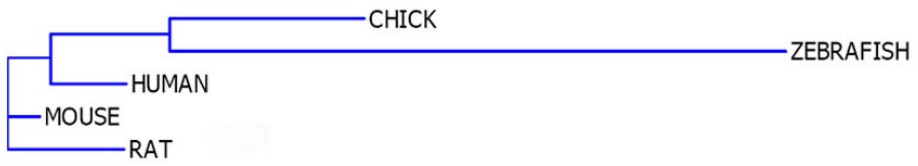

B

	HUMAN	MOUSE	RAT	CHICKEN	ZEBRAFISH
HUMAN	100	94	90	84	66
MOUSE		100	94	84	66
RAT			100	80	63
CHICKEN				100	66
ZEBRAFISH					100

C

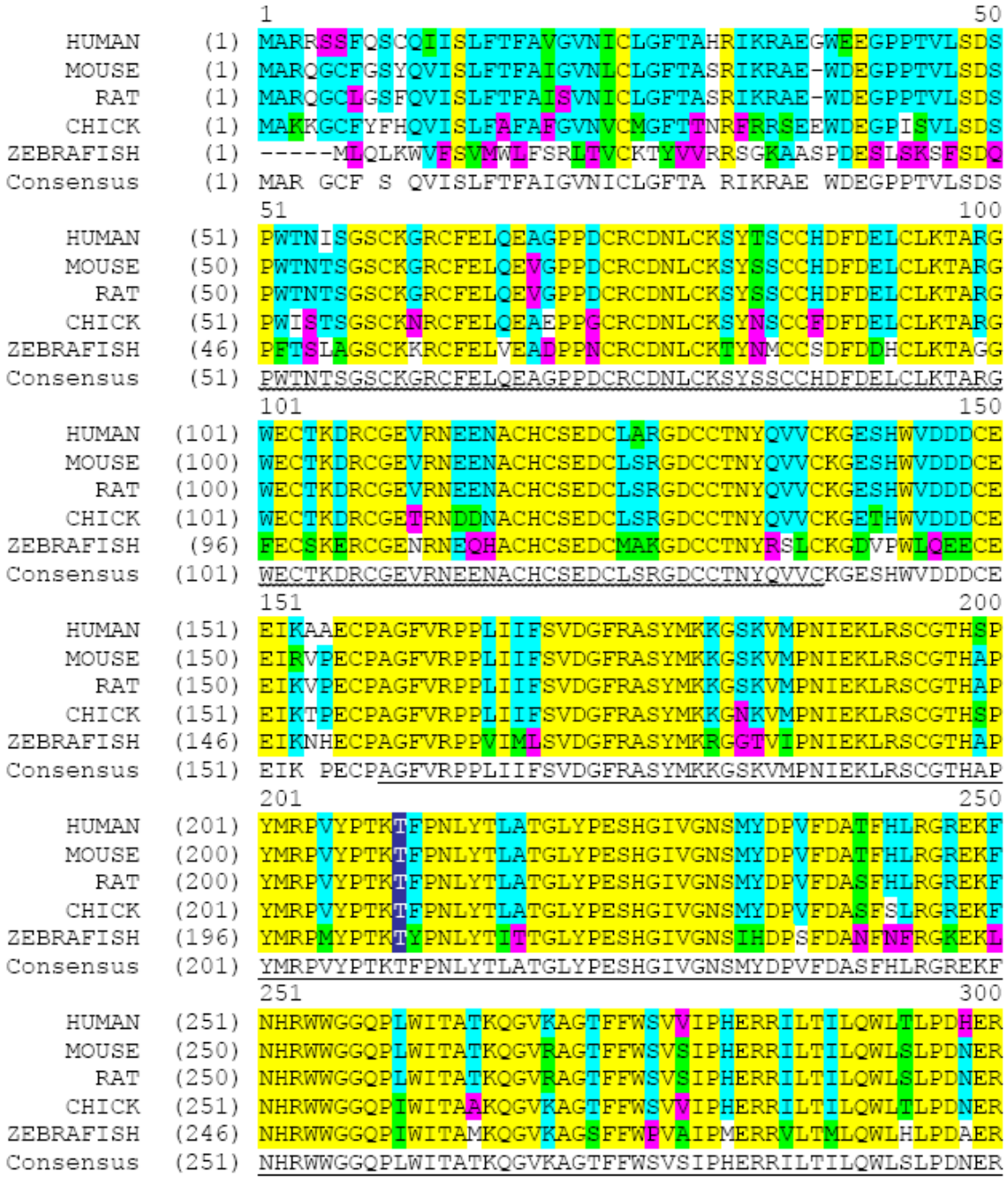
1 50
HUMAN (1) MARRSSFQSCQIISLFTFAVGVNICLGFTAHRIKRAEGWEEGPPTVLSDS
MOUSE (1) MARQGCFGSYQVISLFTFAIGVNLCLGFTASRIKRAE-WDEGPPTVLSDS
RAT (1) MARQGCLGSFQVISLFTFAISVNICLGFTASRIKRAE-WDEGPPTVLSDS
CHICK (1) MAKKGCFYFHQVISLFAFAFGVNVCMGFTTNRFRRSEEWDEGPISVLSDS
ZEBRAFISH (1) -----MLQLKWVFSVMWLFSRLTVCKTYVVRRSGKAASPDESLSKSFSDQ
Consensus (1) MAR GCF S QVISLFTFAIGVNICLGFTA RIKRAE WDEGPPTVLSDS
51 100
HUMAN (51) PWTNISGSCKGRCFELQEAGPPDCRCDNLCKSYTSCCHDFDELCLKTARG
MOUSE (50) PWTNTSGSCKGRCFELQEVGPPDCRCDNLCKSYSSCCHDFDELCLKTARG
RAT (50) PWTNTSGSCKGRCFELQEVGPPDCRCDNLCKSYSSCCHDFDELCLKTARG
CHICK (51) PWISTSGSCKNRCFELQEAEPPGCRCDNLCKSYNSCCFDFDELCLKTARG
ZEBRAFISH (46) PFTSLAGSCKKRCFELVEADPPNCRCDNLCKTYNMCCSDFDDHCLKTAGG
Consensus (51) PWTNTSGSCKGRCFELQEAGPPDCRCDNLCKSYSSCCHDFDELCLKTARG
101 150
HUMAN (101) WECTKDRCGEVRNEENACHCSEDCLARGDCCTNYQVVCKGESHWVDDDCE
MOUSE (100) WECTKDRCGEVRNEENACHCSEDCLSRGDCCTNYQVVCKGESHWVDDDCE
RAT (100) WECTKDRCGEVRNEENACHCSEDCLSRGDCCTNYQVVCKGESHWVDDDCE
CHICK (101) WECTKDRCGETRNDDNACHCSEDCLSRGDCCTNYQVVCKGETHWVDDDCE
ZEBRAFISH (96) FECSKERCGENRNEQHACHCSEDCMAKGDCCTNYRSLCKGDVPWLQEECE
Consensus (101) WECTKDRCGEVRNEENACHCSEDCLSRGDCCTNYQVVCKGESHWVDDDCE
151 200
HUMAN (151) EIKAAECPAGFVRPPLIIFSVDGFRASYMKKGSKVMPNIEKLRSCGTHSP
MOUSE (150) EIRVPECPAGFVRPPLIIFSVDGFRASYMKKGSKVMPNIEKLRSCGTHAP
RAT (150) EIKVPECPAGFVRPPLIIFSVDGFRASYMKKGSKVMPNIEKLRSCGTHAP
CHICK (151) EIKTPECPAGFVRPPLIIFSVDGFRASYMKKGNKVMPNIEKLRSCGTHSP
ZEBRAFISH (146) EIKNHECPAGFVRPPVIMLSVDGFRASYMKRGGTVIPNIEKLRSCGTHAP
Consensus (151) EIK PECPAGFVRPPLIIFSVDGFRASYMKKGSKVMPNIEKLRSCGTHAP
201 250
HUMAN (201) YMRPVYPTKTFPNLYTLATGLYPESHGIVGNSMYDPVFDATFHLRGREKF
MOUSE (200) YMRPVYPTKTFPNLYTLATGLYPESHGIVGNSMYDPVFDATFHLRGREKF
RAT (200) YMRPVYPTKTFPNLYTLATGLYPESHGIVGNSMYDPVFDASFHLRGREKF
CHICK (201) YMRPVYPTKTFPNLYTLATGLYPESHGIVGNSMYDPVFDASFSLRGREKF
ZEBRAFISH (196) YMRPMYPTKTYPNLYTITTGLYPESHGIVGNSIHDPSFDANFNFRGKEKL
Consensus (201) YMRPVYPTKTFPNLYTLATGLYPESHGIVGNSMYDPVFDASFHLRGREKF
251 300
HUMAN (251) NHRWWGGQPLWITATKQGVKAGTFFWSVVIPHERRILTILQWLTLPDHER
MOUSE (250) NHRWWGGQPLWITATKQGVRAGTFFWSVSIPHERRILTILQWLSLPDNER
RAT (250) NHRWWGGQPLWITATKQGVRAGTFFWSVSIPHERRILTILQWLSLPDNER
CHICK (251) NHRWWGGQPIWITAAKQGVKAGTFFWSVVIPHERRILTILQWLTLPDNER
ZEBRAFISH (246) NHRWWGGQPIWITAMKQGVKAGSFFWPVAIPMERRVLTMLQWLHLPDAER
Consensus (251) NHRWWGGQPLWITATKQGVKAGTFFWSVSIPHERRILTILQWLSLPDNER

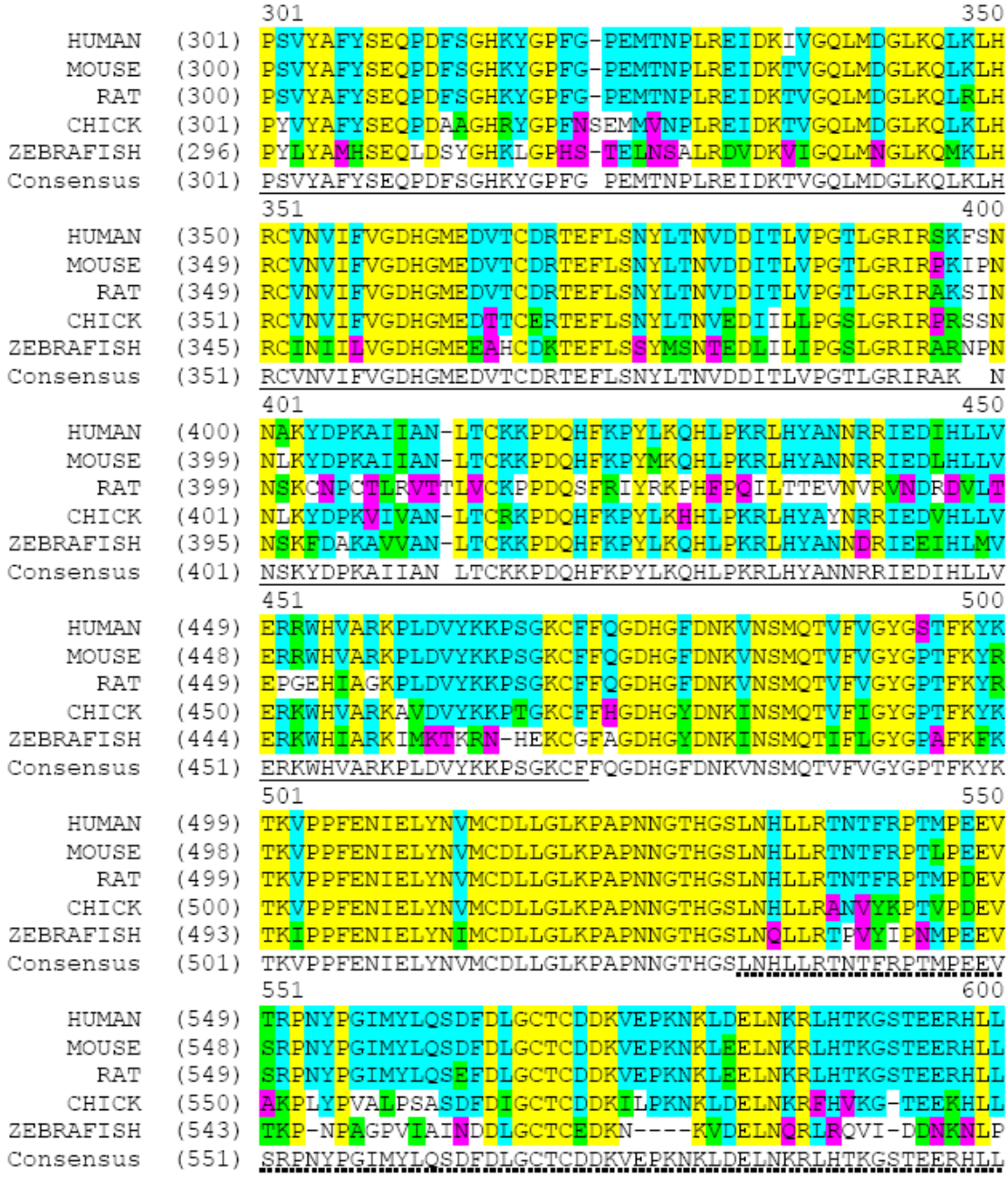
301 350
HUMAN (301) PSVYAFYSEQPDFSGHKYGPFG-PEMTNPLREIDKIVGQLMDGLKQLKLH
MOUSE (300) PSVYAFYSEQPDFSGHKYGPFG-PEMTNPLREIDKTVGQLMDGLKQLKLH
RAT (300) PSVYAFYSEQPDFSGHKYGPFG-PEMTNPLREIDKTVGQLMDGLKQLRLH
CHICK (301) PYVYAFYSEQPDAAGHRYGPFNSEMMVNPLREIDKTVGQLMDGLKQLKLH
ZEBRAFISH (296) PYLYAMHSEQLDSYGHKLGPHS-TELNSALRDVDKVIGQLMNGLKQMKLH
Consensus (301) PSVYAFYSEQPDFSGHKYGPFG PEMTNPLREIDKTVGQLMDGLKQLKLH
351 400
HUMAN (350) RCVNVIFVGDHGMEDVTCDRTEFLSNYLTNVDDITLVPGTLGRIRSKFSN
MOUSE (349) RCVNVIFVGDHGMEDVTCDRTEFLSNYLTNVDDITLVPGTLGRIRPKIPN
RAT (349) RCVNVIFVGDHGMEDVTCDRTEFLSNYLTNVDDITLVPGTLGRIRAKSIN
CHICK (351) RCVNVIFVGDHGMEDTTCERTEFLSNYLTNVEDIILLPGSLGRIRPRSSN
ZEBRAFISH (345) RCINIILVGDHGMEEAHCDKTEFLSSYMSNTEDLILIPGSLGRIRARNPN
Consensus (351) RCVNVIFVGDHGMEDVTCDRTEFLSNYLTNVDDITLVPGTLGRIRAK N
401 450
HUMAN (400) NAKYDPKAIIAN-LTCKKPDQHFKPYLKQHLPKRLHYANNRRIEDIHLLV
MOUSE (399) NLKYDPKAIIAN-LTCKKPDQHFKPYMKQHLPKRLHYANNRRIEDLHLLV
RAT (399) NSKCNPCTLRVTTLVCKPPDQSFRIYRKPHFPQILTTEVNVRVNDRDVLT
CHICK (401) NLKYDPKVIVAN-LTCRKPDQHFKPYLKHHLPKRLHYAYNRRIEDVHLLV
ZEBRAFISH (395) NSKFDAKAVVAN-LTCKKPDQHFKPYLKQHLPKRLHYANNDRIEEIHLMV
Consensus (401) NSKYDPKAIIAN LTCKKPDQHFKPYLKQHLPKRLHYANNRRIEDIHLLV
451 500
HUMAN (449) ERRWHVARKPLDVYKKPSGKCFFQGDHGFDNKVNSMQTVFVGYGSTFKYK
MOUSE (448) ERRWHVARKPLDVYKKPSGKCFFQGDHGFDNKVNSMQTVFVGYGPTFKYR
RAT (449) EPGEHIAGKPLDVYKKPSGKCFFQGDHGFDNKVNSMQTVFVGYGPTFKYR
CHICK (450) ERKWHVARKAVDVYKKPTGKCFFHGDHGYDNKINSMQTVFIGYGPTFKYK
ZEBRAFISH (444) ERKWHIARKIMKTKRN-HEKCGFAGDHGYDNKINSMQTIFLGYGPAFKFK
Consensus (451) ERKWHVARKPLDVYKKPSGKCFFQGDHGFDNKVNSMQTVFVGYGPTFKYK
501 550
HUMAN (499) TKVPPFENIELYNVMCDLLGLKPAPNNGTHGSLNHLLRTNTFRPTMPEEV
MOUSE (498) TKVPPFENIELYNVMCDLLGLKPAPNNGTHGSLNHLLRTNTFRPTLPEEV
RAT (499) TKVPPFENIELYNVMCDLLGLKPAPNNGTHGSLNHLLRTNTFRPTMPDEV
CHICK (500) TKVPPFENIELYNVMCDLLGLKPAPNNGTHGSLNHLLRANVYKPTVPDEV
ZEBRAFISH (493) TKIPPFENIELYNIMCDLLGLKPAPNNGTHGSLNQLLRTPVYIPNMPEEV
Consensus (501) TKVPPFENIELYNVMCDLLGLKPAPNNGTHGSLNHLLRTNTFRPTMPEEV
551 600
HUMAN (549) TRPNYPGIMYLQSDFDLGCTCDDKVEPKNKLDELNKRLHTKGSTEERHLL
MOUSE (548) SRPNYPGIMYLQSDFDLGCTCDDKVEPKNKLEELNKRLHTKGSTEERHLL
RAT (549) SRPNYPGIMYLQSEFDLGCTCDDKVEPKNKLEELNKRLHTKGSTEERHLL
CHICK (550) AKPLYPVALPSASDFDIGCTCDDKILPKNKLDELNKRFHVKG-TEEKHLL
ZEBRAFISH (543) TKP-NPAGPVIAINDDLGCTCEDKN----KVDELNQRLRQVI-DDNKNLP
Consensus (551) SRPNYPGIMYLQSDFDLGCTCDDKVEPKNKLDELNKRLHTKGSTEERHLL

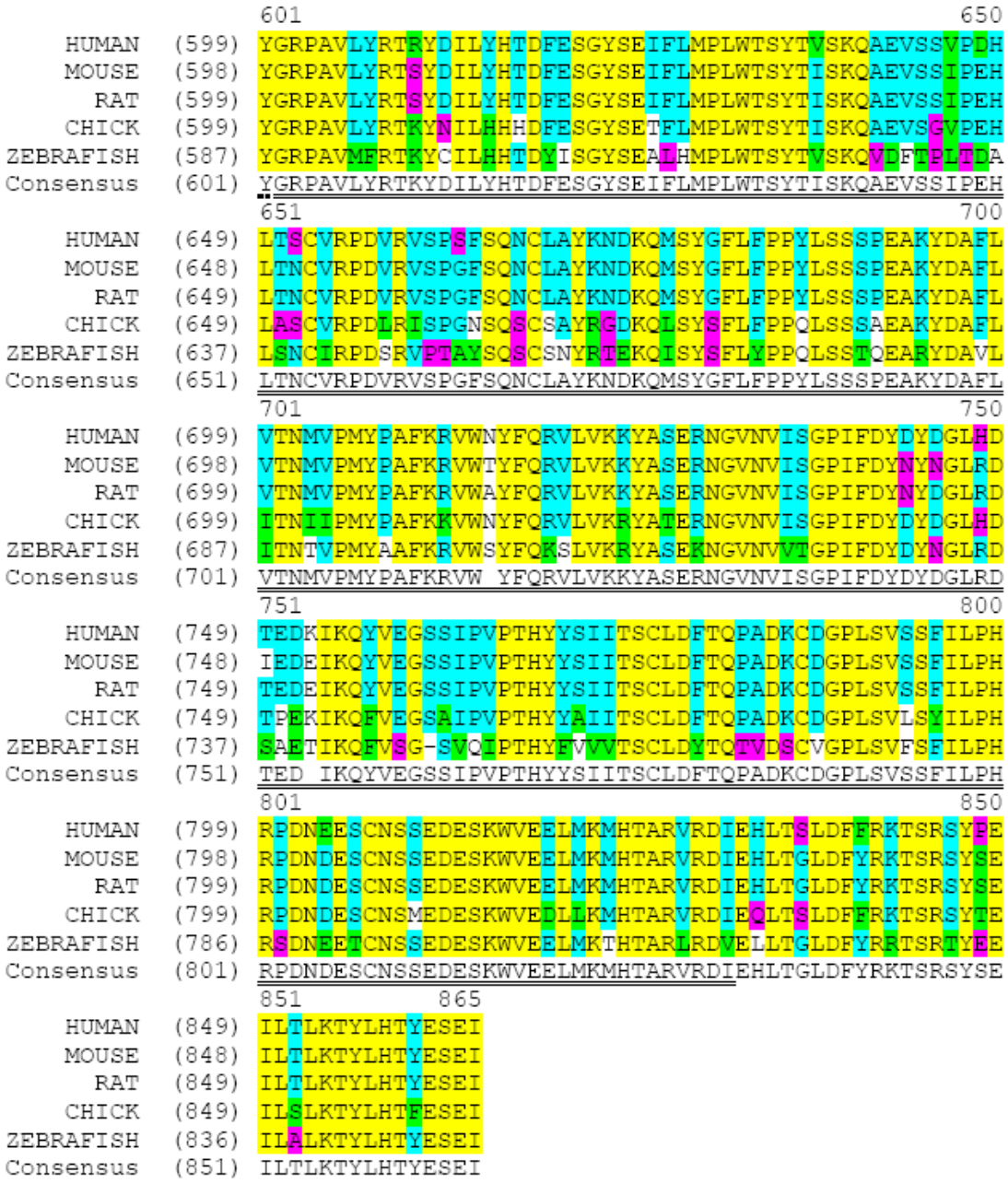
601 650
HUMAN (599) YGRPAVLYRTRYDILYHTDFESGYSEIFLMPLWTSYTVSKQAEVSSVPDH
MOUSE (598) YGRPAVLYRTSYDILYHTDFESGYSEIFLMPLWTSYTISKQAEVSSIPEH
RAT (599) YGRPAVLYRTSYDILYHTDFESGYSEIFLMPLWTSYTISKQAEVSSIPEH
CHICK (599) YGRPAVLYRTKYNILHHHDFESGYSETFLMPLWTSYTISKQAEVSGVPEH
ZEBRAFISH (587) YGRPAVMFRTKYCILHHTDYISGYSEALHMPLWTSYTVSKQVDFTPLTDA
Consensus (601) YGRPAVLYRTKYDILYHTDFESGYSEIFLMPLWTSYTISKQAEVSSIPEH
651 700
HUMAN (649) LTSCVRPDVRVSPSFSQNCLAYKNDKQMSYGFLFPPYLSSSPEAKYDAFL
MOUSE (648) LTNCVRPDVRVSPGFSQNCLAYKNDKQMSYGFLFPPYLSSSPEAKYDAFL
RAT (649) LTNCVRPDVRVSPGFSQNCLAYKNDKQMSYGFLFPPYLSSSPEAKYDAFL
CHICK (649) LASCVRPDLRISPGNSQSCSAYRGDKQLSYSFLFPPQLSSSAEAKYDAFL
ZEBRAFISH (637) LSNCIRPDSRVPTAYSQSCSNYRTEKQISYSFLYPPQLSSTQEARYDAVL
Consensus (651) LTNCVRPDVRVSPGFSQNCLAYKNDKQMSYGFLFPPYLSSSPEAKYDAFL
701 750
HUMAN (699) VTNMVPMYPAFKRVWNYFQRVLVKKYASERNGVNVISGPIFDYDYDGLHD
MOUSE (698) VTNMVPMYPAFKRVWTYFQRVLVKKYASERNGVNVISGPIFDYNYNGLRD
RAT (699) VTNMVPMYPAFKRVWAYFQRVLVKKYASERNGVNVISGPIFDYNYDGLRD
CHICK (699) ITNIIPMYPAFKKVWNYFQRVLVKRYATERNGVNVISGPIFDYDYDGLHD
ZEBRAFISH (687) ITNTVPMYAAFKRVWSYFQKSLVKRYASEKNGVNVVTGPIFDYDYNGLRD
Consensus (701) VTNMVPMYPAFKRVW YFQRVLVKKYASERNGVNVISGPIFDYDYDGLRD
751 800
HUMAN (749) TEDKIKQYVEGSSIPVPTHYYSIITSCLDFTQPADKCDGPLSVSSFILPH
MOUSE (748) IEDEIKQYVEGSSIPVPTHYYSIITSCLDFTQPADKCDGPLSVSSFILPH
RAT (749) TEDEIKQYVEGSSIPVPTHYYSIITSCLDFTQPADKCDGPLSVSSFILPH
CHICK (749) TPEKIKQFVEGSAIPVPTHYYAIITSCLDFTQPADKCDGPLSVLSYILPH
ZEBRAFISH (737) SAETIKQFVSG-SVQIPTHYFVVVTSCLDYTQTVDSCVGPLSVFSFILPH
Consensus (751) TED IKQYVEGSSIPVPTHYYSIITSCLDFTQPADKCDGPLSVSSFILPH
801 850
HUMAN (799) RPDNEESCNSSEDESKWVEELMKMHTARVRDIEHLTSLDFFRKTSRSYPE
MOUSE (798) RPDNDESCNSSEDESKWVEELMKMHTARVRDIEHLTGLDFYRKTSRSYSE
RAT (799) RPDNDESCNSSEDESKWVEELMKMHTARVRDIEHLTGLDFYRKTSRSYSE
CHICK (799) RPDNDESCNSMEDESKWVEDLLKMHTARVRDIEQLTSLDFFRKTSRSYTE
ZEBRAFISH (786) RSDNEETCNSSEDESKWVEELMKTHTARLRDVELLTGLDFYRRTSRTYEE
Consensus (801) RPDNDESCNSSEDESKWVEELMKMHTARVRDIEHLTGLDFYRKTSRSYSE
851 865
HUMAN (849) ILTLKTYLHTYESEI
MOUSE (848) ILTLKTYLHTYESEI
RAT (849) ILTLKTYLHTYESEI
CHICK (849) ILSLKTYLHTFESEI
ZEBRAFISH (836) ILALKTYLHTYESEI
Consensus (851) ILTLKTYLHTYESEI

Figure 4.2. ***atx* is expressed in the anterior pharyngeal arches, developing vasculature, hypochord, trabecula cranii and cephalic floor plate in the developing zebrafish.** Whole mount in situ hybridization was conducted on embryos at various developmental stages. (A) Developmental expression of ATX in embryos staged at 36hpf, 48hpf, 60hpf and 72hpf. Left panel of pictures are lateral views, anterior is to the right. Right panel of pictures are dorsal views; anterior is to the top. Scale bar: 100μm. (B) Expression of ATX compared to cephalic floor plate markers at 48hpf. Dorsal is to the top. Scale bar: 50μm. Abbreviations: cfp, cephalic floor plate; h, hypochord; ha, hyoid arch; hv, head vessels; ma, mandibular arch; pcv, posterior cardinal vein; pf, pectoral fin buds; pll, posterior lateral line; tr, trabecula cranii.

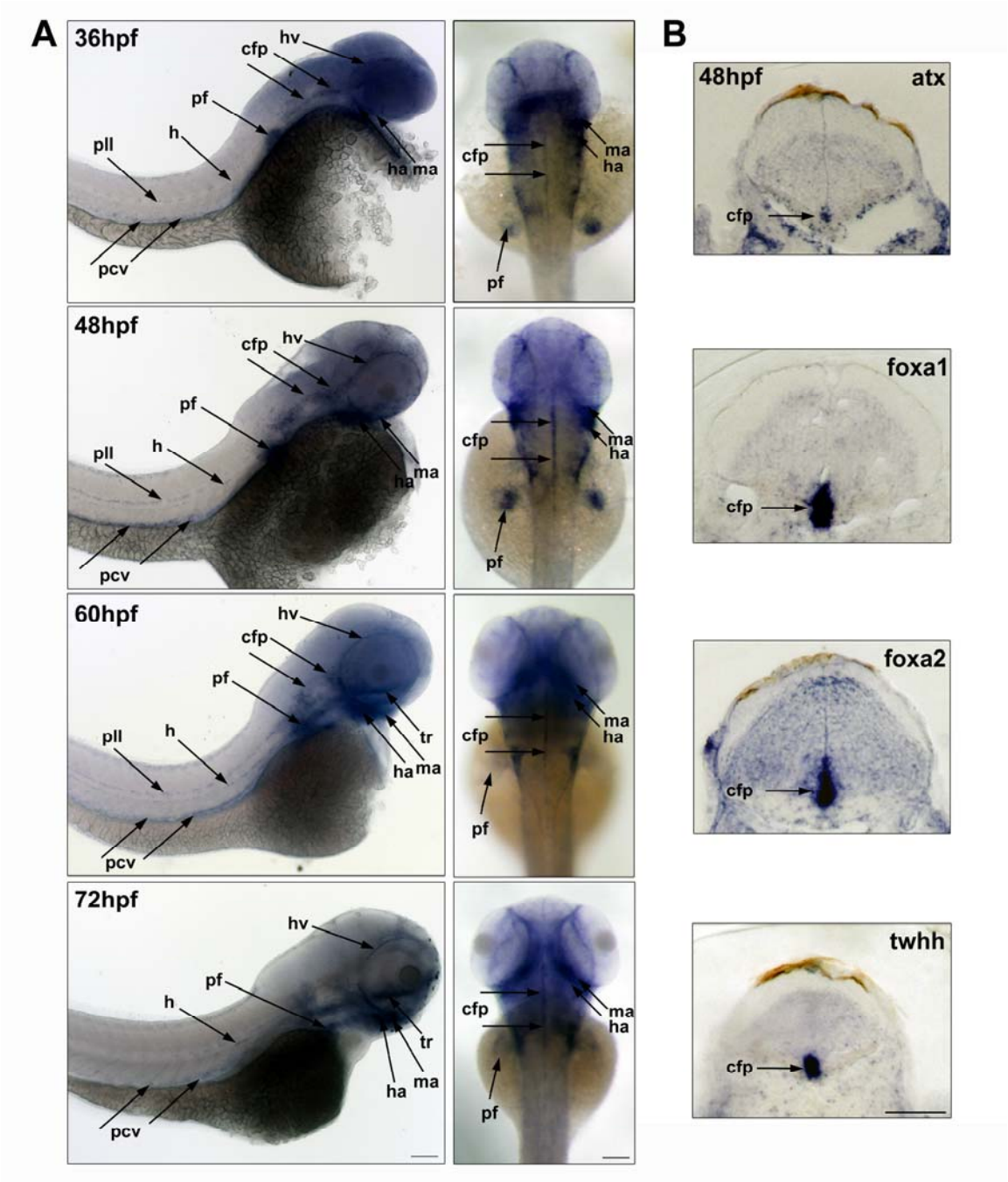
A
36hpf
hv
cfp
pf
h
pll
ha
ma
pcv
cfp
ma
ha
pf
48hpf
hv
cfp
pf
h
pll
ha
ma
pcv
cfp
ma
ha
pf
60hpf
hv
cfp
pf
h
pll
tr
ha
ma
pcv
cfp
ma
ha
pf
72hpf
hv
pf
h
tr
ha
ma
pcv
cfp
ma
ha
pf
B
48hpf
atx
cfp
foxa1
cfp
foxa2
cfp
twhh
cfp

Figure 4.3. **ATX is expressed by differentiating oligodendrocytes in the ventral hindbrain.** Double-fluorescent whole mount *in situ* hybridization using probes specific for *atx* and *plp1b* was performed using embryos at 72hpf. Transverse sections are shown; dorsal is to the top. Arrows indicate expression of *atx* and *plp1b* in the same two cells. Images were obtained by confocal microscopy and represent 2D projections of stacks of 0.488 µm optical sections. Dorsal is to the top. Scale bar: 20 µm.

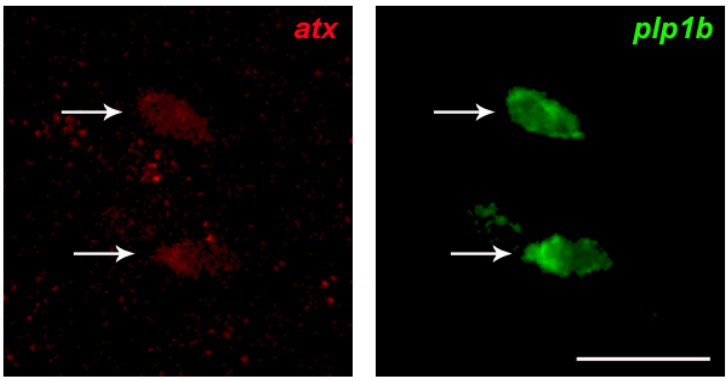
atx
plp1b

Figure 4.4. **Antisense morpholinos designed against ATX successfully inhibit translation of *atx* or splicing of *atx* pre-mRNA.** Embryos were injected with morpholinos designed against translation of ATX (*atx* TL MO) and pre-mRNA splicing (*atx* E2I2 MO) along with their respective 5-base pair mismatch controls (Control). (A) Western blots of 66hpf embryo homogenates were probed with a zebrafish-specific anti-ATX antibody and β-actin for normalization. Bar graphs depicting densitometry analysis of ATX protein bands normalized to β-actin are shown as percent of control (control = 100%). A representative Western blot is shown. (B). RT-PCR analysis of mRNA from control and *atx* E2I2 MO-treated embryos at 66hpf. A representative DNA gel and picture depicting exons and location of primers are shown. Abbrev. E, exon; P, primer.

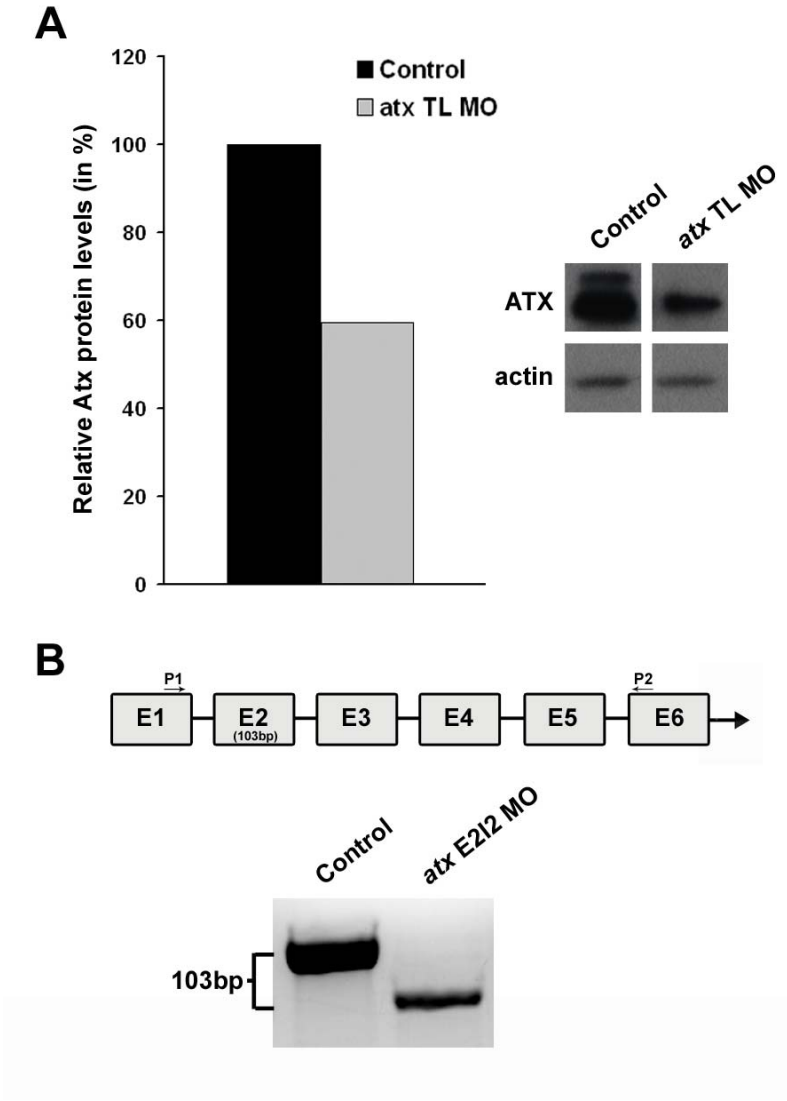
A
120
100
80
60
40
20
0
Relative Atx protein levels (in %)
Control
atx TL MO
Control
atx TL MO
ATX
actin
B
P1
P2
E1
E2
(103bp)
E3
E4
E5
E6
Control
atx E2I2 MO
103bp

Figure 4.5. **Reduction of ATX expression leads to a reduction in the appearance of *mbp*-positive oligodendrocytes.** Embryos were injected with *atx* TL, *atx* E2I2 MOs or their respective controls and staged to 66hpf. (A-C) Whole mount *in situ* hybridization using an RNA probe specific to myelin basic protein (*mbp*). Representative examples of control (A) and *atx* TL MO (B-C) embryos are shown. MBP expression phenotypes in the hindbrain were classified as normal (A), reduced (B) or absent (C) (arrows). No apparent changes were observed in *mbp* expression in Schwann cells myelinating the lateral line system of the PNS (arrowheads). Dorsal views, anterior is to the top. Scale bar: 100 μm. (D-E) Bar graphs depicting percentages of embryos with normal and reduced/absent phenotypes after injection of *atx* TL MO (D) *atx* E2I2 MO (E) or respective control MO (D and E). (F) Bar graph depicting the number of *mbp*-positive oligodendrocytes in *atx* TL MO –injected embryos set as a percentage of control (mean of control = 100%). (G-H) Bar graphs depicting *mbp* mRNA levels as percentage of control (mean of control = 100%) for embryos injected with the atx TL MO (G) and atx E2I2 MO (H). Means ± SEM of five (D), four (E and F) and three (G and H) independent experiments are shown. Stars indicate overall two-tailed significance levels of $P < 0.05$ as determined by Student's *t*-test.

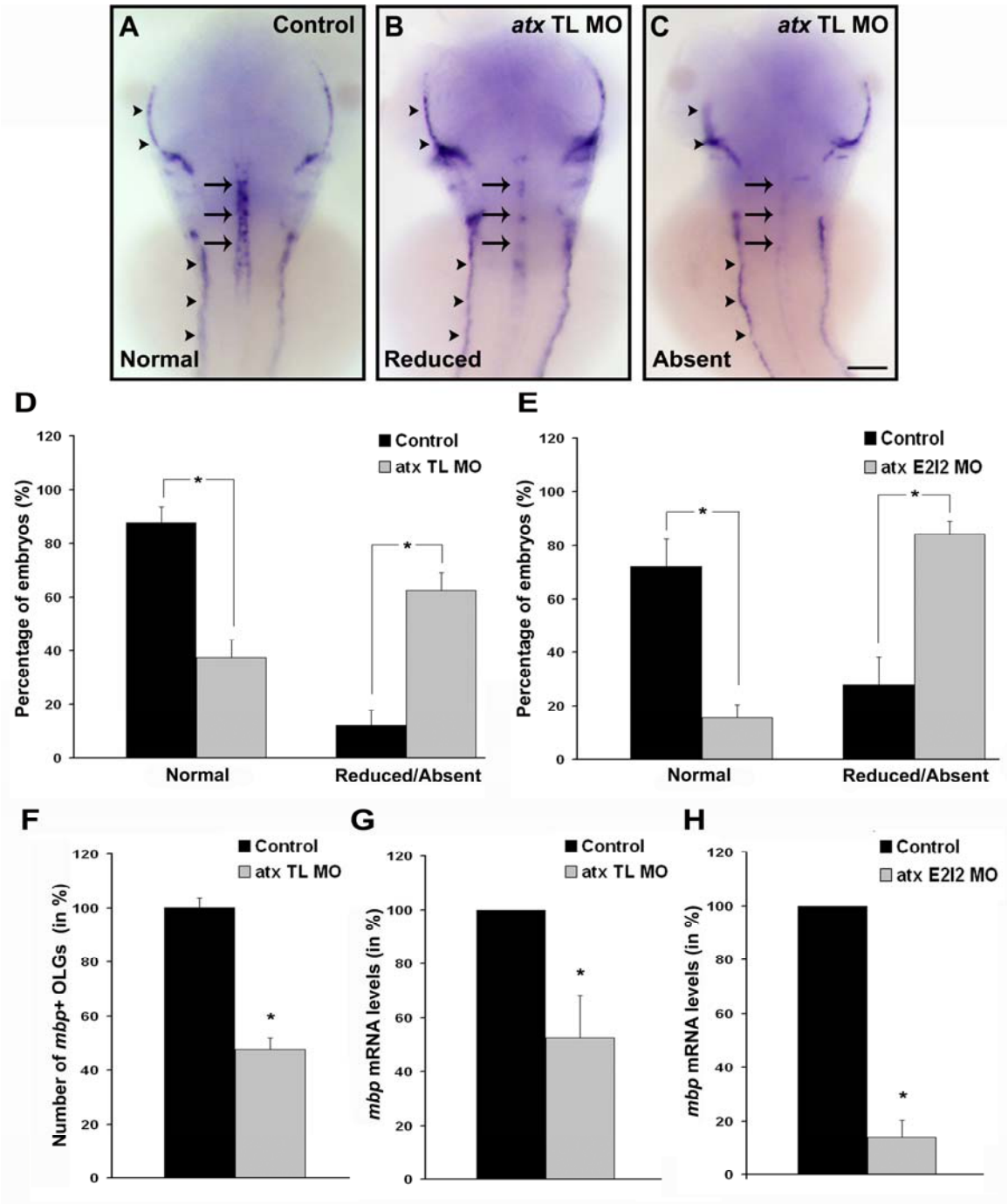
A
Control
Normal
B
atx TL MO
Reduced
C
atx TL MO
Absent
D
Control
atx TL MO
Percentage of embryos (%)
Normal
Reduced/Absent
E
Control
atx E2I2 MO
Percentage of embryos (%)
Normal
Reduced/Absent
F
Control
atx TL MO
Number of mbp+ OLGs (in %)
G
Control
atx TL MO
mbp mRNA levels (in %)
H
Control
atx E2I2 MO
mbp mRNA levels (in %)

Figure 4.6. **The reduction in the appearance of *mbp*-positive oligodendrocytes is not due to a compromised axonal network.** Embryos were injected with either *atx* TL MO or control MO and staged to 48hpf. (A-D) Representative examples of embryos stained with an antibody against anti-acetylated α-tubulin. Shown are head (A) and trunk (C) of control embryos and head (B) and trunk (D) of *atx* TL MO-injected embryos. Images were obtained by confocal microscopy and represent 2D projections of stacks of 5.7μm optical sections. A and C: Dorsal views, anterior is to the top, scale bar: 100μm, B and D: Lateral views, anterior is to the left, scale bar: 100μm.

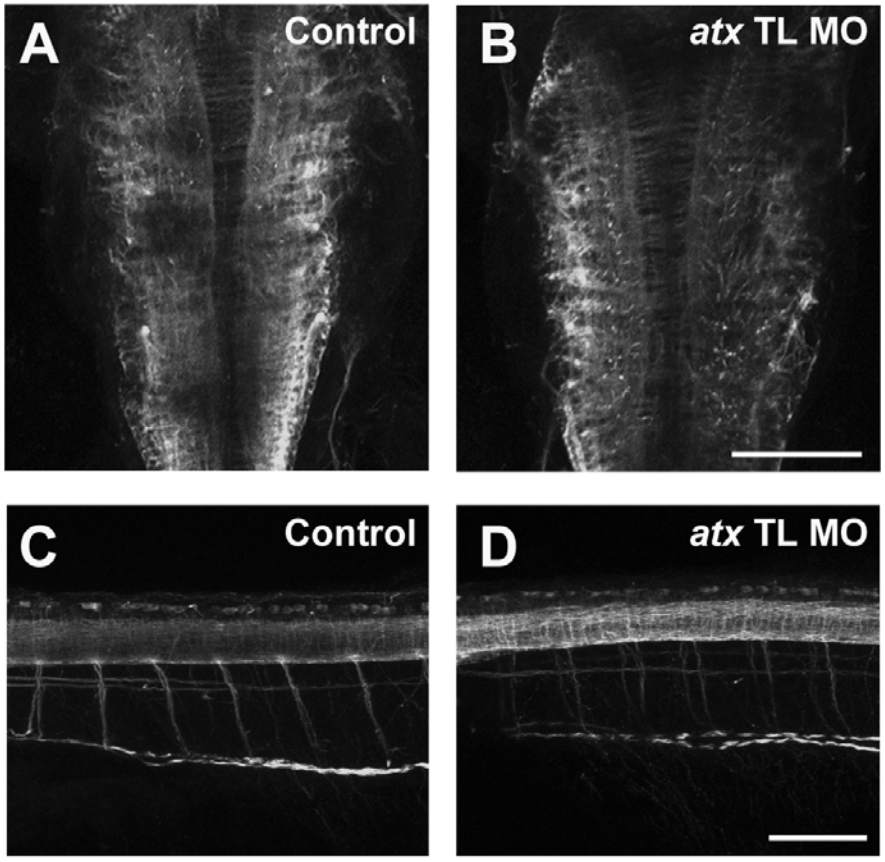
A
Control
B
atx TL MO
C
Control
D
atx TL MO

Figure 4.7. **Reduction of ATX expression leads to a reduction in *plp1b* and *claudink* mRNA levels.** Embryos were injected with *atx* TL MO, *atx* E2I2 MO or their respective control MOs and staged to 66hpf. RNA was isolated from pooled embryos and relative levels of mRNA were determined with qRT-PCR. (A and B) Bar graphs depicting mRNA levels of *plp1b* and *cldnk* in embryos injected with the *atx* TL MO (A) and the *atx* E2I2 MO (B). Data are shown as percent of control (mean of control = 100%). Means ± SEM of three independent experiments are shown. Stars indicate overall two-tailed significance levels of $P < 0.05$ as determined by Student's *t*-test.

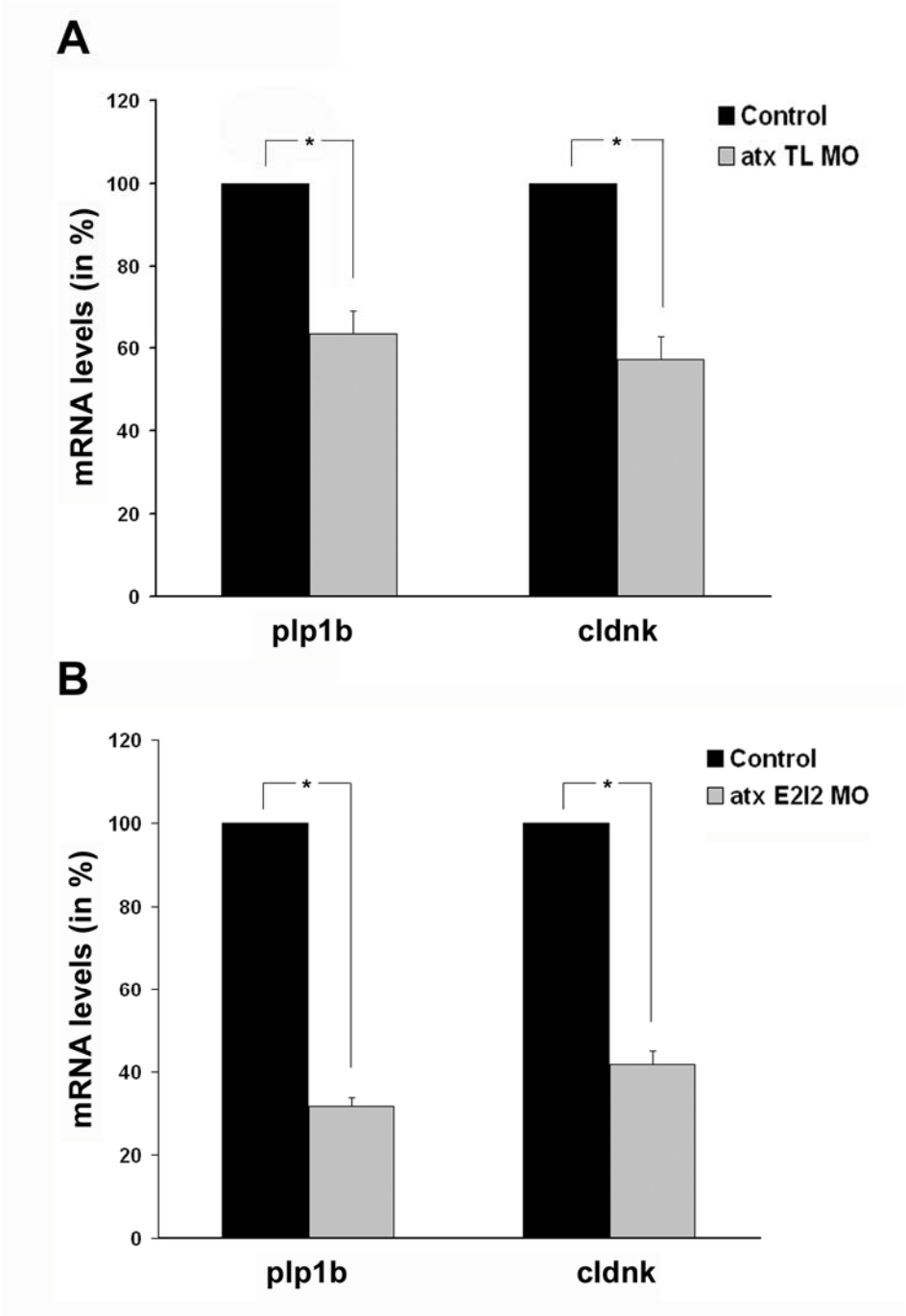
A
120
100
80
60
40
20
0
mRNA levels (in %)
*
*
Control
atx TL MO
plp1b
cldnk
B
120
100
80
60
40
20
0
mRNA levels (in %)
*
*
Control
atx E2l2 MO
plp1b
cldnk

Figure 4.8. **Reduction of ATX expression leads to a reduction in the appearance of *olig1*-positive oligodendrocytes.** Embryos were injected with *atx* TL, *atx* E2I2 MO or their respective control MOs and staged to 66hpf. (A-B) Representative examples of whole mount *in situ* hybridizations using mRNA probes specific for *olig1*. Representative examples of control (A) and *atx* TL MO (B) injected fish are shown. Lateral views, anterior is to the right. Scale bar: 100μm for A and B. (C-D) Bar graphs depicting the number of *olig1*-positive oligodendrocytes (C) and *olig1* mRNA levels (D) shown in percent of control (mean of control = 100%) and as determined by qRT-PCR. Means ± SEM of four (C) and three (D) independent experiments are shown. Stars indicate overall two-tailed significance levels of $P < 0.05$ as determined by Student's *t*-test.

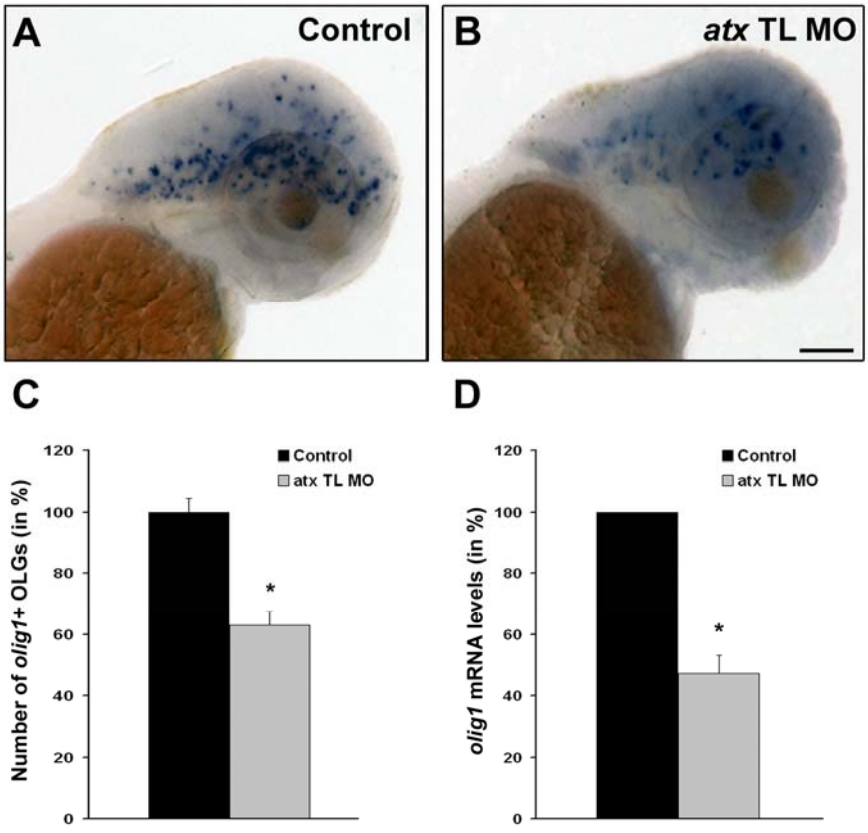
A
Control
B
atx TL MO
C
Number of olig1+ OLGs (in %)
120
100
80
60
40
20
0
Control
atx TL MO
*
D
olig1 mRNA levels (in %)
120
100
80
60
40
20
0
Control
atx TL MO
*

CHAPTER 5

Final Conclusions

In order for oligodendrocytes to develop and differentiate properly to ultimately function in myelination, they must undergo tightly regulated stages of development. Changes in gene regulation as well as morphological remodeling must occur in parallel and at the appropriate times. The data presented here, as well as previous data from our laboratory (Fox et al., 2003; Fox et al., 2004; Dennis et al., 2008; Nogaroli et al., 2009), support the idea that ATX plays an important functional role in the developmental program of oligodendrocytes by regulating both of these processes.

More specifically, recent data presented in chapter two suggest that ATX, through the production of LPA, is necessary for the expression of *mbp* and establishment of membranous structures during later stages of oligodendrocyte development. Chapter four identified ATX as necessary for the timely appearance of *olig1*-positive OPCs, a novel functional role not previously described. Currently the mechanisms leading to this early stage phenotype are unknown, but it is clear that ATX is necessary for this process at least during zebrafish development.

Until now, ATX's function has not been found associated with early stages of oligodendrocyte development. OPCs do not express ATX endogenously and it was therefore assumed that ATX would not be necessary for their development. The finding that *atx* is expressed in the cephalic floor plate at the time when oligodendrocytes are being specified and during their early development, as well

as the notion that ATX is a secreted protein, led to the hypothesis that it could regulate early oligodendrocyte development both in the zebrafish and in higher vertebrates (chapter four and (Bachner et al., 1999; Ohuchi et al., 2007)).

Chapter four identified that the presence of ATX *in vivo* is necessary for early stages of oligodendrocyte development before the expression of *olig1*, one of the earliest markers used to identify oligodendrocytes in the zebrafish (Li et al., 2007a; Schebesta and Serluca, 2009). Reduced numbers of *olig1*-positive oligodendrocytes could be a result from ATX-mediated regulation of oligodendrocyte specification, early differentiation or proliferation as described in more detail in chapter four. However, at this point the mechanisms for this regulatory role of ATX is unclear as is the contribution of each of ATX's functionally characterized domains.

The *in vitro* data presented in chapter two demonstrate that LPA, a product of ATX's lysoPLD domain, can promote the establishment of membranous structures and based on the data presented in chapters two and four, it appears likely that ATX, via the generation of LPA, promotes *mbp* expression in differentiating oligodendrocytes.

LPA-mediated signaling involves binding to G-protein-coupled receptors, LPA1-3 in oligodendrocytes as described in chapter one, and can initiate many different signaling cascades via activation of at least three different G_{α} proteins: $G_{\alpha i}$, $G_{\alpha q}$ and $G_{\alpha 12/13}$ (Swarthout and Walling, 2000; Fukushima and Chun, 2001). In order to induce cell shape changes, LPA can activate signaling cascades leading to the activation of the Rho family of GTPases, known for their roles in

regulating signaling pathways linking the extracellular environment to the organization of the actin cytoskeleton as well as controlling microtubule dynamics and other functions (Hall, 1998; Etienne-Manneville and Hall, 2002; Moolenaar et al., 2004). Rho GTPases are expressed by oligodendrocytes (Liang et al., 2004; Erschbamer et al., 2005) and more specifically, the Rho GTPase family members, RhoA and Rac1 have been associated with membrane formation in oligodendrocytes (Thurnherr et al., 2006; Czopka et al., 2009) indicating that activation of these Rho GTPases could be activated and responsible for LPA-induced membranous structure formation in our studies. Regulation of *mbp* expression, alternately, appears to occur independently of this signaling pathway (Czopka et al., 2009) suggesting that membrane formation and gene expression are regulated by different downstream signaling pathways. This strongly argues in favor of a specific role of signaling through the Rho GTPases in regulating myelin membrane formation, while it appears marginal with regard to *mbp* expression.

LPA-induced increases in *mbp* mRNA levels could potentially be a result of activation of the *mbp* promoter as its activity increases as oligodendrocytes differentiate in culture (Wei et al., 2005). LPA has been shown to have the capability for promoter activation in myelinating cells as demonstrated in Schwann cells, where LPA activates the p_0 promoter via multiple signaling pathways, resulting in its increased expression levels (Li et al., 2003).

In oligodendrocytes, expression and phosphorylation levels of CREB (cyclic AMP-response element binding protein) are important factors regulating

their differentiation (Sato-Bigbee and Yu, 1993; Sato-Bigbee et al., 1994), and different signal transduction systems may regulate CREB activation in oligodendrocytes (Sato-Bigbee et al., 1999). In particular, application of a cAMP analogue and subsequent activation of CREB can stimulate expression of *mbp* in cell culture (Sato-Bigbee and DeVries, 1996; Afshari et al., 2001). These increases in *mbp* expression were observed after 24 hours (Afshari et al., 2001), much longer than the two hours observed in our *in vitro* studies, indicating that LPA may not directly activate CREB. Consistent with this observation, LPA receptors expressed by oligodendrocytes and in particular LPA1, the major LPA receptor expressed by myelinating oligodendrocytes, does not signal through G_s and consequently not signal activate cAMP dependent pathway through adenylyl cyclase (Swarthout and Walling, 2000; Fukushima and Chun, 2001).

Since LPA may not directly regulate CREB expression, other signaling pathways could be responsible for the increases in *mbp* mRNA levels seen in our studies. p_0 expression in Schwann cells is partially regulated by activation of the MAP (mitogen-activated protein) kinase signaling cascade pathway (Li et al., 2003), composed of kinases that respond to extracellular stimuli leading to transcriptional regulation (Cobb, 1999). LPA could therefore utilize this signaling pathway to induce *mbp* expression. Data supporting this hypothesis include that LPA can activate ERK1/2 (extracellular signal-regulated kinase) (unpublished data and (Stankoff et al., 2002)), a kinase within this pathway, and activation of the MAP kinase pathway has already been shown to regulate *mbp* expression in oligodendrocytes via growth factor stimulation (Du et al., 2006). These data

suggest that LPA-mediated activation of *mbp* expression in our experiments could likely be due to direct signaling through this pathway.

Transcription factors other than CREB can also regulate *mbp* gene expression. The *mbp* promoter region contains binding sites for numerous transcription factors that are known to be involved in transcriptional control of the *mbp* gene. No binding site for CREB has been found (Zhang and Miskimins, 1993) but the cell-specific transcription factors *olig1* and *sox10* can bind to the *mbp* promoter and activate its transcription (Wegner, 2000; Stolt et al., 2002; Wei et al., 2004; Li et al., 2007a). Our *in vivo* studies indicated that down-regulation of ATX resulted in less *olig1*-positive oligodendrocytes. At the present time, we are unsure what developmental mechanism is regulating this observation, but ATX release from the floor plate could potentially regulate the expression of transcription factors such as *olig1* (Lu et al., 2000; Alberta et al., 2001). This activation could then subsequently increase *mbp* expression.

We observed no changes in *mog* or *plp* mRNA expression upon ATX down-regulation indicating that ATX may specifically regulate *mbp* expression. Interestingly, expression of CREB is not necessary for expression of *plp* as it is for *mbp* (Afshari et al., 2001), further supporting the idea that different myelin genes may be regulated differently as may be true for LPA-induced gene expression.

Despite the molecular processes involved, ATX has been shown in this dissertation to be necessary for regulating both early and late stages of oligodendrocyte development. These roles in the zebrafish studies looking at

early differentiation or specification are likely resulting from a paracrine mechanism of ATX released from the floor plate while the later stages of differentiation may be from an autocrine source as demonstrated in *in vitro* studies from our laboratory (Fox et al., 2003; Fox et al., 2004; Dennis et al., 2008; Nogaroli et al., 2009). During later stages of oligodendrocyte differentiation, past the timing of our experiments, we have shown that oligodendrocytes do express *atx* at this time, a preferentially autocrine mechanism may be responsible for promoting further stages of oligodendrocyte differentiation. Expression of *atx* in the floor plate disappeared around the time when expression commenced in oligodendrocytes. The reason for this "switch" in expression is likely because of the transient state of the floor plate (Altman and Bayer, 1984) as well as the location of oligodendrocytes during later stages of development. Oligodendrocytes are first specified adjacent to the floor plate and as they develop, they migrate throughout the brain and spinal cord (Park et al., 2002; Kirby et al., 2006; Schebesta and Serluca, 2009) and are no longer in close proximity to the floor plate. Thus, the expression of *atx* by oligodendrocytes, and its subsequent secretion into the local extracellular environment, may be necessary to further regulate their differentiation, consistent with our *in vitro* data (see Fig. 5.1 for hypothesized scheme).

All of the data obtained from our laboratory so far, including the recent data reported in this dissertation, indicate that ATX may be a major regulator during the entire process of oligodendrocyte development and not just during the later stages as previously thought. The potential for ATX-mediated control over

early and late stages of oligodendrocyte differentiation identify ATX as a potential therapeutic target for MS. Many MS lesions contain premyelinating oligodendrocytes which lack the ability to differentiate limiting their capability to remyelinate (Chang et al., 2002; Kuhlmann et al., 2008). OPCs are also present and recruited to MS lesions initially but may become depleted over time (Kuhlmann et al., 2008). ATX could potentially be responsible for both of these processes as *atx* expression levels are decreased in MS lesions (Comabella and Martin, 2007) which could limit differentiation while protein levels are increased in the cerebrospinal fluid of MS patients (Hammack et al., 2004) which could specify OPCs. Enhanced proliferation and recruitment of OPCs into myelin lesions from the subventricular zone has been previously described in response to demyelination (Nait-Oumesmar et al., 2008) and the presence of elevated ATX levels adjacent to the subventricular zone could result in the increased specification of OPCs. ATX, as a regulator of oligodendrocyte development, could therefore be a crucial molecular player important not only during normal oligodendrocyte development but also necessary for the presence of OPCs and differentiation of oligodendrocytes in MS lesions.

Figure 5.1. **Hypothesized scheme relating the source of ATX and its function.** The presence of ATX in the local extracellular environment of oligodendrocytes is necessary for their proper development. ATX released from the cephalic floor plate regulates early stages of oligodendrocyte development, such as specification or early differentiation. When expression of *atx* disappears in the cephalic floor plate and OPCs have migrated throughout the brain, oligodendrocytes must express and secrete ATX in order to further promote their differentiation during later stages of development.

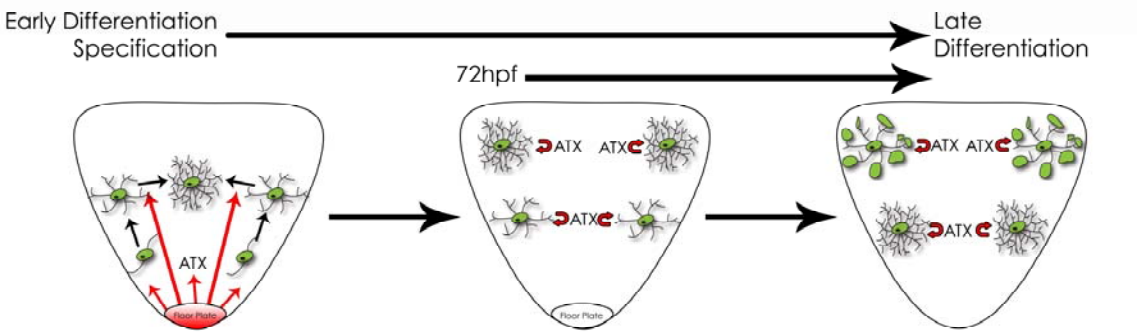
Early Differentiation
Specification
Late
Differentiation
72hpf
ATX
ATX
ATX
ATX
ATX
ATX
Floor Plate
Floor Plate

References

Abramoff M, Magelhaes P, Ram S (2004) Image Processing with image. Journal of Biophotonics Int 11:36-42.

Afshari FS, Chu AK, Sato-Bigbee C (2001) Effect of cyclic AMP on the expression of myelin basic protein species and myelin proteolipid protein in committed oligodendrocytes: differential involvement of the transcription factor CREB. J Neurosci Res 66:37-45.

Ainger K, Avossa D, Diana AS, Barry C, Barbarese E, Carson JH (1997) Transport and localization elements in myelin basic protein mRNA. J Cell Biol 138:1077-1087.

Alberta JA, Park SK, Mora J, Yuk D, Pawlitzky I, Iannarelli P, Vartanian T, Stiles CD, Rowitch DH (2001) Sonic hedgehog is required during an early phase of oligodendrocyte development in mammalian brain. Mol Cell Neurosci 18:434-441.

Altman J, Bayer SA (1984) The development of the rat spinal cord. Adv Anat Embryol Cell Biol 85:1-164.

An S, Bleu T, Hallmark OG, Goetzl EJ (1998) Characterization of a novel subtype of human G protein-coupled receptor for lysophosphatidic acid. J Biol Chem 273:7906-7910.

Arbogast D (2007) Determining the Concentration of your Morpholino in Solution using the NanoDrop ND-1000 Spectrophotometer. In: Gene Tools, LLC.

Armstrong RC (2007) Growth factor regulation of remyelination: behind the growing interest in endogenous cell repair of the CNS. Future Neurol 2:689-697.

Aruga J, Okano H, Mikoshiba K (1991) Identification of the new isoforms of mouse myelin basic protein: the existence of exon 5a. J Neurochem 56:1222-1226.

Avila RL, Tevlin BR, Lees JP, Inouye H, Kirschner DA (2007) Myelin structure and composition in zebrafish. Neurochem Res 32:197-209.

Bachner D, Ahrens M, Betat N, Schroder D, Gross G (1999) Developmental expression analysis of murine autotaxin (ATX). Mech Dev 84:121-125.

Bandoh K, Aoki J, Hosono H, Kobayashi S, Kobayashi T, Murakami-Murofushi K, Tsujimoto M, Arai H, Inoue K (1999) Molecular cloning and characterization of a novel human G-protein-coupled receptor, EDG7, for lysophosphatidic acid. J Biol Chem 274:27776-27785.

Barbarese E, Carson JH, Braun PE (1978) Accumulation of the four myelin basic proteins in mouse brain during development. J Neurochem 31:779-782.

Barbazuk WB, Korf I, Kadavi C, Heyen J, Tate S, Wun E, Bedell JA, McPherson JD, Johnson SL (2000) The syntenic relationship of the zebrafish and human genomes. Genome Res 10:1351-1358.

Bauer NG, Richter-Landsberg C, Ffrench-Constant C (2009) Role of the oligodendroglial cytoskeleton in differentiation and myelination. GLIA 57:1691-1705.

Baumann N, Pham-Dinh D (2001) Biology of oligodendrocyte and myelin in the mammalian central nervous system. Physiol Rev 81:871-927.
Blader P, Strahle U (2000) Zebrafish developmental genetics and central nervous system development. Human Molecular Genetics 9:945-951.
Boggs JM (2006) Myelin basic protein: a multifunctional protein. Cell Mol Life Sci 63:1945-1961.
Bollen M, Gijsbers R, Ceulemans H, Stalmans W, Stefan C (2000) Nucleotide pyrophosphatases/phosphodiesterases on the move. Crit Rev Biochem Mol Biol 35:393-432.
Braun PE, Sandillon F, Edwards A, Matthieu JM, Privat A (1988) Immunocytochemical localization by electron microscopy of 2'3'-cyclic nucleotide 3'-phosphodiesterase in developing oligodendrocytes of normal and mutant brain. J Neurosci 8:3057-3066.
Brend T, Holley SA (2009) Zebrafish whole mount high-resolution double fluorescent in situ hybridization. J Vis Exp.
Brosamle C, Halpern ME (2002) Characterization of myelination in the developing zebrafish. Glia 39:47-57.
Brown LA, Rodaway AR, Schilling TF, Jowett T, Ingham PW, Patient RK, Sharrocks AD (2000) Insights into early vasculogenesis revealed by expression of the ETS-domain transcription factor Fli-1 in wild-type and mutant zebrafish embryos. Mech Dev 90:237-252.
Buckley CE, Goldsmith P, Franklin RJ (2008) Zebrafish myelination: a transparent model for remyelination? Dis Model Mech 1:221-228.
Buckley CE, Marguerie A, Alderton WK, Franklin RJM (2010) Temporal Dynamics of Myelination in the Zebrafish Spinal Cord. Glia 58:802-812.
Cameron-Curry P, Le Douarin NM (1995) Oligodendrocyte precursors originate from both the dorsal and the ventral parts of the spinal cord. Neuron 15:1299-1310.
Campagnoni AT, Macklin WB (1988) Cellular and molecular aspects of myelin protein gene expression. Mol Neurobiol 2:41-89.
Campagnoni AT, Campagnoni CW (2004) Myelin basic protein gene. In: Myelin Biology and Disorders (Lazzarini RA, ed), pp 387-400. San Diego: Elsevier Academic Press.
Campagnoni CW, Carey GD, Campagnoni AT (1978) Synthesis of myelin basic proteins in the developing mouse brain. Arch Biochem Biophys 190:118-125.
Chang A, Tourtellotte WW, Rudick R, Trapp BD (2002) Premyelinating oligodendrocytes in chronic lesions of multiple sclerosis. N Engl J Med 346:165-173.
Chari DM, Blakemore WF (2002) New insights into remyelination failure in multiple sclerosis: implications for glial cell transplantation. Mult Scler 8:271-277.
Clair T, Lee HY, Liotta LA, Stracke ML (1997) Autotaxin is an exoenzyme possessing 5'-nucleotide phosphodiesterase/ATP pyrophosphatase and ATPase activities. J Biol Chem 272:996-1001.
Cobb MH (1999) MAP kinase pathways. Prog Biophys Mol Biol 71:479-500.

Comabella M, Martin R (2007) Genomics in multiple sclerosis--current state and future directions. J Neuroimmunol 187:1-8.
Contos JJ, Ishii I, Fukushima N, Kingsbury MA, Ye X, Kawamura S, Brown JH, Chun J (2002) Characterization of lpa(2) (Edg4) and lpa(1)/lpa(2) (Edg2/Edg4) lysophosphatidic acid receptor knockout mice: signaling deficits without obvious phenotypic abnormality attributable to lpa(2). Mol Cell Biol 22:6921-6929.
Croset M, Brossard N, Polette A, Lagarde M (2000) Characterization of plasma unsaturated lysophosphatidylcholines in human and rat. Biochem J 345 Pt 1:61-67.
Cui HL, Qiao JT (2007) Effect of lysophosphatidic acid on differentiation of embryonic neural stem cells into neuroglial cells in rats in vitro. Sheng Li Xue Bao 59:759-764.
Cui MZ, Laag E, Sun L, Tan M, Zhao G, Xu X (2006) Lysophosphatidic acid induces early growth response gene 1 expression in vascular smooth muscle cells: CRE and SRE mediate the transcription. Arterioscler Thromb Vasc Biol 26:1029-1035.
Czopka T, Von Holst A, Schmidt G, Ffrench-Constant C, Faissner A (2009) Tenascin C and tenascin R similarly prevent the formation of myelin membranes in a RhoA-dependent manner, but antagonistically regulate the expression of myelin basic protein via a separate pathway. GLIA 57:1790-1801.
D'Urso D, Brophy PJ, Staugaitis SM, Gillespie CS, Frey AB, Stempak JG, Colman DR (1990) Protein zero of peripheral nerve myelin: biosynthesis, membrane insertion, and evidence for homotypic interaction. Neuron 4:449-460.
Das AK, Hajra AK (1989) Quantification, characterization and fatty acid composition of lysophosphatidic acid in different rat tissues. Lipids 24:329-333.
Dawson J, Hotchin N, Lax S, Rumsby M (2003) Lysophosphatidic acid induces process retraction in CG-4 line oligodendrocytes and oligodendrocyte precursor cells but not in differentiated oligodendrocytes. J Neurochem 87:947-957.
Deiters A, Garner RA, Lusic H, Govan JM, Dush M, Nascone-Yoder NM, Yoder JA (2010) Photocaged Morpholino Oligomers for the Light-Regulation of Gene Function in Zebrafish and Xenopus Embryos. J Am Chem Soc.
Dennis J, Nogaroli L, Fuss B (2005) Phosphodiesterase-Ialpha/autotaxin (PD-Ialpha/ATX): a multifunctional protein involved in central nervous system development and disease. J Neurosci Res 82:737-742.
Dennis J, White MA, Forrest AD, Yuelling LM, Nogaroli L, Afshari FS, Fox MA, Fuss B (2008) Phosphodiesterase-Ialpha/autotaxin's MORFO domain regulates oligodendroglial process network formation and focal adhesion organization. Mol Cell Neurosci 37:412-424.
Du Y, Lercher LD, Zhou R, Dreyfus CF (2006) Mitogen-activated protein kinase pathway mediates effects of brain-derived neurotrophic factor on

differentiation of basal forebrain oligodendrocytes. J Neurosci Res 84:1692-1702.
Ericson J, Muhr J, Jessell TM, Edlund T (1995) Sonic hedgehog: a common signal for ventral patterning along the rostrocaudal axis of the neural tube. Int J Dev Biol 39:809-816.
Ericson J, Briscoe J, Rashbass P, van Heyningen V, Jessell TM (1997) Graded sonic hedgehog signaling and the specification of cell fate in the ventral neural tube. Cold Spring Harb Symp Quant Biol 62:451-466.
Eriksson J, Lofberg J (2000) Development of the hypochord and dorsal aorta in the zebrafish embryo (Danio rerio). J Morphol 244:167-176.
Erschbamer MK, Hofstetter CP, Olson L (2005) RhoA, RhoB, RhoC, Rac1, Cdc42, and Tc10 mRNA levels in spinal cord, sensory ganglia, and corticospinal tract neurons and long-lasting specific changes following spinal cord injury. J Comp Neurol 484:224-233.
Etienne-Manneville S, Hall A (2002) Rho GTPases in cell biology. Nature 420:629-635.
Ferguson CG, Bigman CS, Richardson RD, van Meeteren LA, Moolenaar WH, Prestwich GD (2006) Fluorogenic phospholipid substrate to detect lysophospholipase D/autotaxin activity. Org Lett 8:2023-2026.
Ferry G, Giganti A, Coge F, Bertaux F, Thiam K, Boutin JA (2007) Functional invalidation of the autotaxin gene by a single amino acid mutation in mouse is lethal. FEBS Lett 581:3572-3578.
Filbin MT, Walsh FS, Trapp BD, Pizzey JA, Tennekoon GI (1990) Role of myelin P0 protein as a homophilic adhesion molecule. Nature 344:871-872.
Fotopoulou S, Oikonomou N, Grigorieva E, Nikitopoulou I, Paparountas T, Thanassopoulou A, Zhao Z, Xu Y, Kontoyiannis DL, Remboutsika E, Aidinis V (2010) ATX expression and LPA signalling are vital for the development of the nervous system. Dev Biol 339:451-464.
Fox MA, Colello RJ, Macklin WB, Fuss B (2003) Phosphodiesterase-Ialpha/autotaxin: a counteradhesive protein expressed by oligodendrocytes during onset of myelination. Mol Cell Neurosci 23:507-519.
Fox MA, Alexander JK, Afshari FS, Colello RJ, Fuss B (2004) Phosphodiesterase-I alpha/autotaxin controls cytoskeletal organization and FAK phosphorylation during myelination. Mol Cell Neurosci 27:140-150.
Fox RJ, Bethoux F, Goldman MD, Cohen JA (2006) Multiple sclerosis: advances in understanding, diagnosing, and treating the underlying disease. Cleve Clin J Med 73:91-102.
Franz T, Waehneldt TV, Neuhoff V, Wachtler K (1981) Central nervous system myelin proteins and glycoproteins in vertebrates: a phylogenetic study. Brain Res 226:245-258.
Fukushima N, Morita Y (2006) Actomyosin-dependent microtubule rearrangement in lysophosphatidic acid-induced neurite remodeling of young cortical neurons. Brain Res 1094:65-75.

Fuss B, Baba H, Phan T, Tuohy VK, Macklin WB (1997) Phosphodiesterase I, a novel adhesion molecule and/or cytokine involved in oligodendrocyte function. J Neurosci 17:9095-9103.
Giganti A, Rodriguez M, Fould B, Moulharat N, Coge F, Chomarat P, Galizzi JP, Valet P, Saulnier-Blache JS, Boutin JA, Ferry G (2008) Murine and human autotaxin alpha, beta, and gamma isoforms: gene organization, tissue distribution, and biochemical characterization. J Biol Chem 283:7776-7789.
Gijsbers R, Aoki J, Arai H, Bollen M (2003) The hydrolysis of lysophospholipids and nucleotides by autotaxin (NPP2) involves a single catalytic site. FEBS Lett 538:60-64.
Goding JW, Grobben B, Slegers H (2003) Physiological and pathophysiological functions of the ecto-nucleotide pyrophosphatase/phosphodiesterase family. Biochim Biophys Acta 1638:1-19.
Gow A (1997) Redefining the lipophilin family of proteolipid proteins. J Neurosci Res 50:659-664.
Gow A, Southwood CM, Li JS, Pariali M, Riordan GP, Brodie SE, Danias J, Bronstein JM, Kachar B, Lazzarini RA (1999) CNS myelin and sertoli cell tight junction strands are absent in Osp/claudin-11 null mice. Cell 99:649-659.
Griffiths I, Klugmann M, Anderson T, Thomson C, Vouyiouklis D, Nave KA (1998a) Current concepts of PLP and its role in the nervous system. Microsc Res Tech 41:344-358.
Griffiths I, Klugmann M, Anderson T, Yool D, Thomson C, Schwab MH, Schneider A, Zimmermann F, McCulloch M, Nadon N, Nave KA (1998b) Axonal swellings and degeneration in mice lacking the major proteolipid of myelin. Science 280:1610-1613.
Hall A (1998) Rho GTPases and the actin cytoskeleton. Science 279:509-514.
Hammack BN, Fung KY, Hunsucker SW, Duncan MW, Burgoon MP, Owens GP, Gilden DH (2004) Proteomic analysis of multiple sclerosis cerebrospinal fluid. Mult Scler 10:245-260.
Hardy R, Reynolds R (1991) Proliferation and differaentiation potential of rat forebrain oligodendroglial progenitors both in vitro and in vivo. Development 111:1061-1080.
Hardy RJ, Friedrich VL, Jr. (1996) Progressive remodeling of the oligodendrocyte process arbor during myelinogenesis. Dev Neurosci 18:243-254.
Hartline DK, Colman DR (2007) Rapid conduction and the evolution of giant axons and myelinated fibers. Curr Biol 17:R29-35.
Hecht JH, Weiner JA, Post SR, Chun J (1996) Ventricular zone gene-1 (vzg-1) encodes a lysophosphophatidic acid receptor expressed in neurogenic regions of the developing cerebral cortex. The Journal of Cell Biology 135:1071-1083.
Jeserich G, Strelau J, Lanwert C (1997) Partial characterization of the 5'-flanking region of trout IP: a Po-like gene containing a PLP-like promoter. J Neurosci Res 50:781-790.

Jeserich G, Klempahn K, Pfeiffer M (2008) Features and functions of oligodendrocytes and myelin proteins of lower vertebrate species. J Mol Neurosci 35:117-126.
Jessell TM, Bovolenta P, Placzek M, Tessier-Lavigne M, Dodd J (1989) Polarity and patterning in the neural tube: the origin and function of the floor plate. Ciba Found Symp 144:255-276; discussion 276-280, 290-255.
Julich D, Hwee Lim C, Round J, Nicolaije C, Schroeder J, Davies A, Geisler R, Lewis J, Jiang YJ, Holley SA (2005) beamter/deltaC and the role of Notch ligands in the zebrafish somite segmentation, hindbrain neurogenesis and hypochord differentiation. Dev Biol 286:391-404.
Kessaris N, Fogarty M, Iannarelli P, Grist M, Wegner M, Richardson WD (2006) Competing waves of oligodendrocytes in the forebrain and postnatal elimination of an embryonic lineage. Nat Neurosci 9:173-179.
Kettenmann H, Ransom BR, eds (2005) Neuroglia, Second Edition. New York, NY: Oxford University Press.
Kimmel CB, Ballard WW, Kimmel SR, Ullmann B, Schilling TF (1995) Stages of embryonic development of the zebrafish. Dev Dyn 203:253-310.
Kimura M, Sato M, Akatsuka A, Saito S, Ando K, Yokoyama M, Katsuki M (1998) Overexpression of a minor component of myelin basic protein isoform (17.2 kDa) can restore myelinogenesis in transgenic shiverer mice. Brain Res 785:245-252.
Kirby BB, Takada N, Latimer AJ, Shin J, Carney TJ, Kelsh RN, Appel B (2006) In vivo time-lapse imaging shows dynamic oligodendrocyte progenitor behavior during zebrafish development. Nat Neurosci 9:1506-1511.
Klemm S, Zimmermann S, Peschel C, Mak TW, Ruland J (2007) Bcl10 and Malt1 control lysophosphatidic acid-induced NF-kappaB activation and cytokine production. Proc Natl Acad Sci U S A 104:134-138.
Knapp PE, Bartlett WP, Skoff RP (1987) Cultured oligodendrocytes mimic in vivo phenotypic characteristics: cell shape, expression of myelin-specific antigens, and membrane production. Dev Biol 120:356-365.
Koh E, Clair T, Woodhouse EC, Schiffmann E, Liotta L, Stracke M (2003) Site-directed mutations in the tumor-associated cytokine, autotaxin, eliminate nucleotide phosphodiesterase, lysophospholipase D, and motogenic activities. Cancer Res 63:2042-2045.
Kotarsky K, Boketoft A, Bristulf J, Nilsson NE, Norberg A, Hansson S, Owman C, Sillard R, Leeb-Lundberg LM, Olde B (2006) Lysophosphatidic acid binds to and activates GPR92, a G protein-coupled receptor highly expressed in gastrointestinal lymphocytes. J Pharmacol Exp Ther 318:619-628.
Kranenburg O, Verlaan I, Moolenaar WH (1999) Gi-mediated tyrosine phosphorylation of Grb2 (growth-factor-receptor-bound protein 2)-bound dynamin-II by lysophosphatidic acid. Biochem J 339 (Pt 1):11-14.
Kristensson K, Holmes KV, Duchala CS, Zeller NK, Lazzarini RA, Dubois-Dalcq M (1986) Increased levels of myelin basic protein transcripts in virus-induced demyelination. Nature 322:544-547.

Kuhlmann T, Miron V, Cui Q, Wegner C, Antel J, Bruck W (2008) Differentiation block of oligodendroglial progenitor cells as a cause for remyelination failure in chronic multiple sclerosis. Brain 131:1749-1758.
Lanwert C, Jeserich G (2001) Structure, heterologous expression, and adhesive properties of the P(0)-like myelin glycoprotein IP1 of trout CNS. Microsc Res Tech 52:637-644.
Lee CW, Rivera R, Gardell S, Dubin AE, Chun J (2006a) GPR92 as a new G12/13- and Gq-coupled lysophosphatidic acid receptor that increases cAMP, LPA5. J Biol Chem 281:23589-23597.
Lee H, Lin CI, Liao JJ, Lee YW, Yang HY, Lee CY, Hsu HY, Wu HL (2004) Lysophospholipids increase ICAM-1 expression in HUVEC through a Gi- and NF-kappaB-dependent mechanism. Am J Physiol Cell Physiol 287:C1657-1666.
Lee HY, Clair T, Mulvaney PT, Woodhouse EC, Aznavoorian S, Liotta LA, Stracke ML (1996) Stimulation of tumor cell motility linked to phosphodiesterase catalytic site of autotaxin. J Biol Chem 271:24408-24412.
Lee J, Gravel M, Zhang R, Thibault P, Braun PE (2005) Process outgrowth in oligodendrocytes is mediated by CNP, a novel microtubule assembly myelin protein. J Cell Biol 170:661-673.
Lee J, Park SY, Lee EK, Park CG, Chung HC, Rha SY, Kim YK, Bae GU, Kim BK, Han JW, Lee HY (2006b) Activation of hypoxia-inducible factor-1alpha is necessary for lysophosphatidic acid-induced vascular endothelial growth factor expression. Clin Cancer Res 12:6351-6358.
Lee SJ, Chan TH, Chen TC, Liao BK, Hwang PP, Lee H (2008) LPA1 is essential for lymphatic vessel development in zebrafish. FASEB J 22:3706-3715.
Lemke G, Axel R (1985) Isolation and sequence of a cDNA encoding the major structural protein of peripheral myelin. Cell 40:501-508.
Li H, Lu Y, Smith HK, Richardson WD (2007a) Olig1 and Sox10 interact synergistically to drive myelin basic protein transcription in oligodendrocytes. J Neurosci 27:14375-14382.
Li W, Zhang B, Tang J, Cao Q, Wu Y, Wu C, Guo J, Ling EA, Liang F (2007b) Sirtuin 2, a mammalian homolog of yeast silent information regulator-2 longevity regulator, is an oligodendroglial protein that decelerates cell differentiation through deacetylating alpha-tubulin. J Neurosci 27:2606-2616.
Li Y, Gonzalez MI, Meinkoth JL, Field J, Kazanietz MG, Tennekoon GI (2003) Lysophosphatidic acid promotes survival and differentiation of rat Schwann cells. J Biol Chem 278:9585-9591.
Liang X, Graghi N, Resh M (2004) Signaling from integrins to fyn to rho family GTPases regulates morphologic differentiation of oligodendrocytes. The Journal of Neuroscience 24:7140-7149.
Lieschke GJ, Currie PD (2007) Animal models of human disease: zebrafish swim into view. Nat Rev Genet 8:353-367.

Liu A, Muggironi M, Marin-Husstege M, Casaccia-Bonnefil P (2003) Oligodendrocyte process outgrowth in vitro is modulated by epigenetic regulation of cytoskeletal severing proteins. GLIA 44:264-274.
Livak KJ, Schmittgen TD (2001) Analysis of relative gene expression data using real-time quantitative PCR and the 2(-Delta Delta C(T)) Method. Methods 25:402-408.
Lu QR, Sun T, Zhu Z, Ma N, Garcia M, Stiles CD, Rowitch DH (2002) Common developmental requirement for Olig function indicates a motor neuron/oligodendrocyte connection. Cell 109:75-86.
Lu QR, Yuk D, Alberta JA, Zhu Z, Pawlitzky I, Chan J, McMahon AP, Stiles CD, Rowitch DH (2000) Sonic hedgehog--regulated oligodendrocyte lineage genes encoding bHLH proteins in the mammalian central nervous system. Neuron 25:317-329.
Lublin FD, Reingold SC (1996) Defining the clinical course of multiple sclerosis: results of an international survey. National Multiple Sclerosis Society (USA) Advisory Committee on Clinical Trials of New Agents in Multiple Sclerosis. Neurology 46:907-911.
Lunn KF, Baas PW, Duncan ID (1997) Microtubule organization and stability in the oligodendrocyte. J Neurosci 17:4921-4932.
Luttrell LM, Daaka Y, Della Rocca GJ, Lefkowitz RJ (1997) G protein-coupled receptors mediate two functionally distinct pathways of tyrosine phosphorylation in rat 1a fibroblasts. Shc phosphorylation and receptor endocytosis correlate with activation of Erk kinases. J Biol Chem 272:31648-31656.
Ma EY, Raible DW (2009) Signaling pathways regulating zebrafish lateral line development. Curr Biol 19:R381-386.
Masse K, Bhamra S, Allsop G, Dale N, Jones EA (2010) Ectophosphodiesterase/nucleotide phosphohydrolase (Enpp) nucleotidases: cloning, conservation and developmental restriction. Int J Dev Biol 54:181-193.
McIntyre TM, Pontsler AV, Silva AR, St Hilaire A, Xu Y, Hinshaw JC, Zimmerman GA, Hama K, Aoki J, Arai H, Prestwich GD (2003) Identification of an intracellular receptor for lysophosphatidic acid (LPA): LPA is a transcellular PPARgamma agonist. Proc Natl Acad Sci U S A 100:131-136.
Miller RH (2002) Regulation of oligodendrocyte development in the vertebrate CNS. Prog Neurobiol 67:451-467.
Miller RH, Payne J, Milner L, Zhang H, Orentas DM (1997) Spinal cord oligodendrocytes develop from a limited number of migratory highly proliferative precursors. J Neurosci Res 50:157-168.
Moller T, Musante DB, Ransom BR (1999) Lysophosphatidic acid-induced calcium signals in cultured rat oligodendrocytes. NeuroReport 10:2929-2932.
Montgomery J, Carton G, Voigt R, Baker C, Diebel C (2000) Sensory processing of water currents by fishes. Philos Trans R Soc Lond B Biol Sci 355:1325-1327.

Moolenaar WH (2002) Lysophospholipids in the limelight: autotaxin takes center stage. J Cell Biol 158:197-199.
Moolenaar WH, van Meeteren LA, Giepmans BN (2004) The ins and outs of lysophosphatidic acid signaling. Bioessays 26:870-881.
Morita K, Sasaki H, Fujimoto K, Furuse M, Tsukita S (1999) Claudin-11/OSP-based tight junctions of myelin sheaths in brain and Sertoli cells in testis. J Cell Biol 145:579-588.
Morris JK, Willard BB, Yin X, Jeserich G, Kinter M, Trapp BD (2004) The 36K protein of zebrafish CNS myelin is a short-chain dehydrogenase. Glia 45:378-391.
Murata J, Lee HY, Clair T, Krutzsch HC, Arestad AA, Sobel ME, Liotta LA, Stracke ML (1994) cDNA cloning of the human tumor motility-stimulating protein, autotaxin, reveals a homology with phosphodiesterases. J Biol Chem 269:30479-30484.
Murph MM, Scaccia LA, Volpicelli LA, Radhakrishna H (2003) Agonist-induced endocytosis of lysophosphatidic acid-coupled LPA1/EDG-2 receptors via a dynamin2- and Rab5-dependent pathway. J Cell Sci 116:1969-1980.
Murphy-Ullrich JE (2001) The de-adhesive activity of matricellular proteins: is intermediate cell adhesion an adaptive state? J Clin Invest 107:785-790.
Nait-Oumesmar B, Picard-Riera N, Kerninon C, Baron-Van Evercooren A (2008) The role of SVZ-derived neural precursors in demyelinating diseases: from animal models to multiple sclerosis. J Neurol Sci 265:26-31.
Nakanaga K, Hama K, Aoki J (2010) Autotaxin--an LPA producing enzyme with diverse functions. J Biochem 148:13-24.
Narita M, Goji J, Nakamura H, Sano K (1994) Molecular cloning, expression, and localization of a brain-specific phosphodiesterase I/nucleotide pyrophosphatase (PD-I alpha) from rat brain. J Biol Chem 269:28235-28242.
Nave KA (2001) Myelin-specific genes and their mutations in the mouse. In: Glial Cell Development (Jessen KR, Richardson WD, eds), pp 176-208. New York: Oxford University Press.
Nave KA, Lai C, Bloom FE, Milner RJ (1987) Splice site selection in the proteolipid protein (PLP) gene transcript and primary structure of the DM-20 protein of central nervous system myelin. Proc Natl Acad Sci U S A 84:5665-5669.
Newman S, Kitamura K, Campagnoni AT (1987) Identification of a cDNA coding for a fifth form of myelin basic protein in mouse. Proc Natl Acad Sci U S A 84:886-890.
Nogaroli L, Yuelling LM, Dennis J, Gorse K, Payne SG, Fuss B (2009) Lysophosphatidic acid can support the formation of membranous structures and an increase in MBP mRNA levels in differentiating oligodendrocytes. Neurochem Res 34:182-193.
Noguchi K, Ishii S, Shimizu T (2003) Identification of p2y9/GPR23 as a novel G protein-coupled receptor for lysophosphatidic acid, structurally distant from the Edg family. J Biol Chem 278:25600-25606.

Ny A, Autiero M, Carmeliet P (2006) Zebrafish and Xenopus tadpoles: small animal models to study angiogenesis and lymphangiogenesis. Exp Cell Res 312:684-693.
Odenthal J, Nusslein-Volhard C (1998) fork head domain genes in zebrafish. Dev Genes Evol 208:245-258.
Odenthal J, van Eeden FJ, Haffter P, Ingham PW, Nusslein-Volhard C (2000) Two distinct cell populations in the floor plate of the zebrafish are induced by different pathways. Dev Biol 219:350-363.
Ohno S (1970) Evolution by gene duplication. New York: Springer-Verlag.
Ohuchi H, Hayashibara Y, Matsuda H, Onoi M, Mitsumori M, Tanaka M, Aoki J, Arai H, Noji S (2007) Diversified expression patterns of autotaxin, a gene for phospholipid-generating enzyme during mouse and chicken development. Dev Dyn 236:1134-1143.
Orentas DM, Hayes JE, Dyer KL, Miller RH (1999) Sonic hedgehog signaling is required during the appearance of spinal cord oligodendrocyte precursors. Development 126:2419-2429.
Park HC, Shin J, Appel B (2004) Spatial and temporal regulation of ventral spinal cord precursor specification by Hedgehog signaling. Development 131:5959-5969.
Park HC, Mehta A, Richardson JS, Appel B (2002) olig2 is required for zebrafish primary motor neuron and oligodendrocyte development. Dev Biol 248:356-368.
Park HC, Shin J, Roberts RK, Appel B (2007) An olig2 reporter gene marks oligodendrocyte precursors in the postembryonic spinal cord of zebrafish. Dev Dyn 236:3402-3407.
Patani R, Balaratnam M, Vora A, Reynolds R (2007) Remyelination can be extensive in multiple sclerosis despite a long disease course. Neuropathol Appl Neurobiol 33:277-287.
Peirson SN, Butler JN, Foster RG (2003) Experimental validation of novel and conventional approaches to quantitative real-time PCR data analysis. Nucleic Acids Res 31:e73.
Pfeiffer SE, Warrington AE, Bansal R (1993) The oligodendrocyte and its many cellular processes. Trends Cell Biol 3:191-197.
Piperno G, LeDizet M, Chang XJ (1987) Microtubules containing acetylated alpha-tubulin in mammalian cells in culture. J Cell Biol 104:289-302.
Placzek M, Briscoe J (2005) The floor plate: multiple cells, multiple signals. Nat Rev Neurosci 6:230-240.
Poncet C, Soula C, Trousse F, Kan P, Hirsinger E, Pourquie O, Duprat AM, Cochard P (1996) Induction of oligodendrocyte progenitors in the trunk neural tube by ventralizing signals: effects of notochord and floor plate grafts, and of sonic hedgehog. Mech Dev 60:13-32.
Postlethwait J, Amores A, Cresko W, Singer A, Yan YL (2004) Subfunction partitioning, the teleost radiation and the annotation of the human genome. Trends Genet 20:481-490.

Postlethwait JH, Woods IG, Ngo-Hazelett P, Yan YL, Kelly PD, Chu F, Huang H, Hill-Force A, Talbot WS (2000) Zebrafish comparative genomics and the origins of vertebrate chromosomes. Genome Res 10:1890-1902.
Pradere JP, Tarnus E, Gres S, Valet P, Saulnier-Blache JS (2007) Secretion and lysophospholipase D activity of autotaxin by adipocytes are controlled by N-glycosylation and signal peptidase. Biochim Biophys Acta 1771:93-102.
Pringle NP, Yu WP, Guthrie S, Roelink H, Lumsden A, Peterson AC, Richardson WD (1996) Determination of neuroepithelial cell fate: induction of the oligodendrocyte lineage by ventral midline cells and sonic hedgehog. Dev Biol 177:30-42.
Readhead C, Takasashi N, Shine HD, Saavedra R, Sidman R, Hood L (1990) Role of myelin basic protein in the formation of central nervous system myelin. Ann N Y Acad Sci 605:280-285.
Reynolds R, Cenci di Bello I, Dawson M, Levine J (2001) The response of adult oligodendrocyte progenitors to demyelination in EAE. Prog Brain Res 132:165-174.
Richardson W, Smith H, Sun T, Pringle N, Hall A, Woodruff R (2000) Oligodendrocyte lineage and the motor neuron connection. Glia 29:136-142.
Richardson WD, Pringle NP, Yu WP, Hall AC (1997) Origins of spinal cord oligodendrocytes: possible developmental and evolutionary relationships with motor neurons. Dev Neurosci 19:58-68.
Richter-Landsberg C (2000) The oligodendroglia cytoskeleton in health and disease. J Neurosci Res 59:11-18.
Richter-Landsberg C (2001) Organization and functional roles of the cytoskeleton in oligodendrocytes. Microsc Res Tech 52:628-636.
Roth MP, Malfroy L, Offer C, Sevin J, Enault G, Borot N, Pontarotti P, Coppin H (1995) The human myelin oligodendrocyte glycoprotein (MOG) gene: complete nucleotide sequence and structural characterization. Genomics 28:241-250.
Salzer JL (1997) Clustering sodium channels at the node of Ranvier: close encounters of the axon-glia kind. Neuron 18:843-846.
Sato-Bigbee C, Pal S, Chu AK (1999) Different neuroligands and signal transduction pathways stimulate CREB phosphorylation at specific developmental stages along oligodendrocyte differentiation. J Neurochem 72:139-147.
Sayas CL, Avila J, Wandosell F (2002) Regulation of neuronal cytoskeleton by lysophosphatidic acid: role of GSK-3. Biochim Biophys Acta 1582:144-153.
Sayers EW et al. (2009) Database resources of the National Center for Biotechnology Information. Nucleic Acids Res 37:D5-15.
Schebesta M, Serluca FC (2009) olig1 expression identifies developing oligodendrocytes in zebrafish and requires hedgehog and notch signaling. Dev Dyn 238:887-898.
Schliess F, Stoffel W (1991) Evolution of the myelin integral membrane proteins of the central nervous system. Biol Chem Hoppe Seyler 372:865-874.

Schneider-Schaulies J, von Brunn A, Schachner M (1990) Recombinant peripheral myelin protein P0 confers both adhesion and neurite outgrowth-promoting properties. J Neurosci Res 27:286-297.
Schweigreiter R, Roots BI, Bandtlow CE, Gould RM (2006) Understanding myelination through studying its evolution. Int Rev Neurobiol 73:219-273.
Schweitzer J, Becker T, Becker CG, Schachner M (2003) Expression of protein zero is increased in lesioned axon pathways in the central nervous system of adult zebrafish. Glia 41:301-317.
Schweitzer J, Becker T, Schachner M, Nave KA, Werner H (2006) Evolution of myelin proteolipid proteins: gene duplication in teleosts and expression pattern divergence. Mol Cell Neurosci 31:161-177.
Shano S, Moriyama R, Chun J, Fukushima N (2008) Lysophosphatidic acid stimulates astrocyte proliferation through LPA1. Neurochem Int 52:216-220.
Smith R, Kavanagh E, Morrison HG, Gould RM (2001) Messenger RNAs located in spiny dogfish oligodendrocyte processes. Biol Bull 201:255-256.
Solly SK, Thomas JL, Monge M, Demerens C, Lubetzki C, Gardinier MV, Matthieu JM, Zalc B (1996) Myelin/oligodendrocyte glycoprotein (MOG) expression is associated with myelin deposition. GLIA 18:39-48.
Song J, Goetz BD, Baas PW, Duncan ID (2001) Cytoskeletal reorganization during the formation of oligodendrocyte processes and branches. Mol Cell Neurosci 17:624-636.
Southwood CM, Peppi M, Dryden S, Tainsky MA, Gow A (2007) Microtubule deacetylases, SirT2 and HDAC6, in the nervous system. Neurochem Res 32:187-195.
Sporkel O, Uschkureit T, Bussow H, Stoffel W (2002) Oligodendrocytes expressing exclusively the DM20 isoform of the proteolipid protein gene: myelination and development. GLIA 37:19-30.
Stankoff B, Barron S, Allard J, Barbin G, Noel F, Aigrot MS, Premont J, Sokoloff P, Zalc B, Lubetzki C (2002) Oligodendroglial expression of Edg-2 receptor: developmental analysis and pharmacological responses to lysophosphatidic acid. Mol Cell Neurosci 20:415-428.
Staugaitis SM, Colman DR, Pedraza L (1996) Membrane adhesion and other functions for the myelin basic proteins. Bioessays 18:13-18.
Stecca B, Southwood CM, Gragerov A, Kelley KA, Friedrich VL, Jr., Gow A (2000) The evolution of lipophilin genes from invertebrates to tetrapods: DM-20 cannot replace proteolipid protein in CNS myelin. J Neurosci 20:4002-4010.
Stemple DL (2005) Structure and function of the notochord: an essential organ for chordate development. Development 132:2503-2512.
Stolt CC, Rehberg S, Ader M, Lommes P, Riethmacher D, Schachner M, Bartsch U, Wegner M (2002) Terminal differentiation of myelin-forming oligodendrocytes depends on the transcription factor Sox10. Genes Dev 16:165-170.

Stracke ML, Krutzsch HC, Unsworth EJ, Arestad A, Cioce V, Schiffmann E, Liotta LA (1992) Identification, purification, and partial sequence analysis of autotaxin, a novel motility-stimulating protein. J Biol Chem 267:2524-2529.
Strahle U, Blader P, Henrique D, Ingham PW (1993) Axial, a zebrafish gene expressed along the developing body axis, shows altered expression in cyclops mutant embryos. Genes Dev 7:1436-1446.
Tabata K, Baba K, Shiraishi A, Ito M, Fujita N (2007) The orphan GPCR GPR87 was deorphanized and shown to be a lysophosphatidic acid receptor. Biochem Biophys Res Commun 363:861-866.
Takada N, Appel B (2010) Identification of genes expressed by zebrafish oligodendrocytes using a differential microarray screen. Dev Dyn 239:2041-2047.
Tanaka M, Okudaira S, Kishi Y, Ohkawa R, Iseki S, Ota M, Noji S, Yatomi Y, Aoki J, Arai H (2006) Autotaxin stabilizes blood vessels and is required for embryonic vasculature by producing lysophosphatidic acid. J Biol Chem 281:25822-25830.
Taylor JS, Braasch I, Frickey T, Meyer A, Van de Peer Y (2003) Genome duplication, a trait shared by 22000 species of ray-finned fish. Genome Res 13:382-390.
Thisse C, Thisse B (2008) High-resolution in situ hybridization to whole-mount zebrafish embryos. Nat Protoc 3:59-69.
Thurnherr T, Benninger Y, Wu X, Chrostek A, Krause SM, Nave KA, Franklin RJ, Brakebusch C, Suter U, Relvas JB (2006) Cdc42 and Rac1 signaling are both required for and act synergistically in the correct formation of myelin sheaths in the CNS. J Neurosci 26:10110-10119.
Tiso N, Filippi A, Benato F, Negrisolo E, Modena N, Vaccari E, Driever W, Argenton F (2009) Differential expression and regulation of olig genes in zebrafish. J Comp Neurol 515:378-396.
Tokumura A, Tsutsumi T, Tsukatani H (1992) Transbilayer movement and metabolic fate of ether-linked phosphatidic acid (1-O-Octadecyl-2-acetyl-sn-glycerol 3-phosphate) in guinea pig peritoneal polymorphonuclear leukocytes. J Biol Chem 267:7275-7283.
Tokumura A, Majima E, Kariya Y, Tominaga K, Kogure K, Yasuda K, Fukuzawa K (2002) Identification of human plasma lysophospholipase D, a lysophosphatidic acid-producing enzyme, as autotaxin, a multifunctional phosphodiesterase. J Biol Chem 277:39436-39442.
Trapp BD, Moench T, Pulley M, Barbosa E, Tennekoon G, Griffin J (1987) Spatial segregation of mRNA encoding myelin-specific proteins. Proc Natl Acad Sci U S A 84:7773-7777.
Umezu-Goto M, Kishi Y, Taira A, Hama K, Dohmae N, Takio K, Yamori T, Mills GB, Inoue K, Aoki J, Arai H (2002) Autotaxin has lysophospholipase D activity leading to tumor cell growth and motility by lysophosphatidic acid production. J Cell Biol 158:227-233.
Urs NM, Jones KT, Salo PD, Severin JE, Trejo J, Radhakrishna H (2005) A requirement for membrane cholesterol in the beta-arrestin- and clathrin-

dependent endocytosis of LPA1 lysophosphatidic acid receptors. J Cell Sci 118:5291-5304.
Valentine WJ, Fujiwara Y, Tsukahara R, Tigyi G (2008) Lysophospholipid signaling: beyond the EDGs. Biochim Biophys Acta 1780:597-605.
van Meeteren LA, Moolenaar WH (2007) Regulation and biological activities of the autotaxin-LPA axis. Prog Lipid Res 46:145-160.
van Meeteren LA, Ruurs P, Stortelers C, Bouwman P, van Rooijen MA, Pradere JP, Pettit TR, Wakelam MJ, Saulnier-Blache JS, Mummery CL, Moolenaar WH, Jonkers J (2006) Autotaxin, a secreted lysophospholipase D, is essential for blood vessel formation during development. Mol Cell Biol 26:5015-5022.
Vandesompele J, De Preter K, Pattyn F, Poppe B, Van Roy N, De Paepe A, Speleman F (2002) Accurate normalization of real-time quantitative RT-PCR data by geometric averaging of multiple internal control genes. Genome Biol 3:RESEARCH0034.
Voas MG, Lyons DA, Naylor SG, Arana N, Rasband MN, Talbot WS (2007) alphaII-spectrin is essential for assembly of the nodes of Ranvier in myelinated axons. Curr Biol 17:562-568.
Volff JN (2005) Genome evolution and biodiversity in teleost fish. Heredity 94:280-294.
Warrington AE, Pfeiffer SE (1992) Proliferation and differentiation of O4+ oligodendrocytes in postnatal rat cerebellum: analysis in unfixed tissue slices using anti-glycolipid antibodies. J Neurosci Res 33:338-353.
Wegner M (2000) Transcriptional control in myelinating glia: flavors and spices. GLIA 31:1-14.
Wei Q, Miskimins WK, Miskimins R (2004) Sox10 acts as a tissue-specific transcription factor enhancing activation of the myelin basic protein gene promoter by p27Kip1 and Sp1. J Neurosci Res 78:796-802.
Wei Q, Miskimins WK, Miskimins R (2005) Stage-specific expression of myelin basic protein in oligodendrocytes involves Nkx2.2-mediated repression that is relieved by the Sp1 transcription factor. J Biol Chem 280:16284-16294.
Weiner JA, Hecht JH, Chun J (1998) Lysophosphatidic acid receptor gene vzg-1/lpA1/edg-2 is expressed by mature oligodendrocytes during myelination in the postnatal murine brain. J Comp Neurol 398:587-598.
Westerfield M (2000) The zebrafish book. A guide for the laboratory use of zebrafish (Danio rerio). 4th Edition. Eugene: University of Oregon Press.
Williams AF, Barclay AN (1988) The immunoglobulin superfamily--domains for cell surface recognition. Annu Rev Immunol 6:381-405.
Wilson R, Brophy PJ (1989) Role for the oligodendrocyte cytoskeleton in myelination. J Neurosci Res 22:439-448.
Wilson SW, Houart C (2004) Early steps in the development of the forebrain. Dev Cell 6:167-181.
Woods IG, Lyons DA, Voas MG, Pogoda HM, Talbot WS (2006) nsf is essential for organization of myelinated axons in zebrafish. Curr Biol 16:636-648.

Wu S, Wu Y, Capecchi MR (2006) Motoneurons and oligodendrocytes are sequentially generated from neural stem cells but do not appear to share common lineage-restricted progenitors in vivo. Development 133:581-590.
Xin M, Yue T, Ma Z, Wu FF, Gow A, Lu QR (2005) Myelinogenesis and axonal recognition by oligodendrocytes in brain are uncoupled in Olig1-null mice. J Neurosci 25:1354-1365.
Yan H, Lu D, Rivkees SA (2003) Lysophosphatidic acid regulates the proliferation and migration of olfactory ensheathing cells in vitro. GLIA 44:26-36.
Yan Y, Lagenaur C, Narayanan V (1993) Molecular cloning of M6: identification of a PLP/DM20 gene family. Neuron 11:423-431.
Yanagida K, Masago K, Nakanishi H, Kihara Y, Hamano F, Tajima Y, Taguchi R, Shimizu T, Ishii S (2009) Identification and characterization of a novel lysophosphatidic acid receptor, p2y5/LPA6. J Biol Chem 284:17731-17741.
Yang AH, Ishii I, Chun J (2002) In vivo roles of lysophospholipid receptors revealed by gene targeting studies in mice. Biochim Biophys Acta 1582:197-203.
Ye X, Hama K, Contos JJ, Anliker B, Inoue A, Skinner MK, Suzuki H, Amano T, Kennedy G, Arai H, Aoki J, Chun J (2005) LPA3-mediated lysophosphatidic acid signalling in embryo implantation and spacing. Nature 435:104-108.
Yoshida M, Colman DR (1996) Parallel evolution and coexpression of the proteolipid proteins and protein zero in vertebrate myelin. Neuron 16:1115-1126.
Yoshida M, Macklin WB (2005) Oligodendrocyte development and myelination in GFP-transgenic zebrafish. J Neurosci Res 81:1-8.
Yu N, Lariosa-Willingham KD, Lin FF, Webb M, Rao TS (2004) Characterization of lysophosphatidic acid and sphingosine-1-phosphate-mediated signal transduction in rat cortical oligodendrocytes. GLIA 45:17-27.
Yuelling LM, Fuss B (2008) Autotaxin (ATX): a multi-functional and multi-modular protein possessing enzymatic lysoPLD activity and matricellular properties. Biochim Biophys Acta 1781:525-530.
Zaslavsky A, Singh LS, Tan H, Ding H, Liang Z, Xu Y (2006) Homo- and hetero-dimerization of LPA/S1P receptors, OGR1 and GPR4. Biochim Biophys Acta 1761:1200-1212.
Zhang X, Miskimins R (1993) Binding at an NFI site is modulated by cyclic AMP-dependent activation of myelin basic protein gene expression. J Neurochem 60:2010-2017.
Zhou Q, Anderson DJ (2002) The bHLH transcription factors OLIG2 and OLIG1 couple neuronal and glial subtype specification. Cell 109:61-73.

Larra Walling Yuelling was born in Long Branch, NJ, on August 12th, 1981. She graduated from Shore Regional High School in 1999. Larra continued her education at Drew University in Madison, New Jersey, where she received a Bachelor of Arts in Neurobiology and a Minor in Mathematics in 2003. From 2003 to 2004, Larra worked as a laboratory technician under the direction of Dr. Karen Chandross in the department of CNS regeneration at Aventis Pharmaceuticals (now Sanofi-Aventis) in Bridgewater, NJ. In the fall of 2004, Larra entered the Neuroscience program at Virginia Commonwealth University and joined the laboratory of Dr. Babette Fuss in the department of Anatomy and Neurobiology in the summer of 2005. Throughout her research career there she was given many opportunities to present her research via posters and oral presentations at national meetings such as the American Society for Neurochemistry and the Society for Neuroscience. At VCU, Larra participated in two Watts Day symposia, two Central Virginia Chapter Society for Neuroscience annual fall poster sessions, the Graduate Student Association annual research presentation session as well as being selected for an oral presentation at the Forbes Day honors colloquium. Larra also earned various awards such as the Jack Denning Burke award in cell biology, the VCU Graduate School Dissertation Assistantship award as well as travel awards from the American Society for Neurochemistry, Central Virginia Chapter of the Society for Neuroscience and the VCU graduate school.

Manuscripts resulting from Larra's work at Virginia Commonwealth University:

Yuelling, L.W., Afshari, F.S., Waggener, C.T., Lister, J.A., Fuss, B. Autotaxin regulates the presence of differentiating oligodendrocytes in the developing CNS of the zebrafish. (in preparation)

Coelho, R.P., Yuelling, L.M., Fuss, B., Sato-Bigbee, C. Neurotrophin-3 targets the translational initiation machinery in oligodendrocytes. Glia 2009, May; 57: 1754-1764.

Nogaroli*, L., Yuelling*, L.M., Dennis, J., Gorse, K., Payne, S.G., and Fuss, B. Lysophosphatidic acid can support the formation of membranous structures and an increase in MBP mRNA levels in differentiating oligodendrocytes. Neurochem. Res. 2009, Jan; 34(1): 182-93.
*Equal contribution

Yuelling, L.M. and Fuss, B. Autotaxin (ATX): a multifunctional protein with lysophospholipase (lysoPLD) activity and matricellular properties. Review. Biochim Biophys Acta. 2008, Sept; 1781(9): 525-530.

Dennis, J., White, M., Forrest A.D., Yuelling L.M., Nogaroli, L., Afshari, F.S., Fox, M.A., and Fuss, B. Phosphodiesterase-1 alpha/Autotaxin's MORFO domain regulates oligodendroglial process network formation and focal adhesion organization. Mol Cell Neurosci. 2008, Feb; 37: 412-424.